

Chapter 8

Mechanically Linked Network and Branched Poly(urethane rotaxane)s with Controllable Polydispersity

8.1 Introduction

Compared to linear counterparts, branched polymers often show new properties such as high solubility, low melt viscosity and low density and thus bring about lots of new applications. Hyperbranched materials can easily be prepared by one-step reactions of AB_x monomers, in which functional groups A and B can react with each other and x is 2 or greater.¹⁻¹² However, there are some limitations in this classical approach. First, the final product is always highly functional, i.e., contains lots of unreacted B, and an additional step is required to decrease or terminate such end-functional groups if necessary. Secondly, groups A and B can not be too reactive. For example, polyurethanes can not be constructed directly from monomers with hydroxy and isocyanate groups and a protective group has to be introduced.¹¹ Finally, the degrees of branching or polydispersity (PDI) and the degree of polymerization (DP) are difficult to control because they are mainly decided by statistics, accessibility of functional groups and reaction rate. Overcoming these limitations remains a great challenge to chemists.

¹ For reviews: a) Dvornic, P. R.; Tomalia, D. A. *Curr. Opinion Coll. Interface Sci.* **1996**, *1*, 221. b) Newkome, G. R.; Moorefield, C. N.; Vogtle, F. “*Dendritic Molecules*”, VCH Publishers, Weinheim, Germany, **1996**. c) Fréchet, J. M. J. *Science*, **1994**, *263*, 1710. d) Fréchet, J. M. J. *J. Macromol. Sci. Pure Appl. Chem.* **1994**, *A31*, 1627.

² Massa, D. J.; Shriner, K. A.; Turner, S. R.; Voit, B. I. *Macromolecules* **1995**, *28*, 3214.

³ Turner, S. R.; Walter, F.; Voit, B. I.; Mourey, T. H. *Macromolecules* **1994**, *27*, 1611.

⁴ Wooley, K. L.; Hawker, C. J.; Lee, R.; Fréchet, J. M. J. *Polym. J.* **1994**, *26*, 187.

⁵ Turner, S. R.; Voit, B. I.; Mourey, T. H. *Macromolecules* **1993**, *26*, 4617.

⁶ Ralph, P.; Hawker, C. J.; Fréchet, J. M. J. *Macromolecules* **1993**, *26*, 4809.

⁷ Miller, T. M.; Neenan, T. X.; Kwock, E. W.; Stein, S. M. *J. Am. Chem. Soc.* **1993**, *115*, 356.

⁸ Uhrich, K. E.; Hawker, C. J.; Fréchet, J. M. J.; Turner, S. R. *Macromolecules* **1992**, *25*, 4583.

⁹ Kim, Y. H. *J. Am. Chem. Soc.* **1992**, *114*, 4947.

¹⁰ Kim, Y. H.; Webster, O. W. *Macromolecules* **1992**, *25*, 5561.

¹¹ Hawker, C. J.; Lee, R.; Fréchet, J. M. J. *J. Am. Chem. Soc.* **1991**, *113*, 4583.

¹² Mathias, L. J.; Carothers, T. W. *J. Am. Chem. Soc.* **1991**, *113*, 4043.

Polyrotaxanes, in which rotaxane units (cyclics threaded by linear species) are incorporated into macromolecules, also have received world-wide attention.¹³⁻²¹ Lots of main chain polyrotaxanes have been prepared with crown ethers as cyclic components.^{13,17-19} Recently, hydrogen bonding between hydroxy groups and the crown ethers was proposed as a driving force for the threading.¹⁸⁻²⁰ Therefore, a crown ether bearing a hydroxy functional group brings about a driving force for the formation of a self-complexed structure **8.1**, which can lead to a novel rotaxane structure **8.3** by an endo esterification with a poly(acid chloride) (Scheme 8.1) as we showed by the formation of a branched and/or crosslinked polymer **8.4**.²⁰

In the present work, this concept is extended and used as a novel strategy to overcome the limitations of classical methods for the preparation of branched and network polymers; that is demonstrated by the syntheses of mechanically linked branched and network polyurethanes.

¹³ For reviews: a) Gibson, H. W. In *Large Ring Molecules*, Semlyen, J. A. ed., J. Wiley and Sons, New York, **1996**, 191. b) Philp, D.; Stoddart, J. F. *Angew. Chem. Int. Ed. Engl.* **1996**, *35*, 1154. c) Amabalino, D. B.; Stoddart, J. F. *Chem. Rev.* **1995**, *95*, 2725. d) Gibson, H. W.; Bheda, M. C.; Engen, P. T. *Prog. Polym. Sci.* **1994**, *19*, 843.

¹⁴ a) Steinbrunn, M. B.; Wenz, G. *Angew. Chem. Int. Ed. Engl.* **1996**, *35*, 2139. b) Weickenmeier, M.; Wenz, G. *Macromol. Rapid. Commun.* **1996**, *17*, 731. c) Wenz, G. *Macromol. Symp.* **1994**, *87*, 11.

¹⁵ a) Born, M.; Ritter, H. *Macromol. Rapid Commun.* **1996**, *17*, 197. b) Born, M.; Ritter, H. *Adv. Mater.* **1996**, *8*, 149. c) Born, M.; Ritter, H. *Angew. Chem. Int. Ed. Engl.* **1995**, *107*, 342.

¹⁶ a) Harada, A.; Okada, M.; Li, J.; Kamachi, M. *Macromolecules* **1995**, *28*, 8406. b) Harada, A.; Li, J.; Kamachi, M. *Macromolecules* **1994**, *27*, 4538.

¹⁷ a) Gibson, H. W.; Liu, S.; Lecavalier, P.; Wu, C.; Shen, Y. X. *J. Am. Chem. Soc.* **1995**, *117*, 852. b) Shen, Y. X.; Xie, D.; Gibson, H. W. *J. Am. Chem. Soc.* **1994**, *116*, 537. c) Gibson, H. W.; Marand, H. *Adv. Mater.* **1993**, *5*, 11.

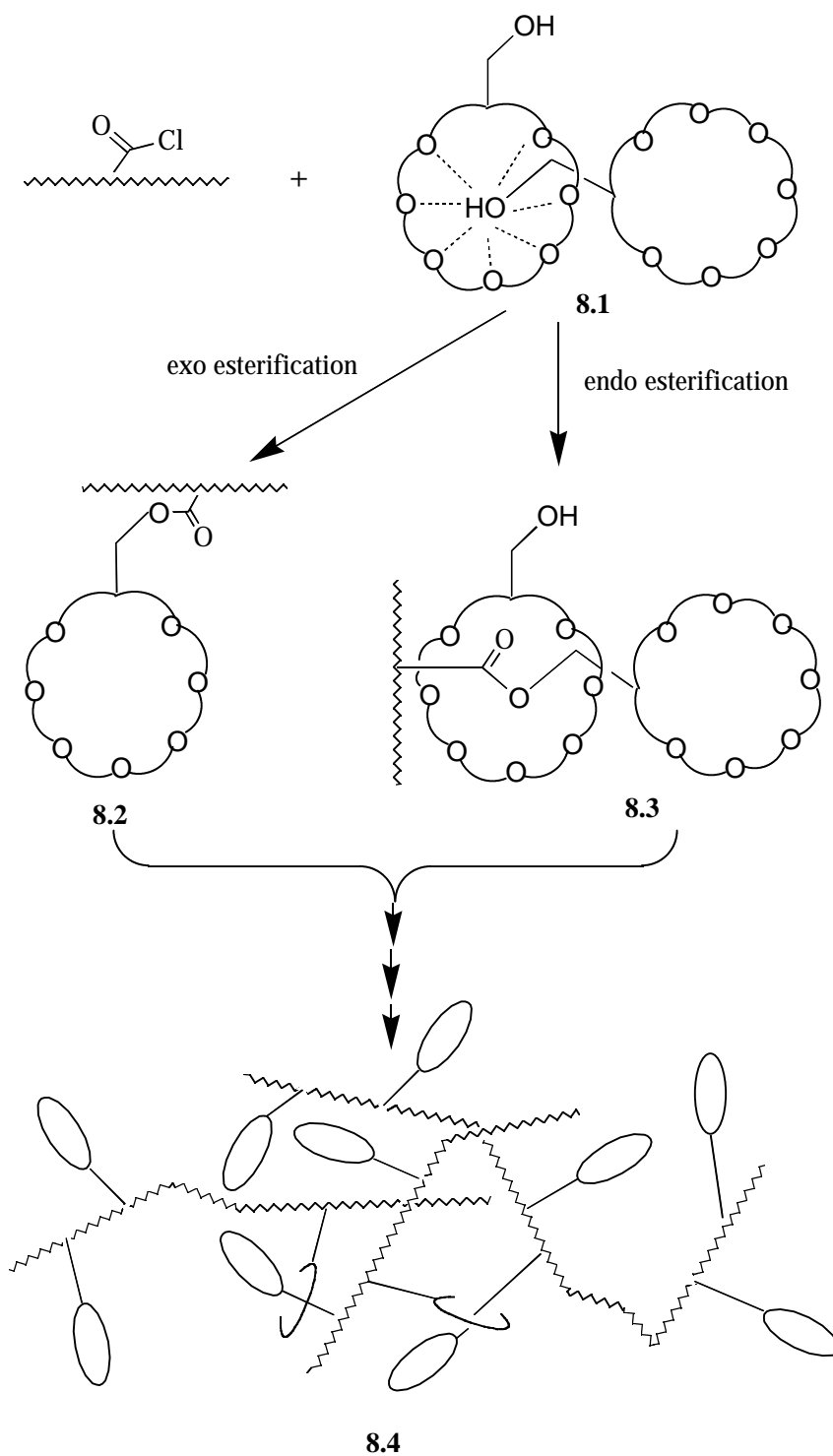
¹⁸ a) Gong, C.; Gibson, H. W. *Macromol. Chem. Phys.*, **1997**, *198*, 2321 and Chapter 4. b) Gibson, H. W.; Liu, S.; Gong, C.; Ji, Q.; Joseph, E. *Macromolecules*, **1997**, *31*, 3711. c) Gong, C.; Gibson, H. W. *Macromolecules* **1996**, *29*, 7029 and chapter 3. d) Gong, C.; Ji, Qing; Glass, T. E.; Gibson, H. W. *Macromolecules*, *30*, 4807 and chapter 5. e) Gibson, H. W.; Liu, S. *Macromol. Symp.* **1996**, *102*, 55. f) Gibson, H. W.; Gong, C.; Liu, S.; Nagvekar, D. *Macromol. Symp.*, in press.

¹⁹ Gong, C.; Gibson, H. W. *Angew. Chem.*, in press and chapter 6.

²⁰ Gong, C.; Gibson, H. W. *J. Am. Chem. Soc.*, **1997**, 5862 and chapter 7.

²¹ a) Gibson, H. W.; Nagvekar, D.; Yamaguchi, N.; Bryant, W. S.; Bhattacharjee, S. *Am. Chem. Soc. Div. Polym. Chem. Polym. Prep.* **1997**, *38(1)*, 64. b) Gibson, H. W.; Nagvekar, D.; Bryant, W. S.; Powell J.; Bhattacharjee, S. *Am. Chem. Soc. Div. Polym. Chem. Polym. Prep.* **1997**, *38(1)*, 115. c) Nagvekar, D. and Gibson, H. W. *Am. Chem. Soc. Div. Polym. Chem. Polym. Prep.* **1996**, *37(2)*, 299. d) Delaviz, Y.; Gibson, H. W. *Macromolecules* **1992**, *25*, 18. e) Delaviz, Y. and Gibson, H. W. *Macromolecules* **1992**, *25*, 4859. f) Gibson, H. W.; Nagvekar, D. S.; Powell, J.; Gong, C.; Bryant, W. S. *Tetrahedron*, in press. g) Delaviz, Y.; Gibson, H. W. *Polym. Commun.* **1991**, *32*, 103.

Scheme 8.1

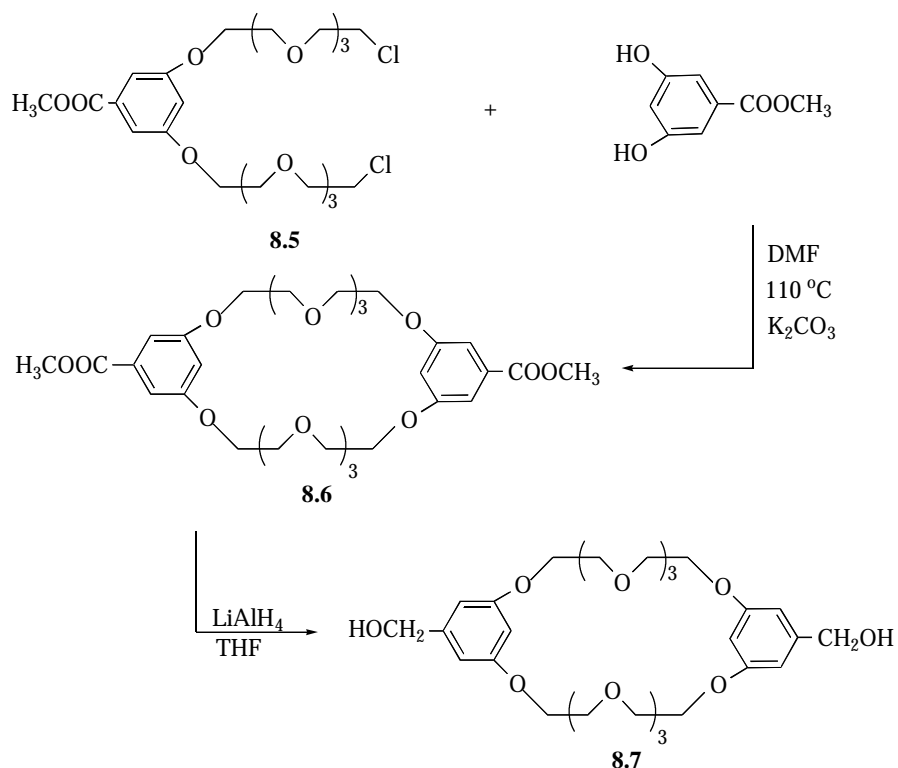


8.2 Results and discussion

8.2.1 Synthesis of bis(hydroxymethyl) BMP32C10 (8.7)

To prepare mechanical linked network and branched polyrotaxanes by polycondensation, a difunctional crown ether is needed. The functional group should complex with the crown ether to provide the driving force for threading, the branching point. Bis(hydroxymethyl) BMP32C10 (**8.7**) is a perfect choice for the above purpose because the hydroxy group can react with diacid chlorides and diisocyanates and can hydrogen bond with the crown ether moiety. Thus **8.7** was prepared by a previous procedure as shown in Scheme 8.2.²²

Scheme 8.2



²² Gibson, H. W.; Nagvekar, D. S. *Can. J. Chem.* **1997**, 75, xxx.

First diester BMP32C10 **8.6** was synthesized by 1+1 combination of dichloride **8.5** and methyl 3,5-dihydroxybenzoate. To insure a highly pseudo-dilute condition, the equimolar solution of dichloride **8.5** and dihydroxybenzoate in a small amount of DMF was added via a syringe pump at a very slow rate to a suspension of potassium carbonate in a large amount of DMF. The purpose is to favor cyclization rather than linear growth. The purification yield was 37 %, which is lower than that reported.²² The possible reason for the low yield is the removal of an impurity separated by chromatography with ether as eluting solvent. No impurity was mentioned in the literature. **8.6** was then converted to bis(hydroxymethyl) BMP32C10 (**8.7**) by the reduction with LiAlH₄ in THF with yield of 87 % after recrystallization in ethanol.

8.2.2 Syntheses of polyurethanes 8-11 and 12a-c.

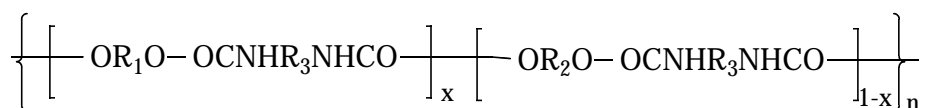
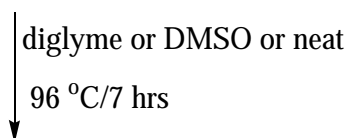
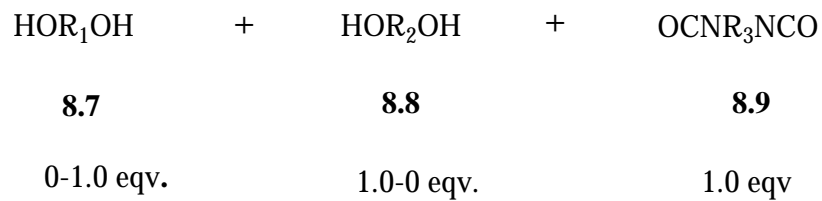
To establish the conditions to achieve high molecular weight, model polyurethane **8.10** was prepared from tetra(ethylene glycol) (**8.8**) and 4,4'-methylenebis(*p*-phenyl isocyanate) (MDI) (**8.9**) by solution polymerization using diglyme as solvent (Table 8.1 and Scheme 8.3). According to GPC measurements (Table 8.2), high molecular weight **8.10** can be obtained within 7 hours at 96 °C. Therefore, the same conditions were applied for copolyurethanes **8.11-13**, which were made from reaction of bis(5-hydroxymethyl-1,3-phenylene)-32-crown-10 (**8.7**) and **8.8** with MDI (**8.9**). The detailed feed composition are specified in Table 8.1 and Scheme 8.3.

Table 8.1 Detailed feed compositions for polyurethanes **8.10-8.14**^a

Polymer	solvent (mL)	8.7 (mmol)	8.8 (mmol)	8.9 (mmol)
8.10	diglyme (58.0)	0.00	18.95	18.95
8.11	diglyme (2.0)	0.1629	0.4865	0.6493
8.12	diglyme (2.0)	0.3250	0.3244	0.6493
8.13	diglyme (1.9)	0.4689	0.1565	0.6254
8.14a	diglyme (1.5)	0.4890	0	0.4890
8.14b	DMSO (1.5)	0.4890	0	0.4890
8.14c	no solvent	0.5392	0	0.5392

a) Polymerization temperature: 96 ± 2 °C; time: 7 h.

Scheme 8.3



8.10: x=0

8.11: x=0.25

8.12: x=0.50

8.13: x=0.75

8.14a-c: x=1.0

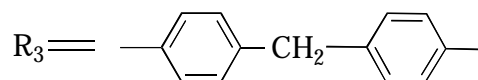
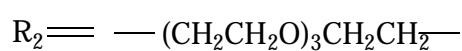
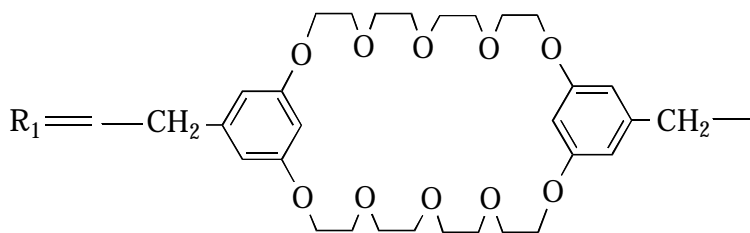


Table 8.2 GPC and DSC results for polyurethanes **8.10-8.14**

Polymer	M_n^a (kg/mol)	M_w^a (kg/mol)	PDI ^a	T_g^b (°C)
8.10	16.6	58.7	3.54	54.0
8.11	8.5	46.4	5.54	55.0
8.12	8.0	109	13.6	57.4
8.13	6.6	161	24.2	59.5
8.14a	11.3	267	23.6	66.4
8.14b	13.2	53.9	4.0	66.2
8.14c	--	--	--	73.9

a) Measured by GPC using universal calibration in NMP at 60 °C.

b) Measured by DSC at a scan rate of 10 °C/minute.

To study the influence of the feed percentage of **8.7** on the PDI of the resulting polyurethanes, the ratio of macrocyclic diol **8.7** vs. **8.8** was increased in the syntheses of **8.10** to **8.13** while the concentration of total hydroxy groups (**8.7** plus **8.8**) was kept at the same value (Table 8.1). To test the effect of solvent on polymer topology, homopolyurethanes **8.14a** and **8.14b** were prepared from the reaction of macrocyclic diol **8.7** with MDI (**8.9**) using different solvents, diglyme for **8.14a** and DMSO for **8.14b**. Finally, **8.14c** was prepared by melt polymerization of **8.8** and **8.9**. The chemical compositions of these polymers were confirmed by proton NMR measurements as exemplified by the spectrum of **8.12** (Figure 8.1).

8.2.3. GPC measurements and mechanism for branching and crosslinking

As the GPC results in Table 8.2 show, copolyurethanes **8.11-8.13** have much higher PDI than model polymer **8.10**. Such high PDI directly indicates that these polymers are essentially branched materials. It is well known that branched polymers and networks can only be generated from starting monomers with functionality greater than 2. How can we

explain the branching structures of polyurethanes **8.11-8.13** since from the point of view of reactive groups only difunctional monomers were used (Scheme 8.3)?

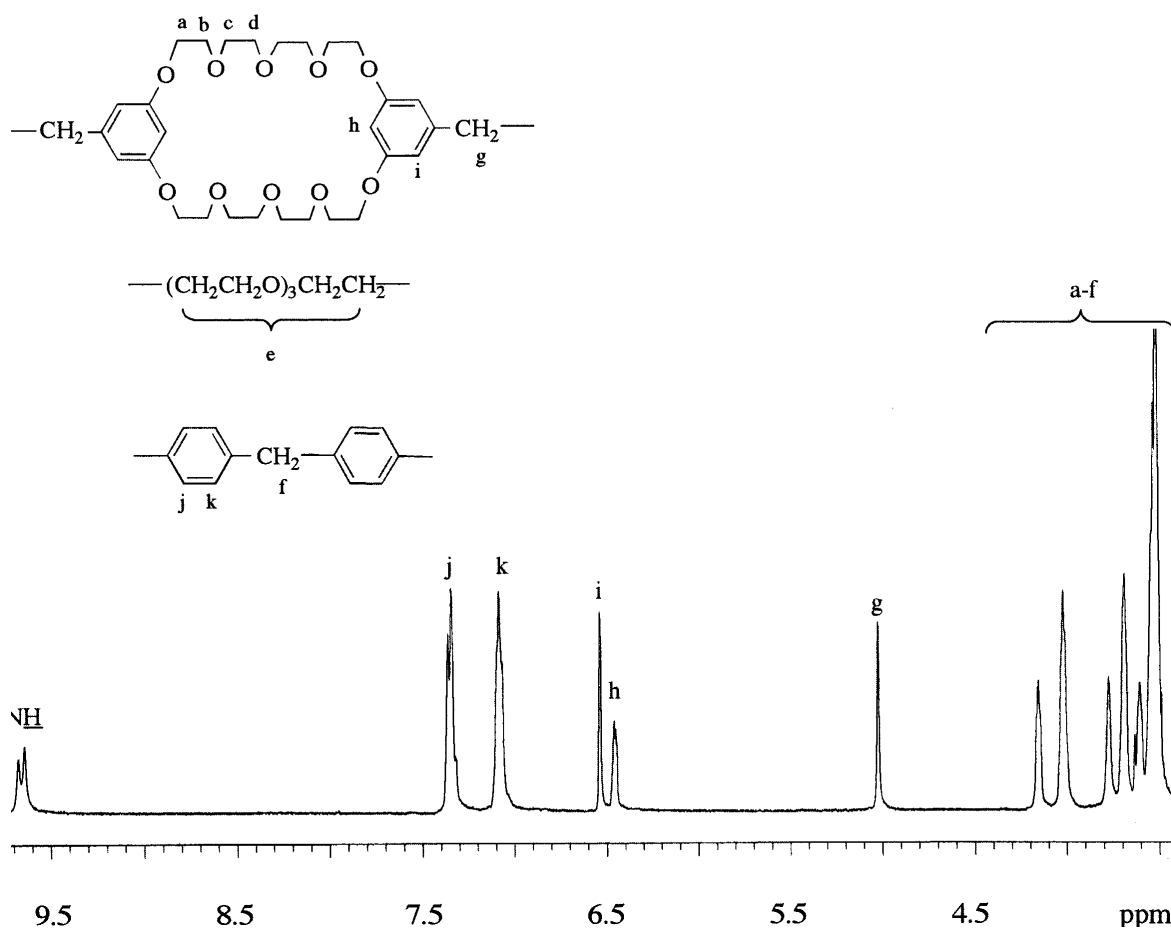
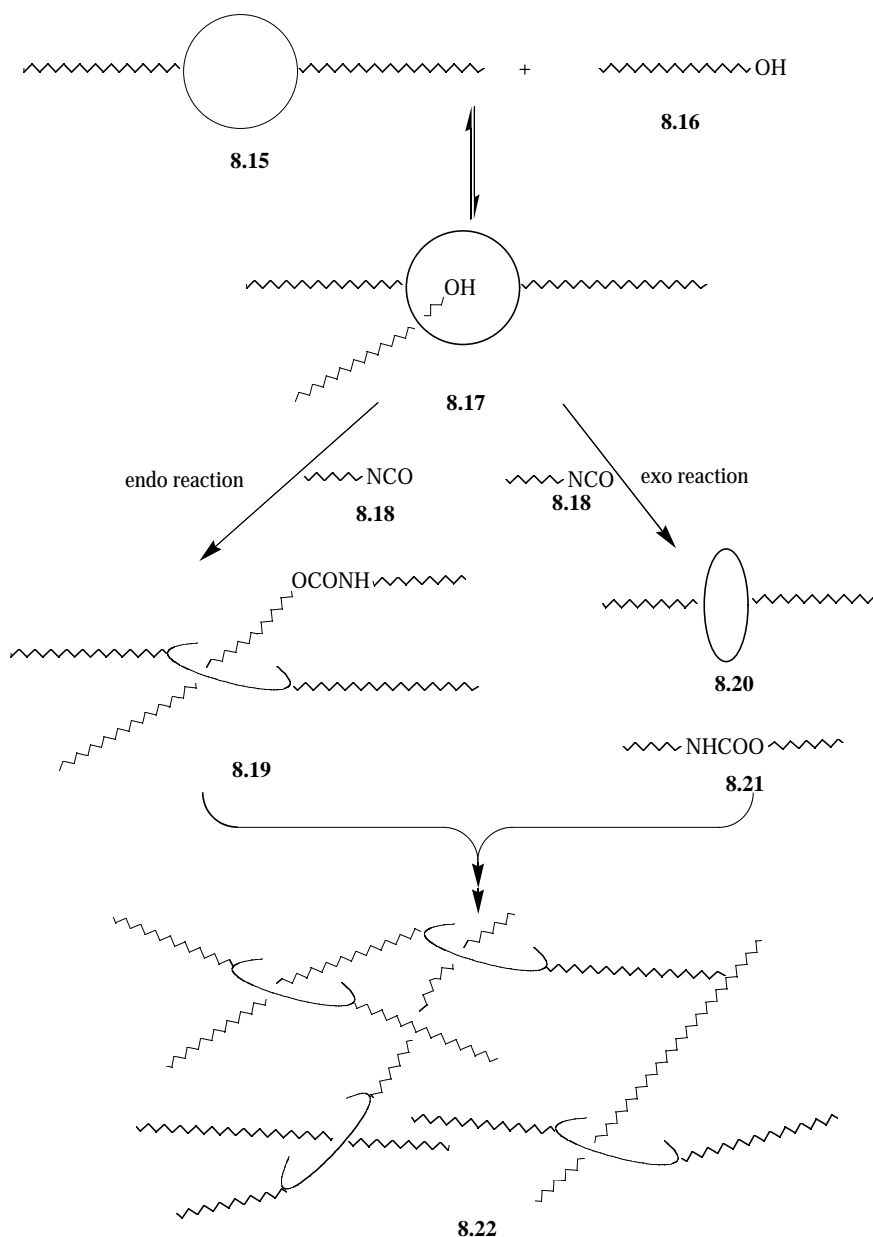


Figure 8.1 400 MHz proton NMR spectrum of polyurethane **8.12** in $\text{DMSO-}d_6$

For the preparation of polyester rotaxanes, we proposed that H-bonding of the crown ethers with -OH groups provides the driving force for threading.¹⁸ Therefore, macrocyclic moieties described as structure **8.15**, macrocyclic diol **8.7** initially and in-chain macrocyclic units during the polymerization, are expected to form various intermediates simplified as structure **8.17** by H-bonding with -OH groups of **8.16**, another macrocyclic diol **8.7** or glycol **8.8** at the start and the terminal -OH groups of polymeric chains during the polymerization (Scheme 8.4). H-bonded complex **8.17** can undergo endo reaction with the isocyanate group of **8.18**, that of MDI (**8.9**) initially and unreacted -NCO groups during the polymerization, to give rotaxane structure **8.19**, a branching or crosslinking point for polyurethanes **8.11-8.13**.

8.17 may also undergo exo reaction to yield normal linear backbone units (structures **8.20** and **8.21**). Ultimately, a novel three dimensional main chain polyrotaxane structure **8.22** is derived. Thus, the branching topology of **8.11-8.13** is produced by the formation of rotaxane units via a physical functionality, the cavity of the macrocycle, i.e., macrocyclic diol **8.7** is trifunctional, having two chemically reactive moieties and a physical linking site, a “topological functionality”.

Scheme 8.4



More interestingly, the PDI of the final polymers increased with the feed ratio of **8.7** vs. **8.8** (Table 8.2) and the relationship is plotted in Figure 8.2. This relationship is consistent with the above hypothesis. First, as more **8.7** and less **8.8** are applied as diol monomers, the concentration of **8.15** increases and thus more intermediate **8.17** and branching units **8.19** are expected (Scheme 8.4). Secondly, it is believed that a macrocycle can not pass through another identical cyclic; thus, in the rotaxanes, macrocycles essentially serve as blocking groups (BG) to prevent dethreading.^{18,20} Therefore, as more **8.7** is applied, there is less dethreading, and consequently a higher branching degree is achieved.

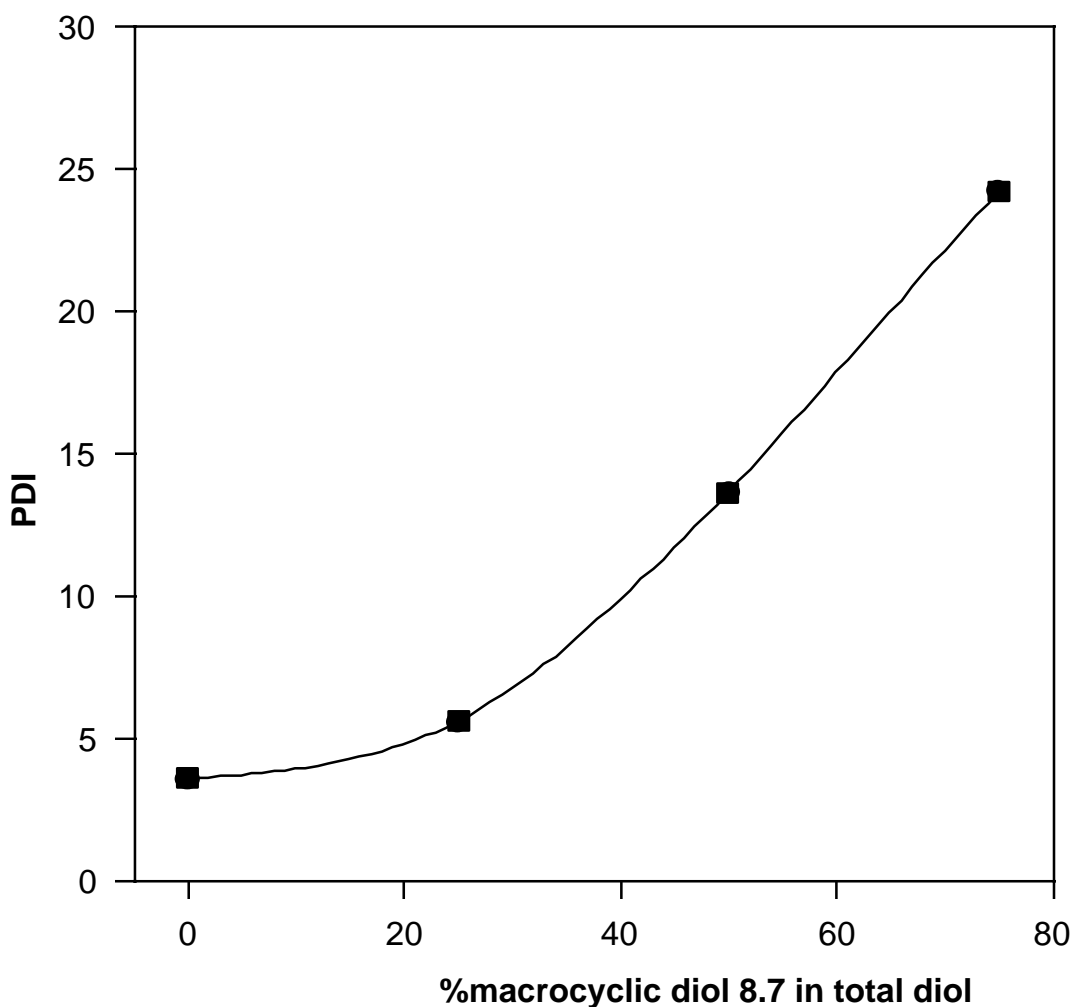


Figure 8.2. The relationship of the polydispersity of polyurethanes 8.10-8.13 vs. the feed percentage of macrocyclic diol 8.7.

It was reported that the strength of H-bonding of crown ethers with -OH moieties is dependent on the polarity of the solvent.²³ Recently, we found that DMSO is a very good solvent to depress or prevent the formation of such H-bonding structures. Therefore, the complex **8.17** and branching points **8.19** (Scheme 8.4) are not expected to form effectively in this solvent. According to GPC analysis, polyurethane **8.14b** prepared with DMSO as solvent indeed has a low PDI (Table 8.2 and Figure 8.3), close to that of model polyurethane **8.10**, and thus it is believed to be linear or to contain only very small amounts of branching rotaxane units, although both PDIs were above two because of the formation of small amounts of allophanate as detected by proton NMR. This result also rules out the possibility that side reactions are responsible for the formation of the branched and/or network polyurethanes. As expected, **8.14a** prepared in diglyme has a very high PDI (Table 8.2 and Figure 8.3). These results further support the proposed mechanism for the formation of branched and network polymers (Scheme 8.4).

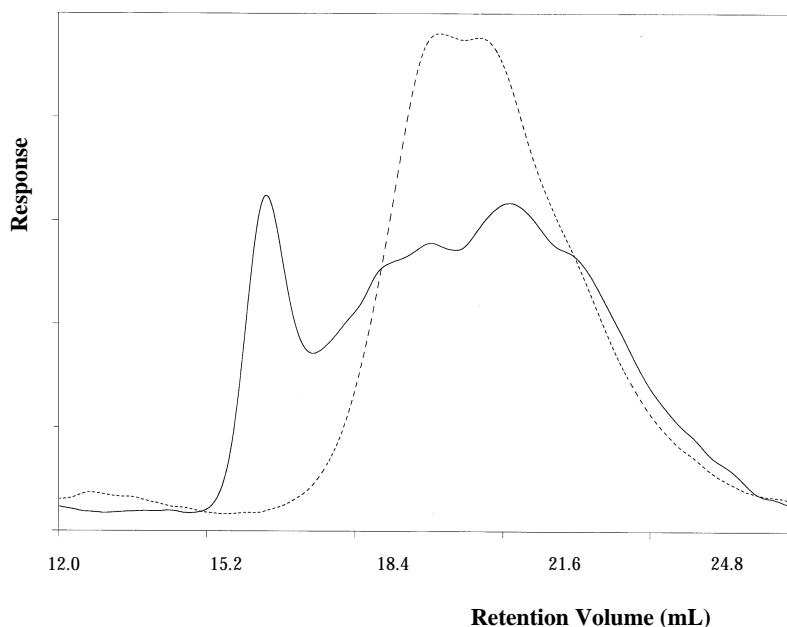


Figure 8.3. The GPC traces of a) polyurethane **8.14a**, solid line and b) polyurethane **8.14b**, dashed line with viscosity detector using NMP as solvent.

²³ Izatt, R. M.; Bradshaw, J. S.; Pawlak, K.; Bruening, R. L.; Tarbet, B. J. *Chem. Rev.*, **1992**, 92, 1261.

Additionally, **8.14c** was prepared by melt polymerization and thus had the highest concentration of H-bonded complex **8.17**. This produced the highest degree of branching as expected; indeed an insoluble network was formed.

8.2.4. NMR Studies

It is well known that threaded macrocycles or backbones can show different chemical shifts from their parent protons because of through-space interactions in the rotaxane structures, especially for macrocycles restricted between blocking groups^{18b,d,e} or other macrocycles.²⁰ In polyurethane **8.14a**, the branching points are main chain rotaxane structures and the threaded macrocycles are confined between other macrocyclic moieties (structures **8.23** and/or **8.24** in Scheme 8.5), since a macrocycle usually can not pass through another identical moiety.²⁰ New signals appear in the spectrum of **8.14a** (Figure 8.4b); this is because of the existence of the rotaxane units (**8.23**, **8.24**), the branching points. The lack of these new signals for **8.14b** (Figure 8.4a) indicates that it contains no rotaxane structures but rather is a linear polymer; this agrees with the GPC results. In addition, the signals h and i of **8.14a** became even more complicated and broader in CDCl₃ (Figure 8.4c) than in DMSO-d₆. We believe that H-bonding between the threaded macrocycle and the in-chain NH group¹⁹ restricts the motion of the macrocycle and thus leads to signal broadening (Scheme 8.5).

The COSY spectrum of **8.14a** shows the couplings consistent with its structure (Figure 8.5); this rules out the possibility that side reactions may cause branching. As expected, the NOESY spectrum (Figure 8.6) of **8.14a** in CDCl₃ indeed showed some through-space interactions. Since proton h is close to protons a, b, c, and d even in the unthreaded cyclic (Scheme 8.5), the correlation does not directly prove the rotaxane structure although it does agree with it. However, the correlations between proton i and the protons a, b, c, and d as well as those of protons k and j with a, b, c, and d do indicate the formation of the rotaxane topology for **8.11-8.13** and **8.14a** (Schemes 8.4 and 8.5) since they do not correlate with each other in unthreaded structures.²⁰ It is necessary to point out that the evidence is still fragile because these correlations were relatively weak and they only showed up after ten hours data collection at a high concentration; this can be ascribed to the low

degree of threading. Therefore, the following study was performed to augment the NOESY results.

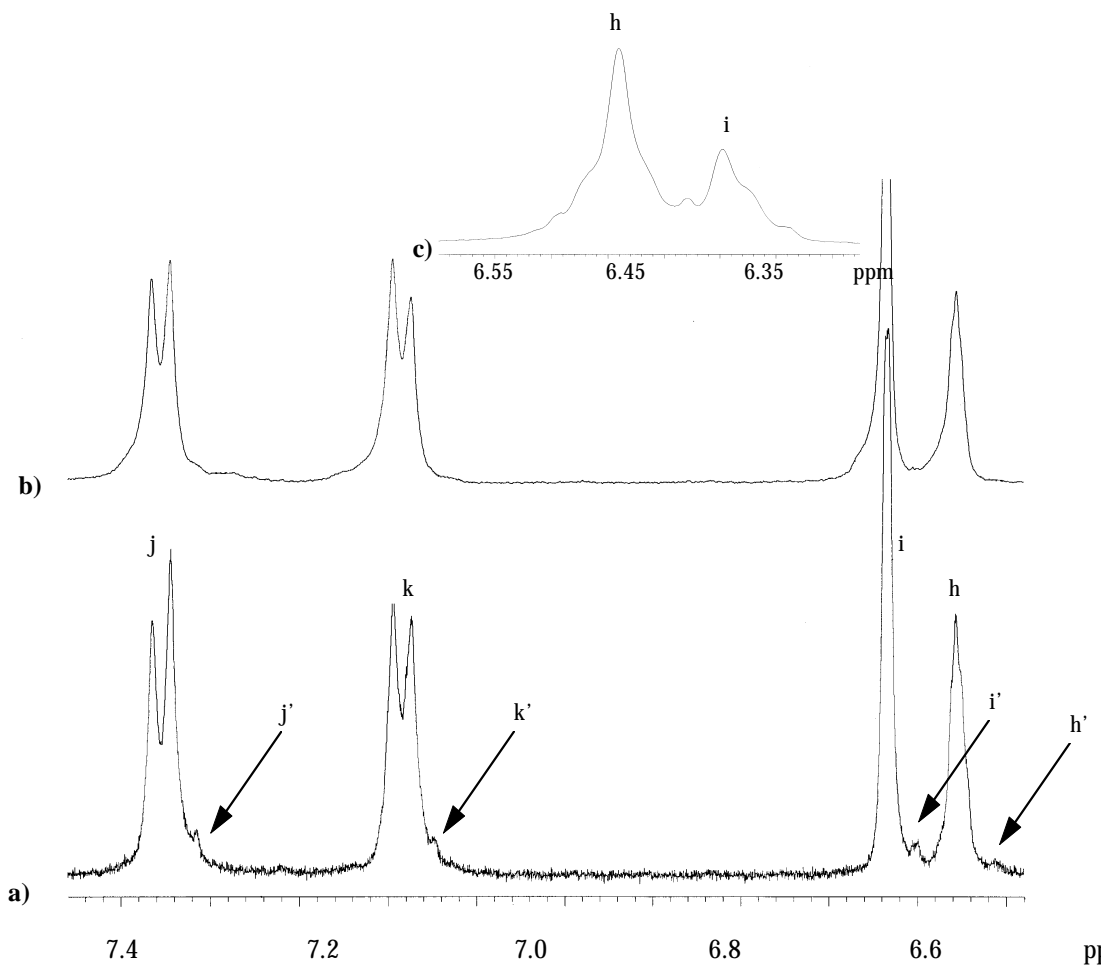
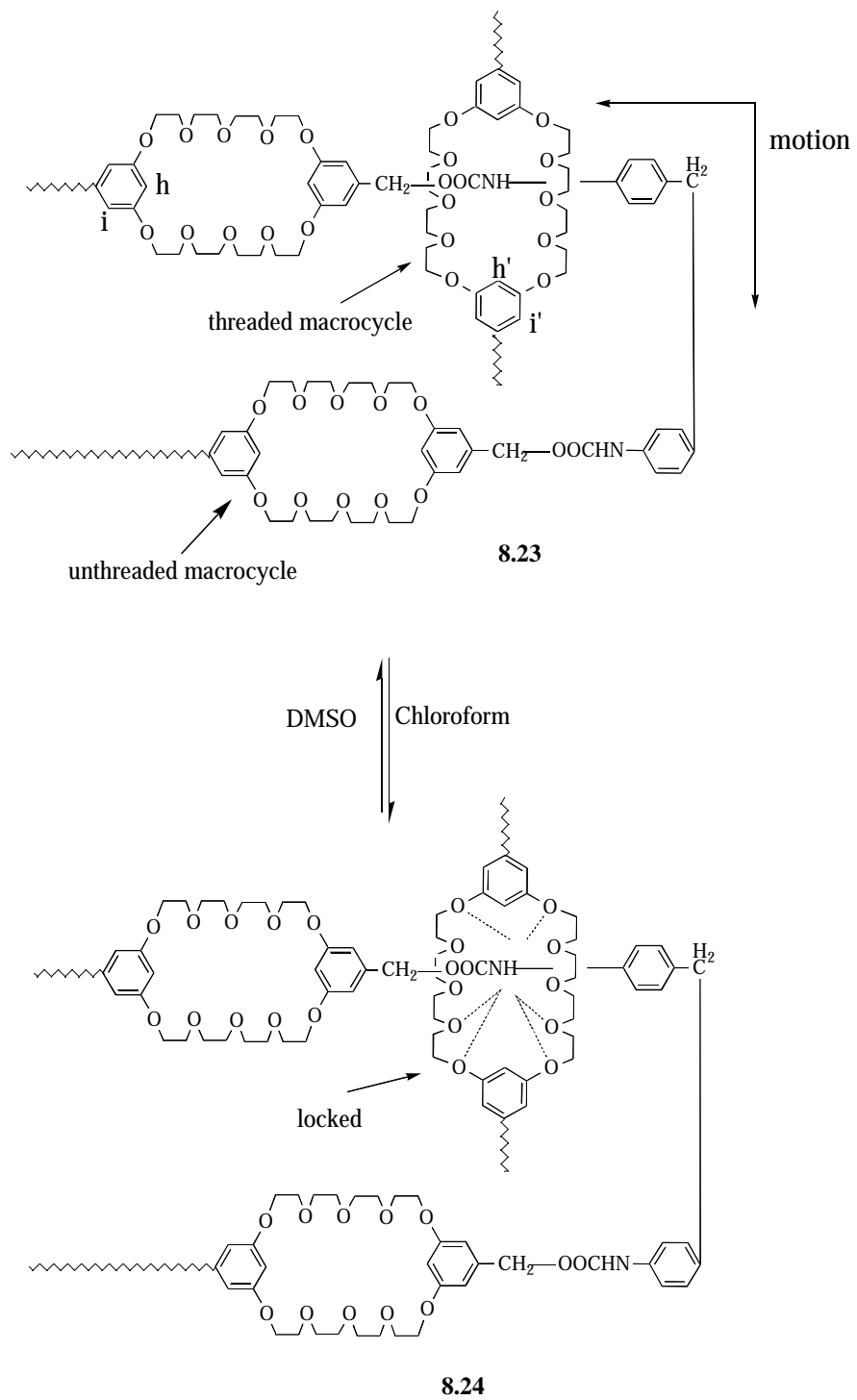


Figure 8.4. The expanded 400 MHz proton NMR spectra of a) 8.14a in DMSO- d_6 , b) 8.14b in DMSO- d_6 and c) 8.14a in CDCl $_3$ (for peak assignments, see Scheme 8.5).

Scheme 8.5



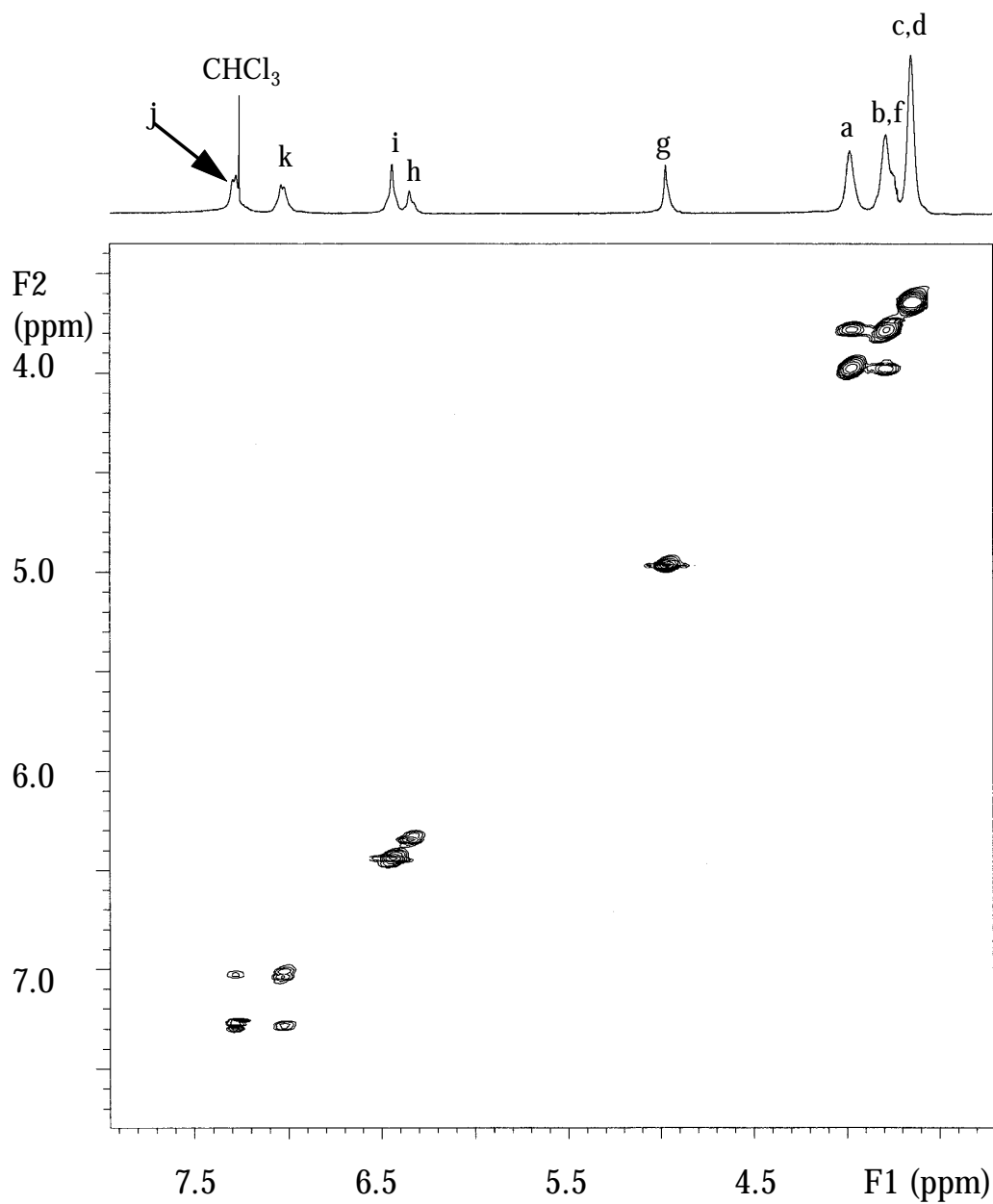


Figure 8.5 The 400 MHz COSY spectrum of 8.14a in CDCl₃ at 26 °C (for peak assignments, see Scheme 8.5).

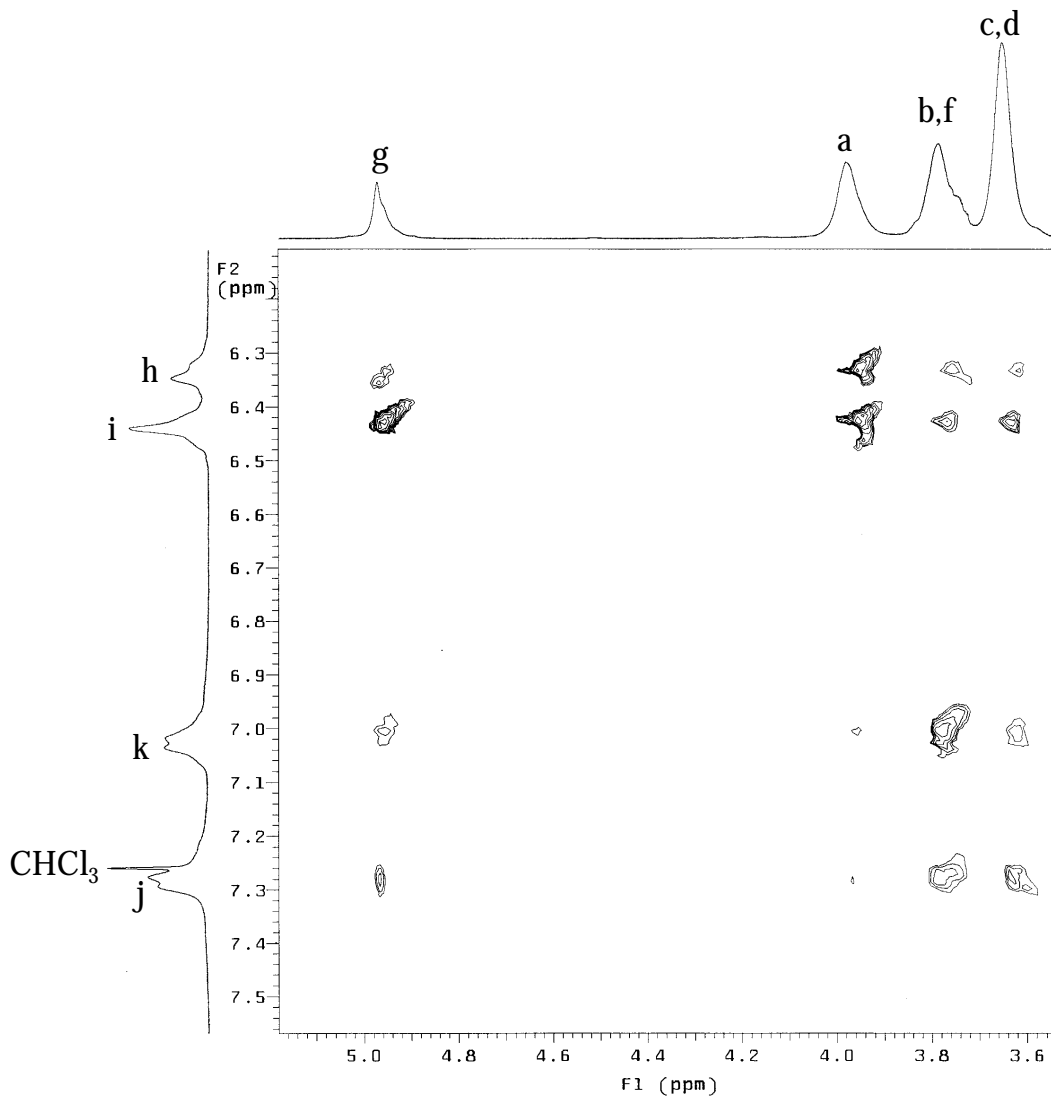


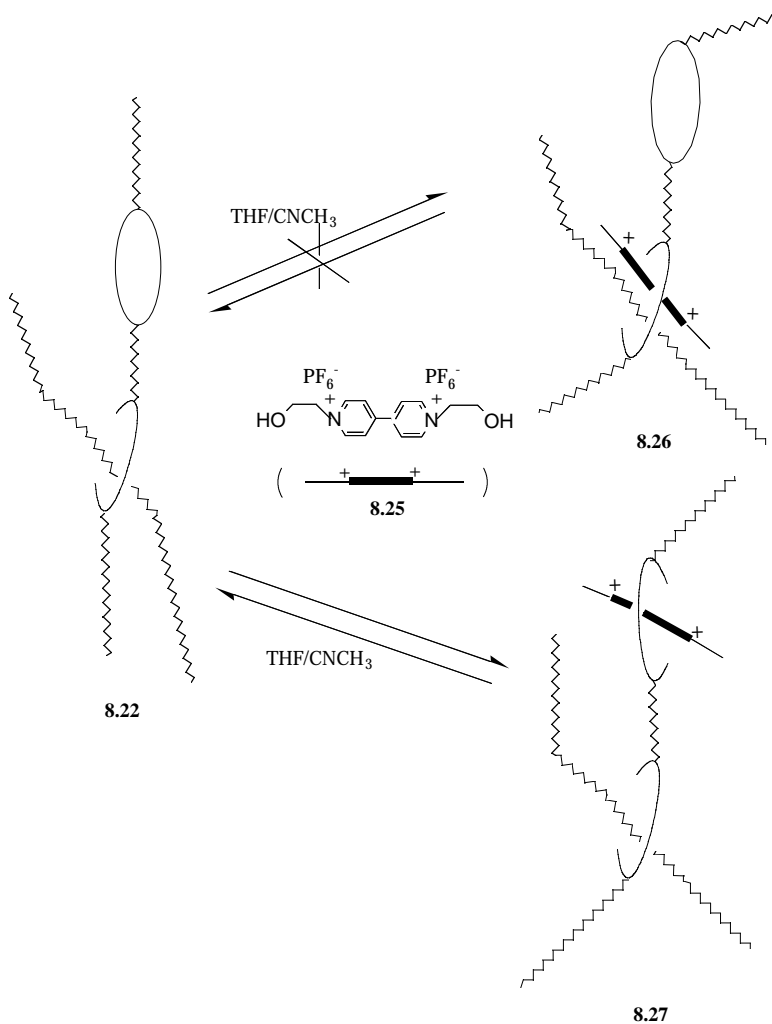
Figure 8.6 The correlated region of 400 MHz NOESY spectrum of 8.14a in CDCl_3 at 26 °C (for peak assignments, see Scheme 8.5)

It is well demonstrated that 4,4'-bipyridinium salts complex with bisphenylene-based crown ethers by charge transfer accompanied by hydrogen bonding and dipole-dipole interactions.^{13,24} Since the complexation between these two components is a fast exchange process, both components display time averaged signals in the proton NMR spectrum.²⁴

²⁴ a) Allwood, B. L.; Spencer, N.; Shahriari-Zavareh, H.; Stoddart, J. F.; Williams, D. J. *J. Chem. Soc., Chem. Commun.* **1987**, 106. b) Asakawa, M.; Ashton, P. R.; Ballardini, R.; Balzani, V.; Belohradsky, M.; Gandolfi, M. T.; Kocian, O.; Prodi, L.; Raymo, F. M.; Stoddart, J. F.; Venturi, M. *J. Am. Chem. Soc.* **1997**, 119, 302.

Recently we prepared new main chain polyrotaxanes by threading *N,N'*-hydroxyethyl-4,4'-bipyridinium 2PF_6^- (**8.25**) through the cavity of in-chain **8.7** units of a poly(ester crown ether).²⁵ Indeed, in this system, the aromatic protons h and i of **8.7** units show time averaged signals shifted upfield relative to the starting polymer.

Scheme 8.6



Therefore, the unthreaded macrocyclic moieties of polyurethane rotaxanes **8.11-8.13** and **8.14a** are expected to complex with **8.25** to afford a pseudorotaxane structure **8.27**, while the threaded units will not have enough room to accommodate **8.25** to produce doubly threaded structure **8.26** (Scheme 8.6). There are no signals from **8.25** in the region of interest

²⁵ Gong, C., Chapter 10.

(Figure 8.7a). In a solution of **8.14a**, a branched rotaxane polymer, and excess **8.25** (Figure 8.7c) major signals h and i were shifted upfield while minor signals h' and i' remained at their original positions relative to **8.14a** itself (Figure 8.7b). Therefore, the signals h' and i' are indeed from self threaded cyclic units, directly proving the formation of mechanically linked (rotaxane) structures of type **8.22** (Scheme 8.4). As expected, **8.14b**, a linear polyurethane, containing no rotaxane branching, i.e., no or only a very small amount of threaded macrocyclic moieties, showed no h' or i' signals after complexation with excess bipyridinium salt (Figure 8.7d).

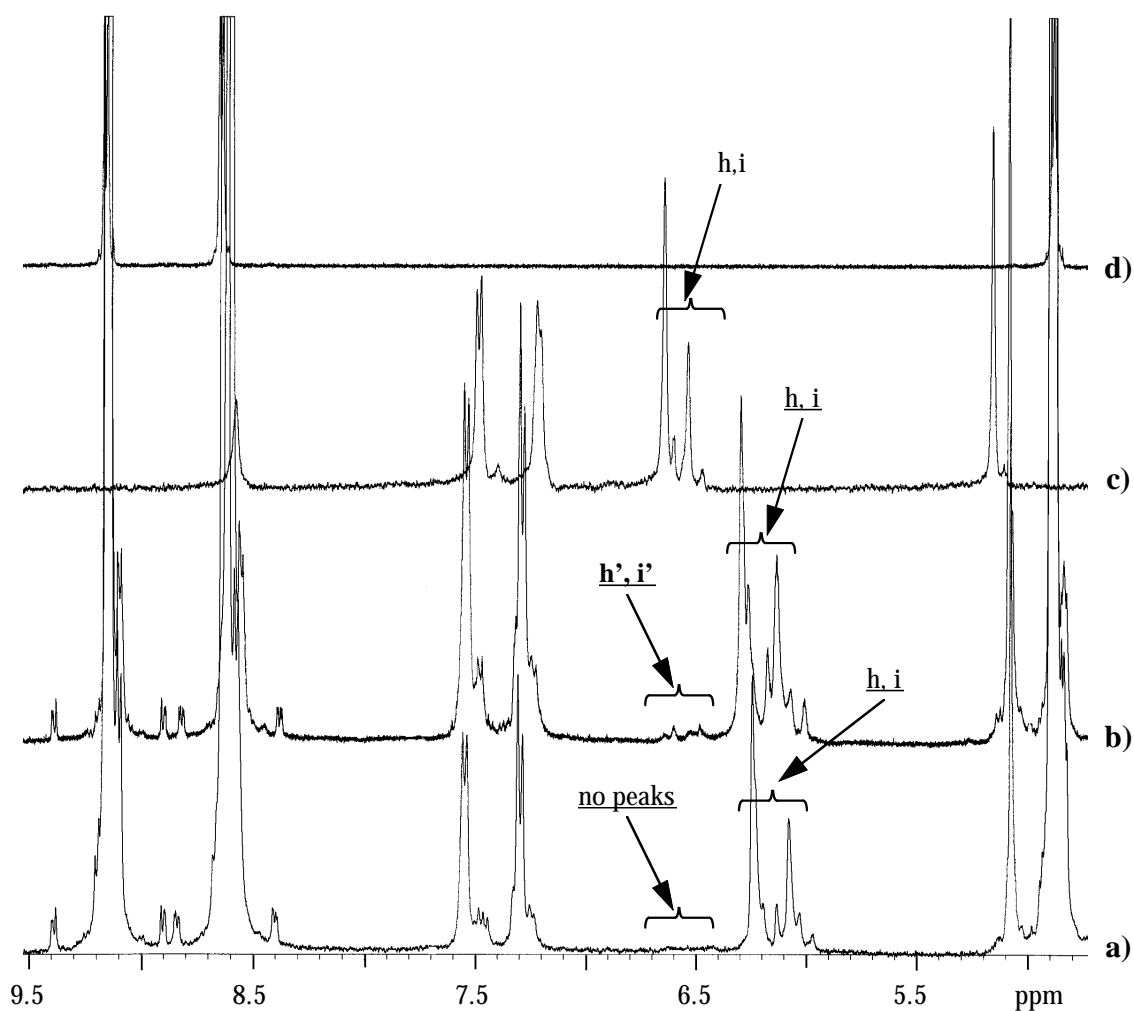


Figure 8.7. The expanded 400 MHz proton NMR spectra of a) **8.25**, b) **8.14a**, c) **8.14a** with excess **8.25** and d) **8.14b** with excess **8.25** in THF-*d*₅/CD₃CN (1:1 by volume) (for peak assignments, see Scheme 8.5).

8.2.5 Thermal properties

All the polyurethanes **8.10-8.13** and **8.14a-c** are amorphous and transparent materials. Since only one glass transition temperature (T_g) (Table 8.2) was observed for each copolyurethane, they are all believed to be random copolymers. The T_g 's of copolyurethanes **8.11-8.13** were between that of homopolyurethane **8.10** (54 °C) and that of homopolymer **8.14a** (66.4 °C). The higher T_g of **8.14a** is attributed to the greater rigidity of macrocycle **8.7** relative to glycol **8.8**. In addition, crosslinked **8.14c** has a T_g higher than those of **8.14a** and **8.14b** because of restricted chain flexibility.

8.3 Conclusions

The present study demonstrated a novel method for the preparation of mechanically linked branched or crosslinked polymers, three dimensional main chain polyrotaxanes. The rotaxane structures were directly proved by complexation studies. More importantly, an approach to control polymeric topology (linear, branched or crosslinked) simply by reaction conditions (solvent or bulk), is provided, i.e., a method to control PDI; this can not be achieved by a classical approach for hyperbranched polymers. In principal, the degree of polymerization can also be adjusted by the feed ratio and the final product may contain no functional groups if monofunctional end-capping agents are used; this level of structural control is again difficult to achieve by a one step approach from AB_x monomers.

The above concept can be used for other condensation polymers, i.e., branched polyesters can be easily prepared by reaction of diacid chlorides with macrocyclic diol **8.7**.^{21b,21f} Since polymer melt viscosity is closely related to topology, i.e., a branched polymer has lower melt viscosity,¹ the present work potentially provides a method to control rheology by adjusting PDI simply by changing the amount of macrocycle **8.7**. In addition, the threaded macrocycle probably can move along the backbone induced by external forces, and thus these polymers are expected to have different mechanical properties, e.g., a higher elongation, compared to chemically bonded branched polymers from classical methods.

8.4 Experimental

General methods

Reagent grade reactants and HPLC or GC grade solvents were used as received from Aldrich except DMSO and diglyme which were dried over sodium hydride and distilled. 4,4'-Bis(2-hydroxyethyl)-N,N'-pyridinium 2PF₆ (**8.25**) was prepared by a well-established procedure.²⁴ ¹H NMR spectra were recorded at ambient temperature on a Varian Unity 400-MHz spectrometer. The NOESY study was performed with a degassed sample at 26 °C with a mixing time of 1 second and relaxation delay of 2 seconds. The absolute molecular weights of the polymers were measured by GPC analyses with a Waters 150C ALC/GPC chromatograph equipped with a differential refractometer detector and an on-line differential viscometric detector (Viscotek 150R) coupled in parallel and the universal calibration was used. The DSC measurements were done with a Perkin Elmer DSC-4 at a scan rate of 10 °C per minute and the data reported here are the midpoints of the transitions in the second heating.

Bis(5-carbomethoxy-1,3-phenylene)-32-crown-10 (**8.6**)

A solution of methyl 3,5-bis(11-chloro-3,6,9-trioxaundecyloxy)benzoate (**8.5**) (7.66 g, 13.7 mmol) and methyl 3,5-dihydroxybenzoate (2.33 g, 13.9 mmol) in DMF (25 ml) was added to a suspension containing K₂CO₃ (19.04 g, 137.7 mmol) and n-Bu₄NI (25 mg) in DMF (800 ml) via syringe pump at the rate of 0.521 ml/hr at 110 °C. After the addition was completed, the mixture was stirred for five days. Then the system was cooled to room temperature. The salt was removed by filtration and solvent by vacuum evaporation. The residue was separated by chromatography with ethyl acetate as eluting solvent. The first fraction was found to be an impurity and the second fraction was the desired product, white solid (3.346 g, 37%, mp: 106.9-107.9 °C, lit.²² 107.2-108.7 °C, 43%). ¹H NMR in CDCl₃: 3.67-3.73 (m, 16H); 3.84 (t, J = 4.8, 8H); 3.87 (s, 6H); 4.10 (t, J = 4.8, 8H), 6.67 (t, J = 2.2, 2H); 7.15 (d, J = 2.2, 4H). ¹³C NMR in CDCl₃: 52.16; 67.83; 69.55; 70.84; 70.91; 106.82; 107.98; 131.79; 159.72; 166.71 (ten peaks as required).

Bis(5-hydroxymethyl-1,3-phenylene)-32-crown-10 (8.7)

To a 250 ml flask was added bis(5-carbomethoxy-1,3-phenylene)-32-crown-10 (**8.6**) (3.10 g, 4.75 mmol) in THF (120 ml). Then 10 ml of LiAlH₄ (10 ml, 1.0 M in THF, 10 mmol) was added to the solution dropwise. The reaction was run for 12 hrs at room temperature. The excess hydride was destroyed by adding ethyl acetate and the solution was diluted with 40 ml of water. Salts were removed by filtration after the system was neutralized with HCl (10 %). The filtrate was extracted with CH₂Cl₂ (3x50 ml). The removal of solvent afforded a white solid which was recrystallized in ethanol to give nice crystals, 2.63 g, 87%; mp: 98.7-99.6 °C, lit.²² 94 %, mp: 99.5-100.4 °C). ¹H NMR in CDCl₃: 1.84 (s, 2H); 3.67-3.84 (m, 16H); 3.83 (t, J = 4.8, 8H); 4.03 (t, J = 4.8, 8H); 4.56 (s, 4H); 6.35 (t, J = 2.2, 2H); 6.49 (d, J = 2.2, 4H). ¹³C NMR in CDCl₃: 65.20; 67.61; 69.70; 70.80; 70.85; 100.89; 105.46; 143.38; 160.03 (9 peaks as required).

Polyurethane 8.10

To a 100 mL flask were added tetra(ethylene glycol) (oven dried at 100 °C) (**8.8**), freshly distilled MDI (**8.9**) and diglyme (Table 8.1). The solution was heated at 96 °C in an oil bath for 7 h. The product was precipitated into a solution of methanol and water (1 L, 1:1) to give a light yellow solid. ¹H NMR (DMSO-d₆, ppm) δ 9.66 (s, 2H, NH), 7.38 (d, 4H, J = 8.3, ArH), 7.10 (d, J = 8.3, 4H, ArH), 4.19 (br s, 4H, OCH₂CH₂(OCH₂CH₂)₂OCH₂CH₂O), 3.79 (s, 2H, ArCH₂Ar), 3.62 (br s, 4H, OCH₂CH₂(OCH₂CH₂)₂OCH₂CH₂O), 3.51 (br s, 8H, OCH₂CH₂(OCH₂CH₂)₂-OCH₂CH₂O).

General Procedure for Copolyurethanes 8.11-8.13

Macrocyclic diol **8.7** and glycol **8.8** were dissolved in anhydrous diglyme (Table 8.1). After the solution was stirred for 0.5 h at 96 °C under the protection of nitrogen, MDI (**8.9**) was added as a solid and reaction proceeded for 7 h. The polymer was precipitated into a mixture of methanol and water (120 mL, 1:1). ¹H NMR (DMSO-d₆, ppm) for **8.11** δ 9.66 (s, 1.5H, NH), 9.44 (s, 0.5H, NH), 7.35 (br s, 4H, ArH), 7.07 (br s, 4H, ArH), 6.52 (br s, 1H, ArH), 6.44 (br s, 0.5H, ArH), 5.00 (s, 1H, ArCH₂O), 4.19 (br s, 3H,

$\text{OCH}_2\text{CH}_2(\text{OCH}_2\text{CH}_2)_2\text{OCH}_2\text{CH}_2\text{O}$), 4.0 (br s, 2H, $\text{ArOCH}_2\text{CH}_2(\text{OCH}_2\text{CH}_2)_2\text{OCH}_2\text{CH}_2\text{OAr}$), 3.78 (br s, 2H, ArCH_2Ar), 3.67 (br s, 2H, $\text{ArOCH}_2\text{CH}_2(\text{OCH}_2\text{CH}_2)_2\text{OCH}_2\text{CH}_2\text{OAr}$), 3.62 (br s, 3H, $\text{OCH}_2\text{CH}_2(\text{OCH}_2\text{CH}_2)_2\text{OCH}_2\text{CH}_2\text{O}$), 3.51 (br m, 10H, $\text{OCH}_2\text{CH}_2(\text{OCH}_2\text{CH}_2)_2\text{-OCH}_2\text{CH}_2\text{O}$ plus $\text{ArOCH}_2\text{CH}_2(\text{OCH}_2\text{CH}_2)_2\text{-OCH}_2\text{CH}_2\text{OAr}$); for **8.12** (Figure 8.1) δ 9.66 (s, 1H, NH), 9.44 (s, 1H, NH), 7.35 (br s, 4H, ArH), 7.07 (br s, 4H, ArH), 6.52 (br s, 2H, ArH), 6.44 (br s, 1H, ArH), 5.00 (s, 2H, ArCH_2O), 4.19 (br s, 4H, $\text{OCH}_2\text{CH}_2(\text{OCH}_2\text{CH}_2)_2\text{OCH}_2\text{CH}_2\text{O}$), 4.0 (br s, 4H, $\text{ArOCH}_2\text{CH}_2(\text{OCH}_2\text{CH}_2)_2\text{OCH}_2\text{CH}_2\text{OAr}$), 3.78 (br s, 2H, ArCH_2Ar), 3.67 (br s, 4H, $\text{ArOCH}_2\text{CH}_2(\text{OCH}_2\text{CH}_2)_2\text{OCH}_2\text{CH}_2\text{OAr}$), 3.62 (br s, 2H, $\text{OCH}_2\text{CH}_2(\text{OCH}_2\text{CH}_2)_2\text{OCH}_2\text{CH}_2\text{O}$), 3.51 (br m, 12H, $\text{OCH}_2\text{CH}_2(\text{OCH}_2\text{CH}_2)_2\text{-OCH}_2\text{CH}_2\text{O}$ plus $\text{ArOCH}_2\text{CH}_2(\text{OCH}_2\text{CH}_2)_2\text{-OCH}_2\text{CH}_2\text{OAr}$); for **8.13** δ 9.66 (s, 0.5H, NH), 9.44 (s, 1.5H, NH), 7.35 (br s, 4H, ArH), 7.07 (br s, 4H, ArH), 6.52 (br s, 3H, ArH), 6.44 (br s, 1.5H, ArH), 5.00 (s, 3H, ArCH_2O), 4.19 (br s, 1H, $\text{OCH}_2\text{CH}_2(\text{OCH}_2\text{CH}_2)_2\text{OCH}_2\text{CH}_2\text{O}$), 4.0 (br s, 6H, $\text{ArOCH}_2\text{CH}_2(\text{OCH}_2\text{CH}_2)_2\text{OCH}_2\text{CH}_2\text{OAr}$), 3.78 (s br, 2H, ArCH_2Ar), 3.67 (br s, 6H, $\text{ArOCH}_2\text{CH}_2(\text{OCH}_2\text{CH}_2)_2\text{OCH}_2\text{CH}_2\text{OAr}$), 3.62 (br s, 1H, $\text{OCH}_2\text{CH}_2(\text{OCH}_2\text{CH}_2)_2\text{OCH}_2\text{CH}_2\text{O}$), 3.51 (br m, 16H, $\text{OCH}_2\text{CH}_2(\text{OCH}_2\text{CH}_2)_2\text{-OCH}_2\text{CH}_2\text{O}$ plus $\text{ArOCH}_2\text{CH}_2(\text{OCH}_2\text{CH}_2)_2\text{-OCH}_2\text{CH}_2\text{OAr}$);

Polyurethanes **8.14a** and **8.14b**.

Macrocyclic diol **8.7** was dissolved in anhydrous diglyme for **8.14a** and anhydrous DMSO for **8.14b** (Table 8.1). After the solution was stirred for 0.5 h at 96 °C under the protection of nitrogen, MDI (**8.9**) was added slowly as a solid and polymerization was allowed to proceed for 7 h. The polymer solution was precipitated into a mixture of methanol and water (120 mL, 1:1). ^1H NMR (DMSO- d_6 , ppm) for **8.14b** δ 9.64 (s, 2H, NH), 7.35 (d, 2H, $J = 8.3$, ArH), 7.07 (d, $J = 8.3$, 2H, ArH), 6.52 (br s, 4H, ArH), 6.44 (br s, 2H, ArH), 5.00 (s, 4H, ArCH_2O), 4.0 (br s, 8H, $\text{ArOCH}_2\text{CH}_2(\text{OCH}_2\text{CH}_2)_2\text{OCH}_2\text{CH}_2\text{OAr}$), 3.76 (s, 2H, ArCH_2Ar), 3.67 (br s, 8H, $\text{ArOCH}_2\text{CH}_2(\text{OCH}_2\text{CH}_2)_2\text{OCH}_2\text{CH}_2\text{OAr}$), 3.51 (br m, 16H, $\text{OCH}_2\text{CH}_2(\text{OCH}_2\text{CH}_2)_2\text{-OCH}_2\text{CH}_2\text{O}$).

Polyurethane 8.14c

Macrocyclic diol **8.7** was melted at 120 °C and then cooled to 96 °C. Before **8.7** solidified, MDI (**8.9**) was added as a solid (Table 8.1) and after the transparent solution had stirred for 2 h at this temperature, stirring stopped. Polymerization was continued for 5 h and the polymer was poured out before it solidified. No detectable amount of soluble product was obtained by extracting with DMF.

Chapter 9

Poly(arylene ether/“42C14” rotaxane)s

9.1 Introduction

A polyrotaxane,¹⁻¹¹ a polymer bearing rotaxane units, often exhibit different properties from its starting polymer, e.g., higher intrinsic viscosity,^{5d} lower melt viscosity,^{5d} different thermal properties^{2-4,5,7} and solubility,^{7c} depending on both the threading efficiency (m/n, average number of cyclics per repeat unit) and the chemical composition of the threaded cyclic. For example, cyclodextrins (CD) are rigid cyclics and the polymer can be

¹ (a) Gibson, H. W.; Bheda, M. C.; Engen, P. T. *Prog. Polym. Sci.* **1994**, *19*, 843-945. (b) Amabilino, D. B.; Stoddart, J. F. *Chem. Rev.*, **1995**, *95*, 2725-2828. (c) Philp, D.; Stoddart, J. F. *Angew. Chem. Int. Ed. Engl.* **1996**, *35*, 1154-1196. (d) Gibson, H. W. in *Large Ring Molecules*; Semlyen, J. A., ed.; J. Wiley and Sons: New York, **1996**, 191-262. (e) Gong, C.; Gibson, H. W. *Current Opinion in Solid State and Materials Science* **1998**, *2*, in press.

² (a) Wenz, G. *Macromol. Symp.* **1994**, *87*, 11-16. (b) Weickenmeier, M.; Wenz, G. *Macromol. Rapid Commun.* **1996**, *17*, 731-736. (c) Steinbrunn, M. B.; Wenz, G. *Angew. Chem. Int. Ed. Engl.* **1996**, *35*, 2139-2142. (d) Herrmann W.; Keller, B.; Wenz, G. *Macromolecules* **1997**, *30*, 4966.

³ (a) Born, M.; Ritter, H. *Angew. Chem. Int. Ed. Engl.* **1995**, *107*, 342-345. (b) Born, M.; Ritter, H. *Angew. Chem. Int. Ed. Engl.* **1995**, *34*, 309-311. (c) Born, M.; Ritter, H. *Adv. Mater.* **1996**, *8*, 149-151. (d) Noll, O.; Ritter, H. *Macromol. Rapid Commun.* **1997**, *18*, 53.

⁴ (a) Harada, A.; Li, J.; Kamachi, M. *Nature* **1994**, *370*, 126-129. (b) Harada, A.; Li, J.; Kamachi, M. *Macromolecules* **1994**, *27*, 4538-4543. (c) Harada, A.; Okada, M.; Li, J.; Kamachi, M. *Macromolecules* **1995**, *28*, 8406-8411. (d) Harada, A.; Li, J.; Kamachi, M. *J. Chem. Soc., Chem. Commun.* **1997**, 1413-1414.

⁵ (a) Gibson, H. W.; Marand, H. *Adv. Mater.* **1993**, *5*, 11-21. (b) Shen, Y. X.; Xie, D.; Gibson, H. W. *J. Am. Chem. Soc.* **1994**, *116*, 537-548. (c) Gibson, H. W.; Liu, S.; Lecavalier, P.; Wu, C.; Shen, Y. X. *J. Am. Chem. Soc.* **1995**, *117*, 852-874. (d) Gibson, H. W.; Liu, S.; Gong, C.; Ji, Q.; Joseph, E. *Macromolecules* **1997**, *30*, 3711-3727.

⁶ (a) Gong, C.; Gibson, H. W. *Macromolecules* **1996**, *29*, 7029-7033. (b) Gong, C.; Gibson, H. W. *Macromol. Chem. Phys.* **1997**, *198*, 2321-2322. (c) Gong, C.; Gibson, H. W. *J. Am. Chem. Soc.* **1997**, *119*, 5862-5866. (d) Gong, C.; Gibson, H. W. *J. Am. Chem. Soc.* **1997**, 8585. (e) Gong, C.; Ji, Q.; Glass, T. E.; Gibson, H. W. *Macromolecules*. **1997**, 4807.

⁷ a) Gong, C.; Gibson, H. W. *Angew. Chem. Int. Ed. Engl.* **1997**, in press. b) Gong, C.; Glass, T. E.; Gibson, H. W. *Macromolecules*, accepted. c) Gong, C.; Gibson, H. W. *Angew. Chem. Int. Ed. Engl.*, accepted.

⁸ Marand, E.; Hu, Q.; Gibson, H. W.; Veytsman, B. *Macromolecules* **1996**, *29*, 2555-2562.

⁹ Gibson, H. W.; Liu, S.; Shen, Y. X.; Bheda, M. C.; Lee, S.-H.; Wang, F. *NATO ASI Series*, Kluwer Acad. Pub., Dordrecht, the Netherlands, **1995**, Series C, Vol. 456, 41--58.

¹⁰ (a) Mason, P. E.; Parsons, I. W.; Tolley, M. S. *Angew. Chem. Int. Ed. Engl.* **1996**, *35*, 2238-2241.

¹¹ Owen, J.; Hodge, P. *J. Chem. Soc., Chem. Commun.* **1997**, 11-12.

rigidified by threading CD to afford a higher glass transition temperature.²⁻⁴ On the other hand, crown ethers with T_g at about -60 °C are flexible and the derived polyrotaxanes had lower T_g than the corresponding backbone.^{5b}

Crown ether-based polyrotaxanes have been successfully prepared with different backbones, e.g., polyester,^{5a,5c,5d,6a,6c,6e} polyamide,¹² polyurethane^{5b,6d,7} and poly(methacrylate)^{6c} using the crown ether as solvent or monomer. The hydrogen bonding between the crown ether and the acid protons, e.g., OH and NH groups, is proposed as the driving force for threading.⁶⁻⁷ It was reported that crown ethers can complex with metal ions, e.g., K^+ and Na^+ .¹³ Therefore, crown ethers are expected to effectively thread onto poly(arylene ether) backbones because a potassium phenoxide is a reaction intermediate during polymerization of dihalides and diphenols if K_2CO_3 is used as base.¹⁴ The idea was tested using “42C14” and 30C10 as the cyclics and the results are reported in this Chapter.

9.2 Results and Discussion

9.2.1 “42C14”

“42C14” was synthesized first by a well-reported procedure,¹⁵ that is 2+2 combination of tetra(ethylene glycol) and hexa(ethylene glycol) ditosylate under a pseudo-dilute condition. To remove the hydroxy-terminated PEO, the product was treated with poly(methacryloyl chloride) and further purified by recrystallization in acetone. It has been believed to be a single sized macrocycle (42-membered) because of its narrow melting range and the absence of end groups of linear PEO as proved by NMR. However, these evidences do not rule out the existence of other-sized crown ethers.

¹² Bheda, M. C. *Ph.D. Dissertation*, Virginia Polytechnic Institute and State University, 1992.

¹³ Yakshin, V. V.; Abashkin, V. M.; Laskprin, B. N. *Dokl. Chem. Proc. Acad. Sci. USSR (Engl. Trans.)* **1979**, 224, 27.

¹⁴ May, R. *Encyclopedia of Polymer Science and Engineering*, 2nd ed.; J. Wiley and Sons: New York, 1987, Vol 12, pp313.

¹⁵ Gibson, H. W.; Bheda, M. C.; Engen, P. T.; Shen, Y. X.; Sze, J.; Zhang, H.; Gibson, M. D.; Delaviz, Y.; Lee, S.-H.; Wang, F.; Nagvekar, D.; Rancourt, J.; Taylor, L. T. *J. Org. Chem.* **1994**, 59, 2186.

Not until recently was high performance liquid chromatography (HPLC) successfully used to characterize the true compositions of large crown ethers, i.e., “42C14”, “48C16” and “60C20”; the detailed conditions were developed by Xie et al.¹⁶ 30C10 is single sized as proved by its X-ray crystal structure and mass spectroscopy.¹⁷ Its HPLC trace (Figure 9.1) had only one peak in addition to a hydrate peak which appeared in all HPLC traces for different crown ethers.¹⁶ However, for “42C14” from 2+2 combination (Figure 9.1), various peaks were observed under identical conditions and thus proved to be a mixture of various ring sizes. The GPC and mass study also confirmed the fact that this product is a mixture.¹⁸

An 1+1 approach is employed to synthesize pure 42C14 (Scheme 9.1). The precursors, hepta(ethylene glycol) (**9.3**) and hepta(ethylene glycol) ditosylate (**9.4**) were prepared by the methods reported by Erik M. D. Keegstra et al.²⁰ Then equal moles of **9.3** and **9.4** in THF were slowly added to a suspension of THF and NaH using a syringe pump to achieve a high dilute condition to favor the cyclization. The reaction was kept at room temperature to reduce side reactions such as elimination.

¹⁶ Xie, D. *Ph.D. Dissertation*, Virginia Virginia Polytechnic Institute and State University, 1997

¹⁷ Bheda, M. C.; Merola, J. S.; Woodward, W. A.; Vasudevan, V. J.; Gibson, H. W. *J. Org. Chem.* **1994**, *59*, 1684.

¹⁸ “42C14” was prepared by a reported procedure.¹⁵ The detailed GPC study by Prof. Colin Booth and colleagues at the University of Manchester (U.K.) showed it to contain rings up to 400 or so atoms, i.e., ~130 repeat units. MALDI-TOF MS indicates that the largest ring detected was (CH₂CH₂O)_n, n = 142 with MW = 6248; the largest signal corresponded to n = 30, MW = 1320. We thus use quotation marks around the name to designate the size of the crown ether that was the target of the synthesis procedure¹⁵ developed previously, rather than its true size.^{5b-d,15,19}

¹⁹ Lee, S.-H. *Ph.D. Dissertation*, Virginia Virginia Polytechnic Institute and State University, 1997

²⁰ Keegstra, E. M. D.; Zwikker, J. W.; Roest, M. R.; Jenneskens, L. W. *J. Org. Chem.*, **1992**, *57*, 6678.

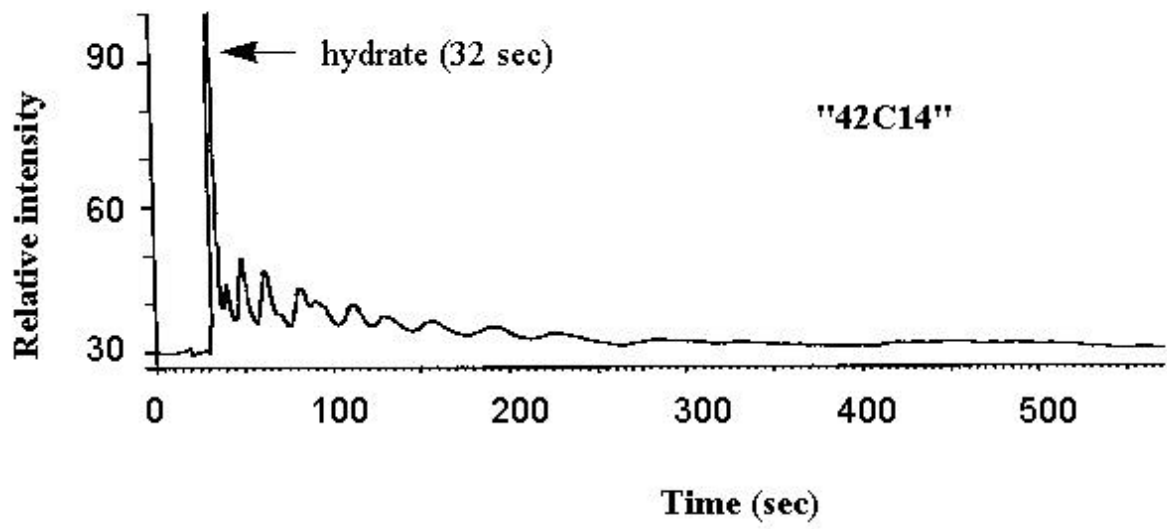
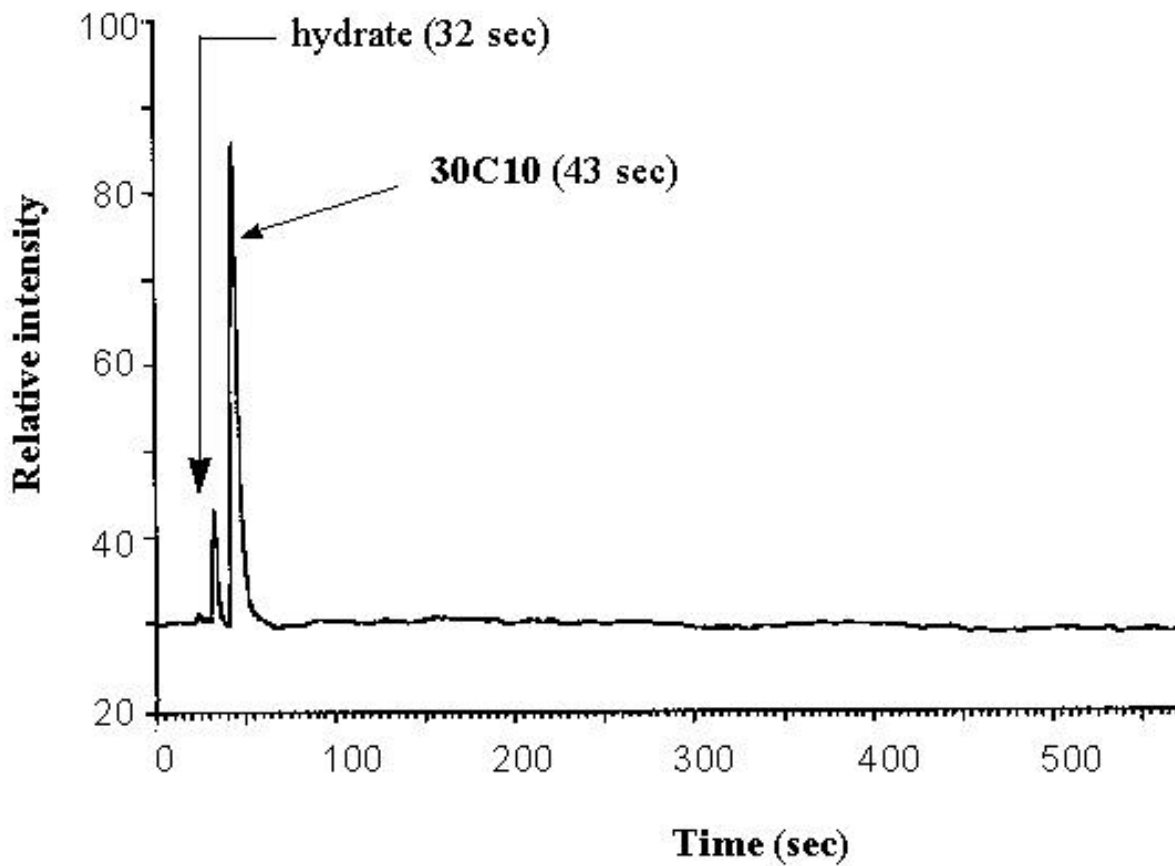
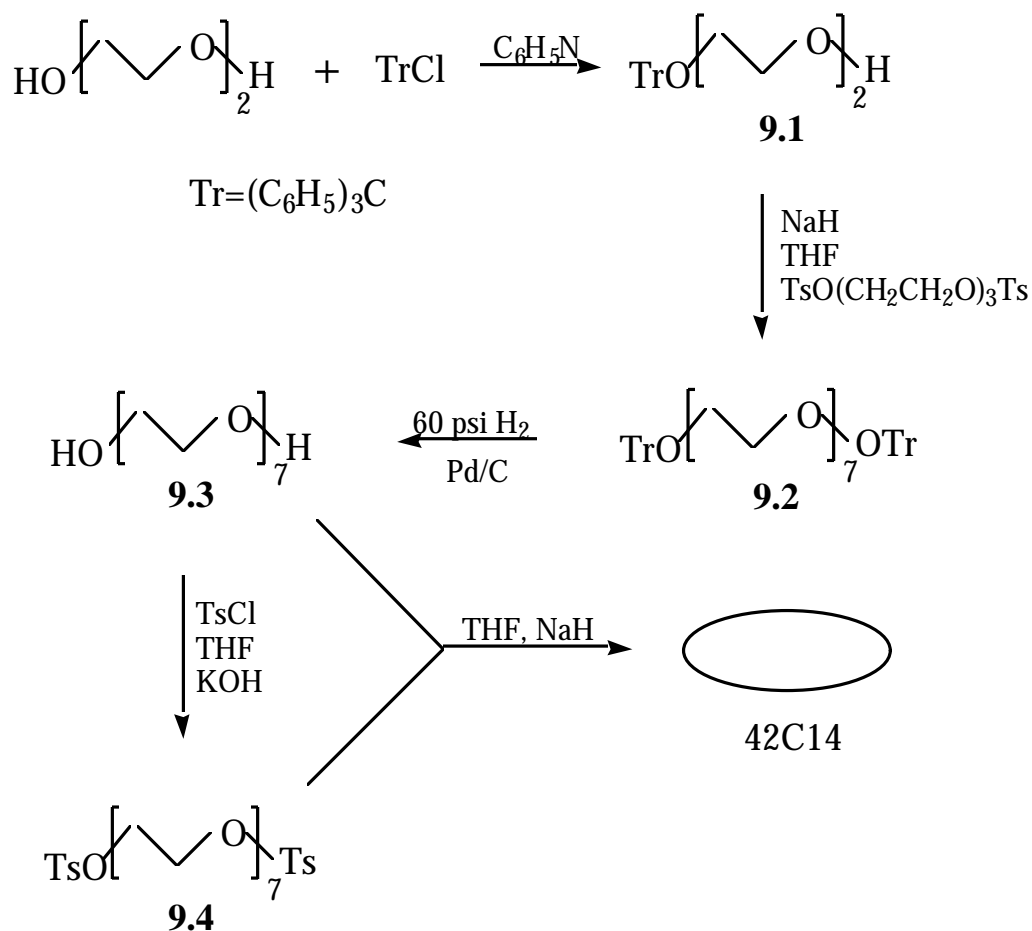


Figure 9.1. RP-HPLC traces of 30C10 and "42C14" by 2+2 combination (C18, 70/30 water/acetonitrile, 2 mL/min, RI detector).

Different from that of previous “42C14”, its HPLC trace (Figure 9.2) has a major peak (80 %). The LC-Mass (616, molecular ion) confirmed that the peak is indeed from 42C14. Therefore, this new procedure is effective for the preparation of single sized large sized (>32) crown ethers. However, it involves multiple steps and purification of the product by chromatography and/or recrystallization using various solvents was not successful.

Scheme 9.1



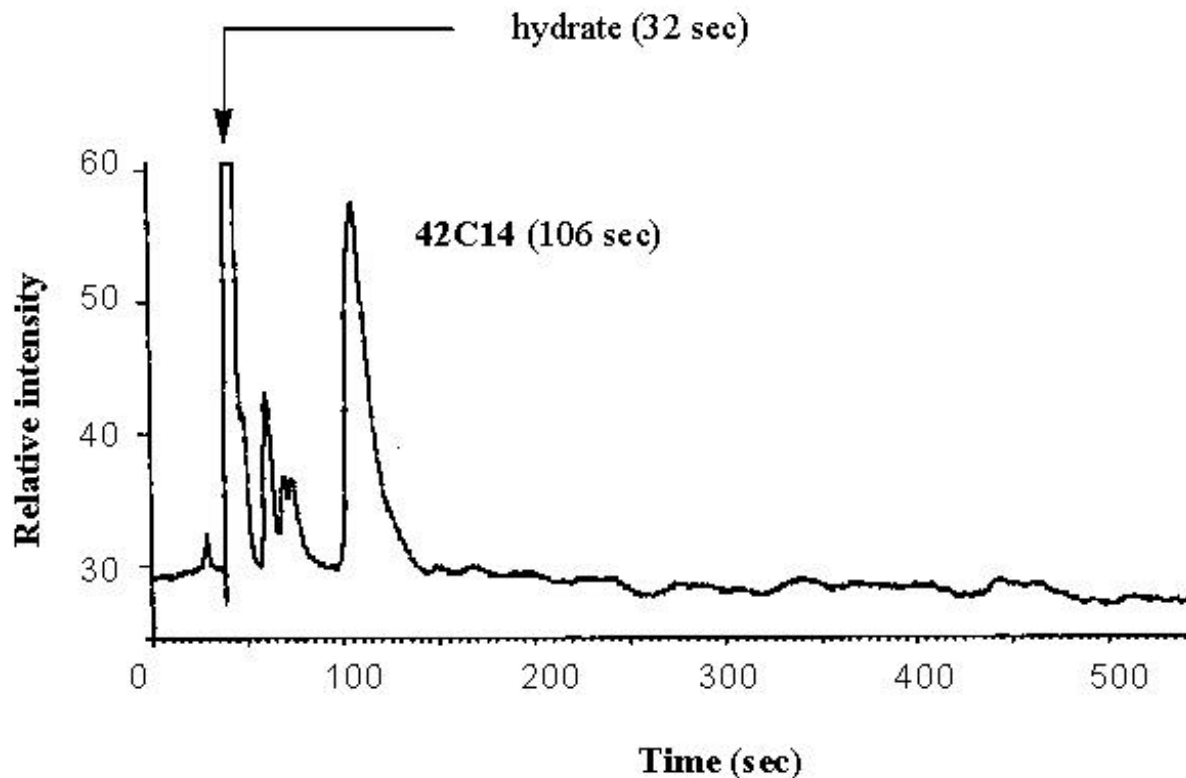


Figure 9.2. RP-HPLC trace of 42C14 by 1+1 combination (C18, 70/30 water/acetonitrile, 2 mL/min, RI detector).

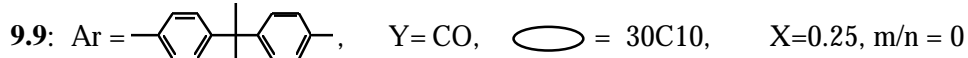
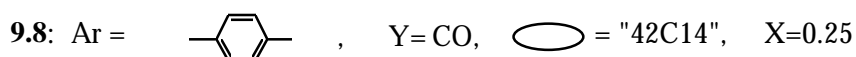
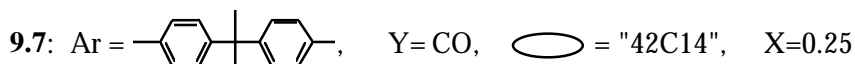
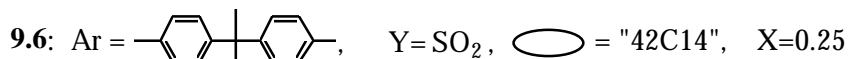
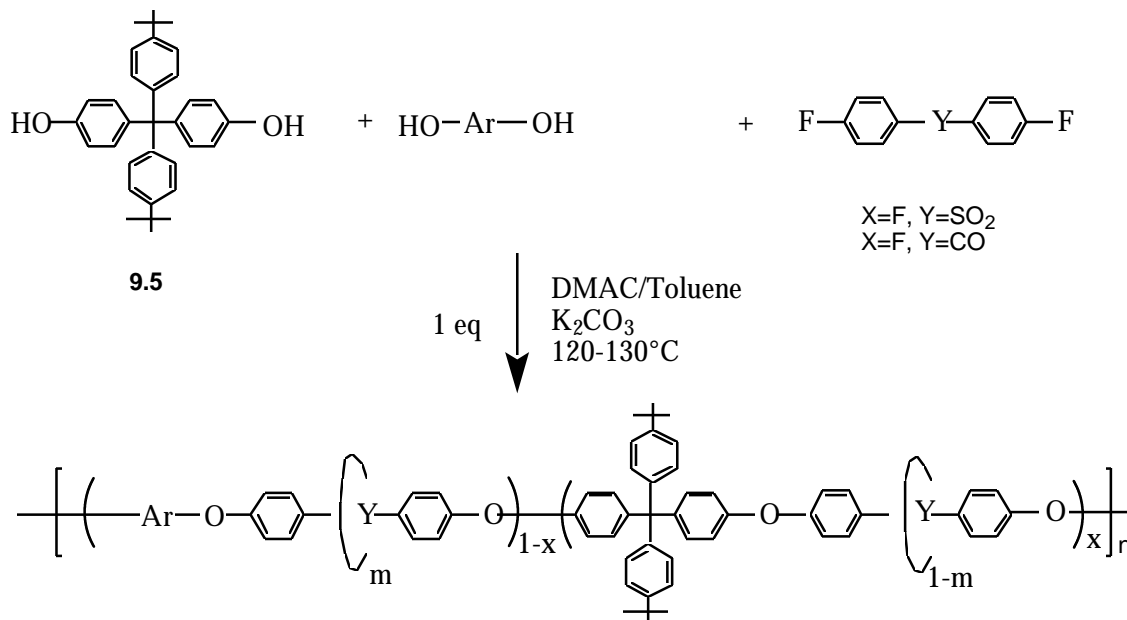
9.2.2 Poly(ether sulfone/"42C14" rotaxane) (9.6), poly(ether ketone/"42C14" rotaxane) (9.7), poly(ether ether ketone/"42C14" rotaxane) (9.8) and poly(ether ketone/30C10 rotaxane) (9.9).

i. Preparation and purification.

Poly(arylene ether/"42C14" rotaxane)s **9.6**, **9.7** and **9.8** were prepared by aromatic nucleophilic substitution reactions between bisphenols (diol BG **9.5**, bisphenol-A or hydroquinone) and difluorides in the presence of K_2CO_3 and "42C14" (Scheme 9.2). The reaction temperature was controlled at 130 ± 5 °C and water was removed by azeotropic refluxing of a mixture of toluene and N,N-dimethylacetamide (DMAc). The feed ratios of the crown ether vs. the total diol, "42C14" for **9.6**, **9.7**

and **9.8** or 30C10 for **9.9** were kept at 1:1. Both **9.6** and **9.7** were soluble throughout the reaction period. However, polyrotaxane **9.8** started to precipitate after 2 hrs due to its poor solubility despite threaded “42C14”.

Scheme 9.2



For polyrotaxanes **9.6**, **9.7** and **9.9**, the unthreaded “42C14” or 30C10 were removed by precipitation into water, a solvent poor for the backbones but good for “42C14”. For polyrotaxane **9.8**, while no precipitation can be performed, most of unthreaded “42C14” remained in the reaction solution and thus were removed by

simple filtration. In order to remove other free “42C14” probably trapped in polymer, the product was further purified by milling and washing with water.

ii. Characterization

It was demonstrated that free crown ether can be detected by GPC measurement provided that the retention volumes for polymer and the crown ether are well separated.^{6c} However, the molecular weights of polyrotaxanes **9.6** and **9.7** (Figure 9.3a and b) were low and close to that^{5b} of “42C14” (Figure 9.3c) and thus **9.6** or **9.7** can not be simply proved to be free of “42C14” by their GPC.¹⁶ The tail at high retention volume in GPC traces of **9.6** and **9.7** may be from the low molecular mass aromatic cyclics formed during polymerization or residual “42C14” trapped in polymer.¹⁶

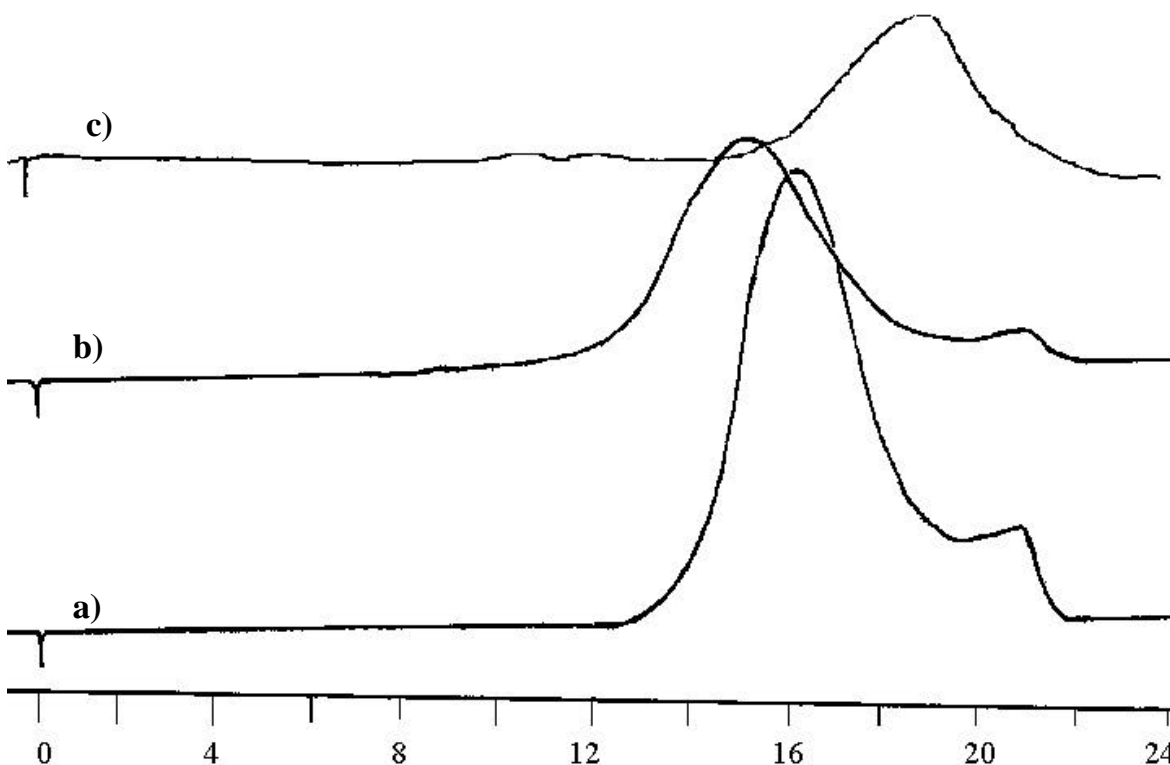


Figure 9.3 The GPC traces of a) polyrotaxane **9.7**, b) polyrotaxane **9.6** and c) “42C14”^{5b} in CHCl₃ (flow rate = 1 mL/min., RI detector).

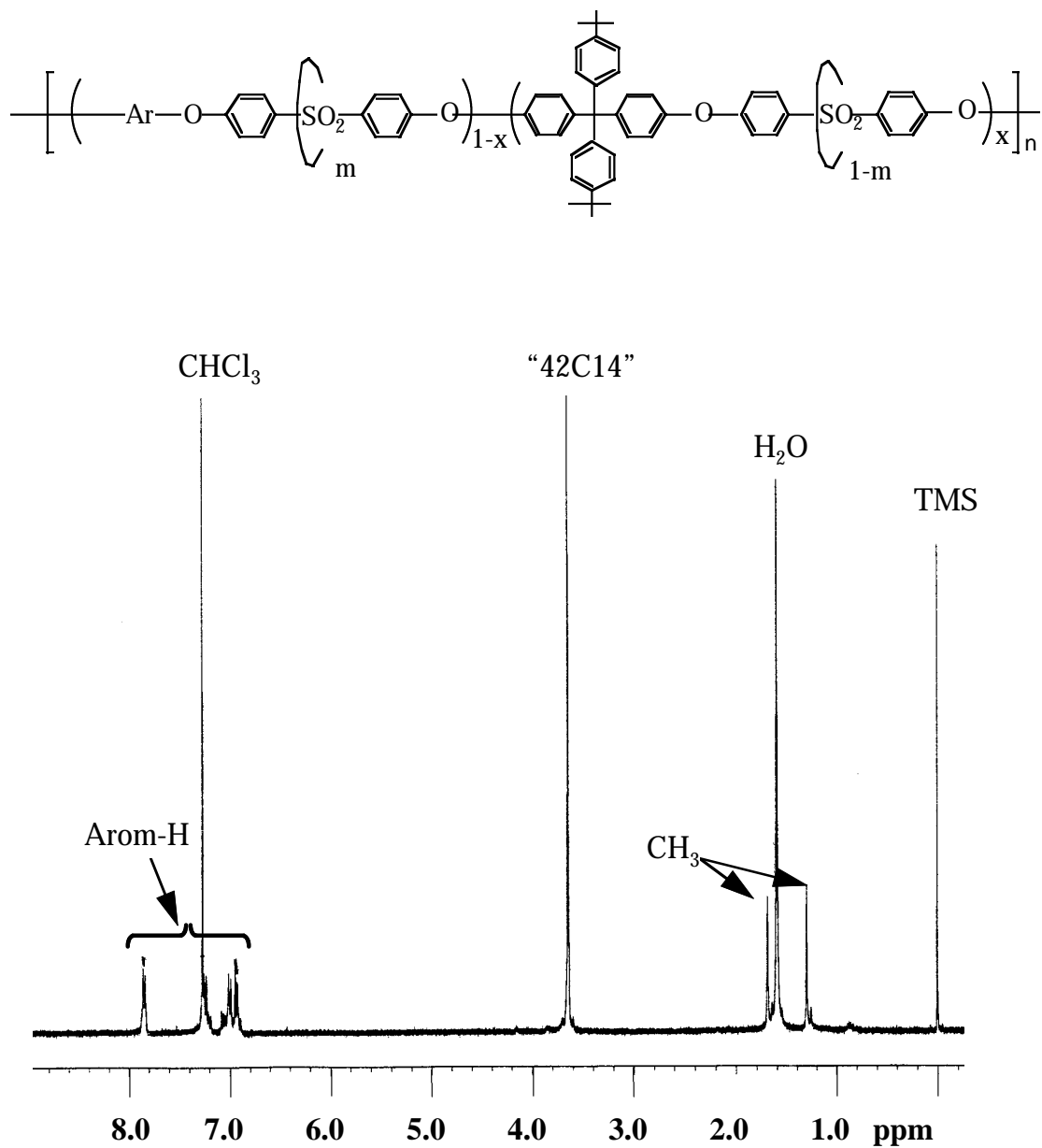


Figure 9.4 400 MHz proton NMR spectrum of poly(ether sulfone/"42C14" rotaxane) **9.6** in CDCl₃

As shown in their proton NMR spectra (Figure 9.4 for **9.6** and Figure 9.5 for **9.7**), "42C14" indeed existed in these materials as manifested by the signal at 3.65 ppm. However, no chemical shift change was observed while 30C10 in polyester and polyurethane rotaxane was shifted upfield if BG was used.⁶ It is known that the

chemical shift change is caused by through-space interaction of the protons close to each other.⁶ Since “42C14” is a mixture the threaded crown ether is much larger than 30C10 as proved by the fact that 30C10 can not be threaded for **9.9**. The large size increases the distance between backbone and the cyclics and thus surely weakens through-space interaction; this explains why there were no chemical shift changes in polyrotaxanes **9.6** and **9.7**. According to the integrals in proton NMR, the threading efficiencies of polyrotaxane **9.6** and **9.7** were calculated (Table 9.1).⁶

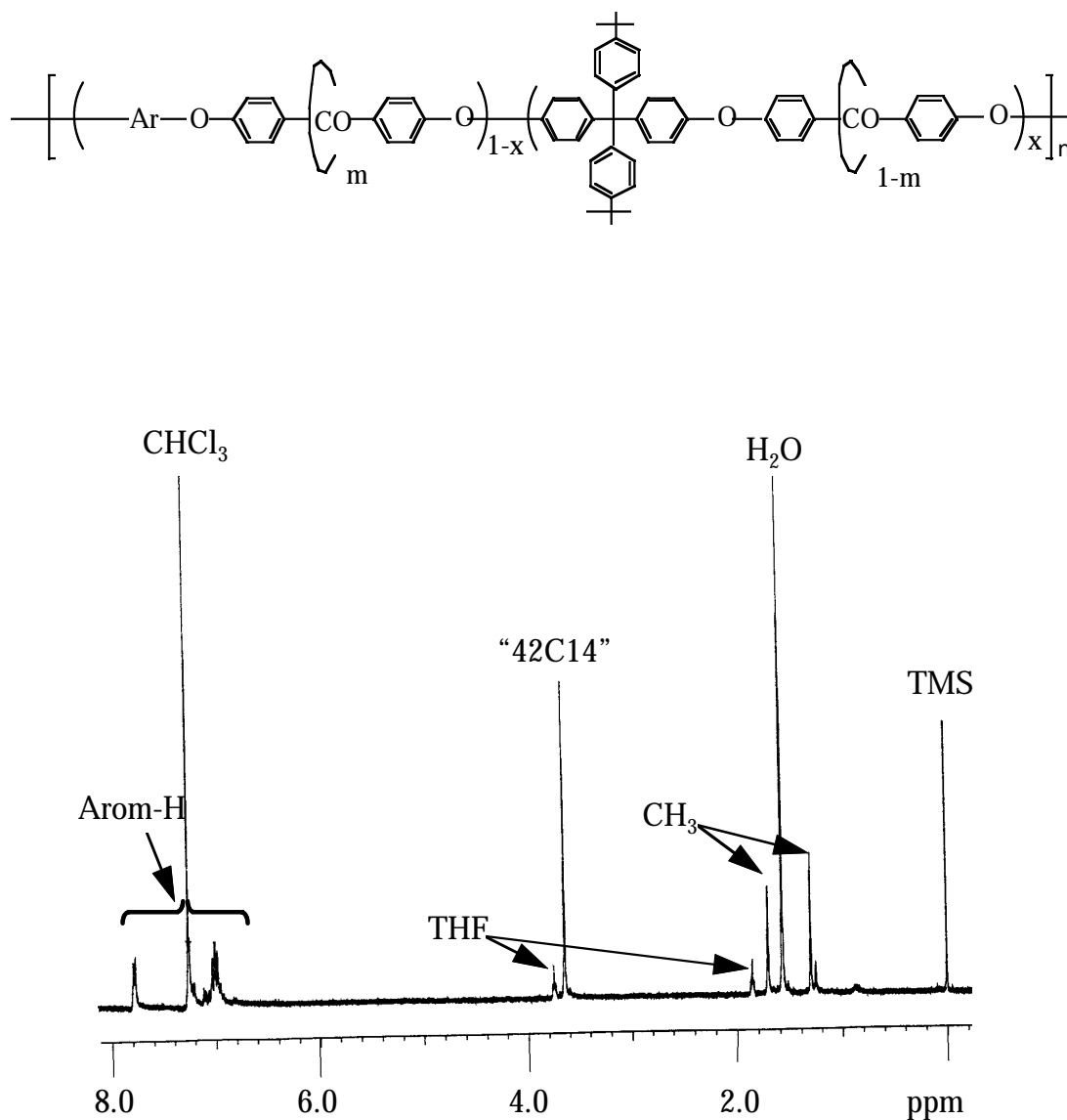


Figure 9.5 400 MHz proton NMR spectrum of poly(ether ketone/“42C14” rotaxane) **9.7** in CDCl₃

Table 9.1 The threading efficiencies of polyrotaxanes **9.6-9.9**

Product	m/n ^c			wt% of cyclic
	1st ppt	2nd ppt	3rd ppt	
9.6 ^a	0.31	0.28	0.22	22
9.7 ^a	0.39	0.14	0.16	18
9.8 ^b	>0	>0	>0	>0
9.9 ^a	0	0	0	0

a) precipitation into water 3 times.

b) Filtration of the polymerization solution to afford **9.9** and then further purification by milling and washing with water 3 times (stirring in water for 24 hrs)

c) Calculated based on MW of 616 for “42C14”.

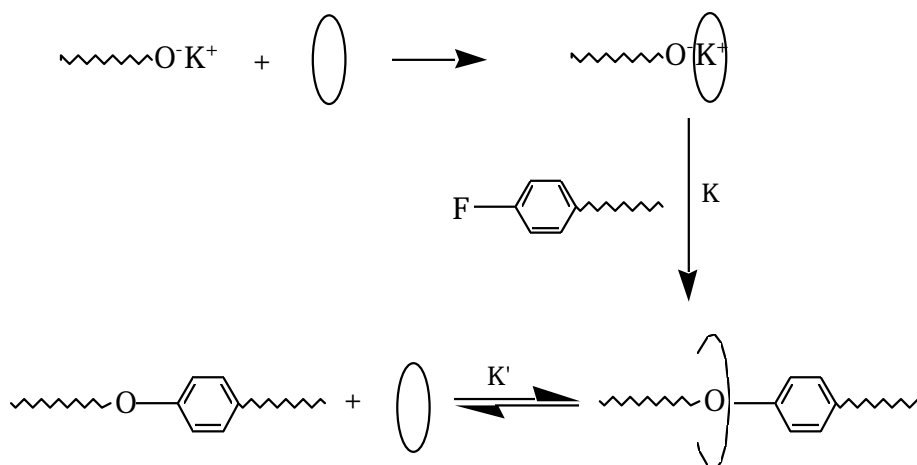
In terms of polyrotaxane synthesis with 30C10 as the cyclic, it is unsuccessful because for **9.9**, after purification no 30C10 was detected in its proton NMR spectrum. However, this was very useful in terms of characterization of **9.6** and **9.7**. No threading for **9.9** proved i) that no side reactions, e.g., ring opening, were responsible for the threading in **9.6**, **9.7**, and **9.8** and ii) the employed purification methods can effectively remove unthreaded crown ethers. Thus the detected crown ethers for the polyrotaxanes **9.6** and **9.7** are not simple mixtures or copolymer segments but indeed threaded onto the backbones. A similar model study was also done by Xie with 18C6, giving the exact same results.¹⁶

Because **9.8** was insoluble in any common solvent, the existence of “42C14” after purification could not be simply detected by solution state NMR but indeed detected in solid state NMR as discussed later in this chapter.

In the experimental procedure, the cyclic concentration is low. Significant threading (Table 9.1) can only be attributed to the possible strong complexation between K⁺ and “42C14” (Scheme 9.3).¹³ 30C10 was not threaded probably due to its small ring size. Similar to polyester backbones,⁶ polyrotaxanes **9.6** and **9.7** have no specific retaining force for threaded crown ether. Thus the threading efficiencies

for **9.6** and **9.7** are expected to be higher than those without BG because BG can mechanically confine the threaded crown ether and decrease dethreading during polymerization.⁶ However, the threading efficiencies of **9.6** and **9.7** are only slightly higher than those¹⁶ without BG; this is probably because BG units can only block the macrocycles smaller than 42-membered rings while most of the crown ethers from threaded “42C14” are probably greater than that size.¹⁸

Scheme 9.3



iii. Solid State NMR

The polymer properties are always related to its molecular motion, e.g., the glass transition temperature resulting from relaxation of local chain. Since a polyrotaxane is essentially a molecular composite consisting of threaded cyclic and the backbone, the motions of both components under certain conditions are very important in terms of understanding its properties.

Solid state NMR is a very useful technique for detection of such molecular motion.²¹ ¹³C NMR in the solid state is usually recorded with magic-angle spinning (MAS) in two ways, cross-polarization (CP) and direct-polarization (DP). In CP ¹³C MAS, the proton is first hit by radio frequency (rf) and the magnetization is transferred to the carbons via static dipolar interaction in a CP period. The relaxation of protons is very fast and thus all carbons of the measured sample are detected. In

²¹ Beckham, H. W.; Spiess, H. W. *NMR Basic Principles and Progress* **1994**, 32, 163-209.

DP ^{13}C MAS, the carbon is hit directly by rf. Because the relaxation of unmobile carbons is very slow, they are absent in the spectra and only those carbons in “liquid-like” states are detected. Therefore, the combination of CP- ^{13}C and DP- ^{13}C spectra can give information on molecular motion.

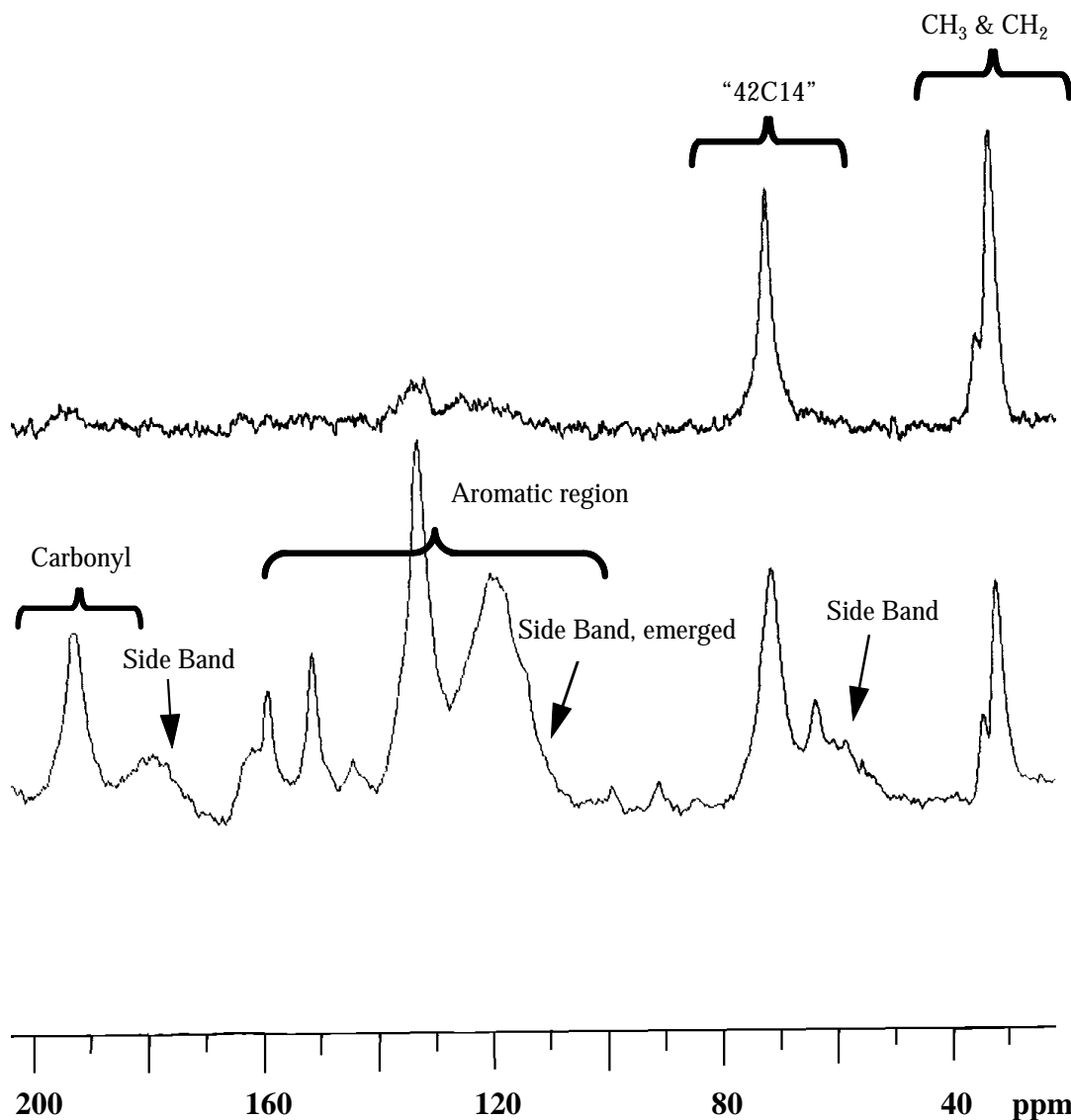


Figure 9.6 The 6 KHz ^{13}C solid state NMR of polyrotaxane 9.8 with a) DP and B) CP model at room temperature.

Interestingly, the signal of “42C14” appeared in both CP- and DP- ^{13}C spectra of 9.8 (Figure 9.6); indicating i) “42C14” is indeed threaded in 9.8 and ii) “42C14” is

mobile and while the backbone is frozen at room temperature, the measurement temperature. This observation can be attributed to the low glass transition temperature of “42C14” (-60 °C) and the great rigidity of the backbone. As expected, the signal of “42C14” also appeared in both CP- and DP- ^{13}C spectra of **9.7** (Figure 9.7) for the same reason. Thus these polyrotaxanes can be viewed as composites consisting of rubbery and rigid components (backbone). The observed motion will surely contribute to their ultimate mechanical properties, e.g., high impact strength. The relationship of the motion and the properties can be a very interesting research topic in the future. Because spinning side bands (SSB) (Figure 9.6) overlapped with the signal of “42C14” in **9.8**, no m/n could be calculated. To do so, the spectrum needs to be improved by total depression of spinning side bands (TOSS).

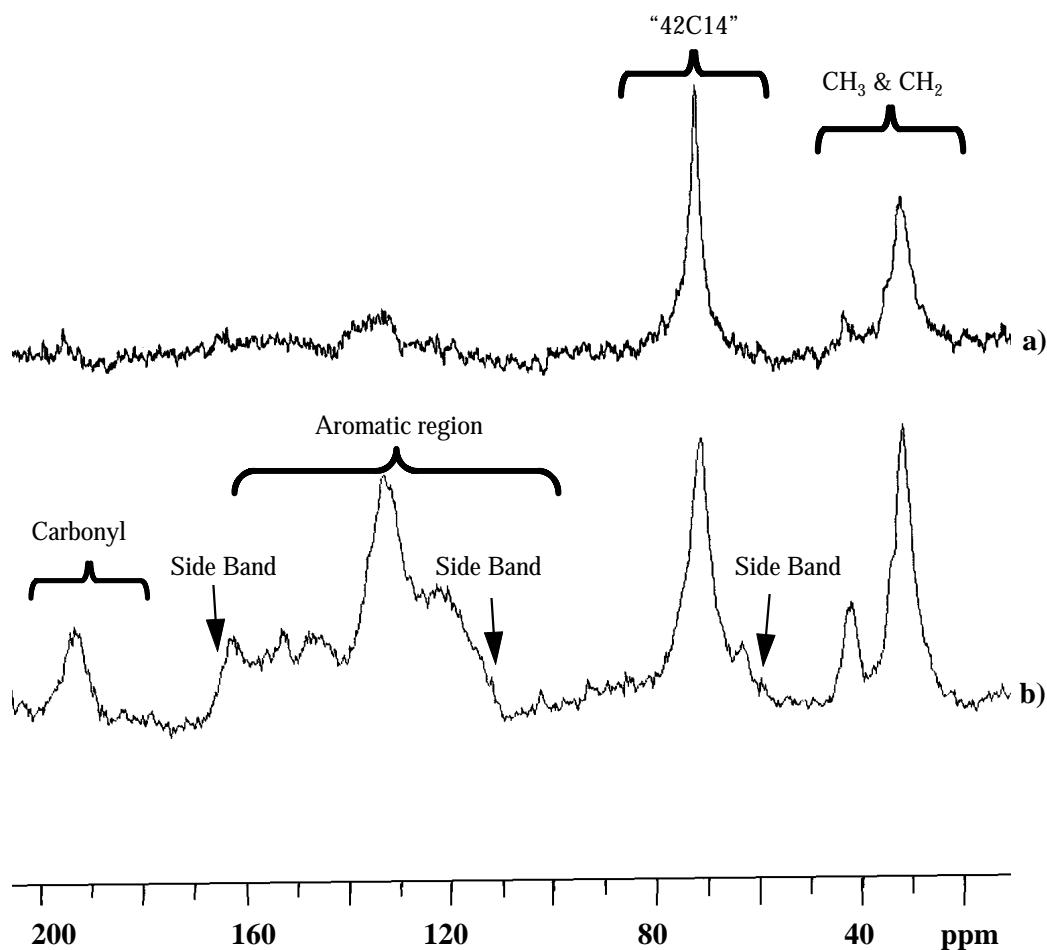


Figure 9.7 The 6 kHz ^{13}C solid state NMR of polyrotaxane **9.7** with a) DP and B) CP model at room temperature.

9.4 Conclusions.

“42C14” prepared by a reported 2+2 method is a mixture of the cyclics with different sizes. An approach toward single sized 42C14 was demonstrated by 1+1 approach. However, the separation procedure was not successful in providing pure 42C14.

Diphenolic BG was successfully used for the preparation of poly(arylene ether/“42C14” rotaxane)s. The threading is believed to be driven by complexation of the K^+ counterion of the phenolates and the crown ether. Interestingly, threaded “42C14” is still mobile at room temperature as proved by solid state NMR spectra.

9.5 Experimental

Chemical Reagents and Measurements

All chemicals were reagent grade and used directly as received from Aldrich unless otherwise specified. All solvents were HPLC or GC grade. 30C10¹¹ and “42C14”¹³ were prepared by well-established procedures. Solution state NMR spectra, reported in ppm, were obtained on a 400 MHz Varian spectrometer using $CDCl_3$ with Me_4Si as an internal standard. Solid state NMR spectra were recorded on Bruker D5X 300 at 6 kHz MAS speed and room temperature with recycle delay for DP at 1 sec. The relative molecular weights of polymers were measured by GPC in $CHCl_3$ at 30 °C with a Waters 150C ALC/GPC chromatograph equipped with a differential refractometer detector using PS standards. HPLC analyses were performed on an ISCO dual pump HPLC system comprising two Model 2350 pumps with Novapak C18 column. A Waters differential refractometer R401 was connected for analyses of crown ethers. The system was interfaced with the ISCO ChemResearch Chromatographic Data Management/System for data analyses.

“42-Crown-14” by 2+2 combination

NaH (1.00 mole) was washed twice with n-hexane and transferred into a flask with 500 mL of THF. Tetra(ethylene glycol) (0.327 mol) in 500 mL was added slowly and the mixture was stirred for two hours. Then the system was diluted to 2.5 L with THF.

Tri(ethylene glycol) ditosylate (0.316 mol) in 500 mL of THF was added dropwise over 24 hrs and refluxed for additional 24 hrs. After cooling the system, some water (8 mL) was added to destroy the excess NaH. The precipitate was filtered and the remaining solution was evaporated. A reddish-purple oil was obtained and it solidified in 40 minutes. The solid was recrystallized in acetone four times. Crude 42-crown-14 (44.0 g), poly(methylmethacryloyl chloride) (18.0 g) and pyridine (5 mL) were added to dry THF (400 mL). The mixture was stirred for 24 hrs under the protection of nitrogen at room temperature, then refluxed for 1.5 hrs. After the system had been cooled down, the mixture was precipitated into methanol (2x750 mL). The glycols and methanol reacted with the poly(methacryloyl chloride), and the resultant copolymer of methyl methacrylate and glycol methacrylate was completely insoluble in the methanol. After removal of solvent from the filtrate, the product was dissolved in methylene chloride and the solution was passed through a silica gel column (3 cm). The product was further purified by recrystallization from acetone (3x250 mL). 33 g dry white solid was obtained (yield of purification: 75%, overall yield: 34%; mp: 52.8-54.8 °C (Lit.¹⁵ 55°C). ¹H NMR: 3.64 (s, -O-CH₂-).

42C14 by 1+1 combination method

i. 7,7,7-triphenyl-3,6-dioxahexanol 9.1

Pyridine (178.5 g, 2.25 mol) and di(ethylene glycol) (1.593 kg, 15.00 mol) were added to a 3 L flask. Upon heating the solution to 45 °C, triphenylmethyl chloride (360 g, 1.29 mol) was added while the solution was being vigorously stirred. The reaction ran for another day. After cooling down the system, the solution was extracted with toluene (3x250 mL). Upon the removal of toluene, the residue was dissolved in CH₂Cl₂. The white product recrystallized from the solution upon being cooled to -20 °C. The white product was recrystallized in a mixture of ethyl acetate and hexane (800 mL, 2:1) to afford nice white crystals. Dry product (332g, 76%) was obtained, mp: 112.0-114.3 °C (Lit.²⁰: 112.7-114.5 °C). ¹H NMR: 7.48-7.45 (m, 6H); 7.32-7.22 (m, 9H); 3.77-3.73 (m, 2H); 3.68 (t, J=5, 2H); 3.364-3.361 (m, 2H); 3.27 (t, J=5); 2.14 (t, J=5.6, 1H). ¹³C NMR: 143.98; 128.67; 127.77; 126.97; 86.70; 72.24; 70.59; 63.33; 61.87.

ii. 1,1,1,24,24,24-hexaphenyl-2,5,8,11,14,17,20,23,26-nonaoxahepta-cosane (9.2)

NaH (60%, 32 g, 0.80 mol) washed with hexane (2x100 mL) was transferred to a 5L flask with 500 ml of THF under the protection of nitrogen. Compound **9.1** (186.0 g, 0.534 mol) in 1L of THF was added dropwise to the system and the mixture was stirred for another day. Then tri(ethylene glycol) ditosylate (122.24 g, 0.26690 mol) in THF (500 mL) was added and stirred for 5 days. The salt was removed by filtration and the solvent was removed by vacuum evaporation of the filtrate. The residue was dissolved in CH₂Cl₂ and washed with water (2x250 mL). The removal of the methylene chloride afforded a clear viscous liquid (206 g 95 %). ¹H NMR:¹⁸ 7.47-7.44 (m, 12H); 7.30-7.19 (m, 18H); 3.69-3.61 (m, 24H); 3.23 (t, J=5.4, 4H). ¹³C NMR: 144.10; 128.70; 127.74; 126.90; 86.50; 70.76; 70.68; 70.65; 70.58; 70.54; 63.30.

iii. Hepta(ethylene glycol) (9.3)

Compound **9.2** (75.00 g, 92.47 mmol) was dissolved in 250 ml of CH₂Cl₂ in a 500 mL high pressure flask and 1.5 g of palladium on activated carbon (10%) was added as catalyst. The reaction was run at 60 psi of hydrogen for 5 days. The catalyst was removed by filtration. Upon the removal of solvent, the residue was dissolved in 300 mL of boiling MeOH. After the solution had been cooled to -20 °C, the by-product, triphenylmethane, from the reaction precipitated and was filtered. Upon the removal of MeOH, the residue was poured into 200 ml of hot hexane and stirred to remove traces of this by-product. The final product was a clear viscous liquid (27.4 g, 91 %). ¹H NMR:²⁰ 3.73-3.70 (m, 4H); 3.67-3.64 (m, 20H); 3.61-3.59 (m, 4H); 3.22 (s, broad, 2H, disappeared upon the addition of D₂O). ¹³C NMR: 72.58; 70.53; 70.45; 70.43; 70.19; 61.62.

iv. Hepta(ethylene glycol) ditosylate (9.4)

Hepta(ethylene glycol) (**9.3**) (38.00 g, 116.5 mmol) and tosyl chloride (45.30 g, 237.6 mmol) were dissolved in 300 mL of THF in a 3L flask. Upon cooling the solution to below 0 °C, 53.0 g (0.945 mol) of KOH in water (200 mL) were added to the system over two hrs while the solution was vigorously stirred. The mixture was stirred for another day below 0

°C. The salt was removed by filtration and solvent by vacuum evaporation. The residue was dissolved in 150 mL of CHCl₃ and washed with water (2x100 ml). The final product was a clear liquid (66.7 g, 90 %). ¹H NMR:²⁰ 7.79-7.77 (m, 4H); 7.36-7.32 (m, 4H); 4.14 (t, J=4.8, 4H); 3.68-3.57 (m, 24H); 2.43 (s, 6H); ¹³C NMR: 144.77; 129.79; 128.04; 127.95; 70.71; 70.57; 70.52; 70.48; 69.23; 68.64; 21.62.

42C14 by 1+1 combination method

Hepta(ethylene glycol) (**9.3**) (2.5074 g, 7.684 mmol) and ditosylate **9.4** (4.877 g, 7.684 mmol) were dissolved in 39 mL of THF in a 50 mL syringe. The solution was added to a suspension of NaH (90%, 2.5 g, 56 mmol) in THF (600 ml) and hexane (150 mL) at the speed of 0.98 mL per hour. After the reaction ran for another 48 hrs, the solution was filtered to remove salt. The removal of the solvent afforded a deep red liquid. The product was purified by silica gel chromatography using diethyl ether, yield: 40 %. ¹H NMR: following main peaks: 3.68 (s), 3.65 (s), 3.64 (s). 3.65 ppm signal is from 42C14, 3.64 ppm is probably from 42C14-catenane,¹⁹ and 3.69 is from small crown ether, e.g., 21C7.

General Procedure for poly(arylene ether rotaxane)s: Poly(ether sulfone/42C14 rotaxane) 9.6

Recrystallized diflorobenzosulfone (406.8 mg, 1.6 mmol), diphenolic BG **9.5** (185.8 mg, 0.4 mmol), bisphenol-A (273.6 mg, 1.2 mmol) were dissolved in DMAc (5 mL) and toluene (10 mL) in a 50 mL flask. Potassium carbonate (2.4 mmol) was used as base. Polymerization was continued for 24 hours. After cooling down, the product was precipitated into water (3X300 mL). 700 mg dry polymer was obtained (yield: 84%). The threading m/n value was 0.22 (weight percentage of crown in polymer was 22.2%), which was determined by the integration of the crown peak and that for the aromatic proton para to the sulfone. ¹H NMR (Figure 9.4): 1.26 (s, 3.6H); 1.69 (s, 4.8H CH₃ of bisphenol-A); 3.65 (s, variable), 6.95-7.79 (m, 17.6H, arom). GPC results: M_n=3.7K, M_w=15.4K, PDI=4.13.

Poly(ether ketone/42C14 rotaxane) 9.7, Poly(ether ether ketone/42C14 rotaxane) 9.8 and Poly(ether ketone/30C10 rotaxane) 9.9

The same preparation and purification procedures as that for **9.6** was applied for all polyrotaxane **9.7-9.9**. However, for **9.9**, the resulting polymer was not soluble in any common solvent. Thus the precipitated product was further purified by multiple milling and washing with water. ^1H NMR for **9.7** (Fig 9.5): 1.26 (s, 3.6H); 1.69 (s, 4.8H CH_3 of bisphenol-A); 3.65 (s, variable, $-\text{OCH}_2-$), 6.95-7.79 (m, 17.6H, arom). ^1H NMR for **9.9**: 1.26 (s, 3.6H); 1.69 (s, 4.8H CH_3 of bisphenol-A); 6.95-7.79 (m, 17.6H, arom). GPC results: $M_n=17.7\text{K}$, $M_w=44.6\text{K}$, $\text{PDI}=2.51$. For **9.8**, see DP- or CP- ^{13}C solid state NMR spectra (Figure 9.6).

Chapter 10

New Classes of Linear and Branched Main Chain Polyrotaxanes by Self-Assembly

10.1 Introduction

In addition to its chemical composition, the properties of a polymer are also related to its topology, e.g., compared to linear counterparts, branched polymers **10.1** (Scheme 10.1) often have lower viscosity and higher solubility.¹⁻¹² Conventionally, branched polymers **10.1** are prepared from one step reactions of AB_x monomers (A and B are reactive groups, x is functionality two or greater). Thus only homopolymers can be obtained by this method and the branched structure is thermally stable up to decomposition since it is chemical bonded.

On the other hand, physically-linked molecular structures, e.g., rotaxanes and catenanes,¹³ opened a new window for polymer scientists in terms of polymer topology. As molecular composites, polyrotaxanes have indeed become an active research topic.¹³ According to the location of the rotaxane unit, polyrotaxanes can be divided into main chain polyrotaxanes, in which the rotaxane moiety is a main chain unit, and side chain

¹ For reviews: (a) Dvornic, P. R.; Tomalia, D. A. *Curr. Opin. Coll. Interface Sci.* **1996**, *1*, 221-235. (b) Fréchet, J. M. J. *Science*, **1994**, *263*, 1710-1715. (c) Fréchet, J. M. J. *J. Macromol. Sci. Pure Appl. Chem.* **1994**, *A31*, 1627.

² Massa, D. J.; Shiriner, K. A.; Turner, S. R.; Voit, B. I. *Macromolecules* **1995**, *28*, 3214-3220.

³ Turner, S. R.; Walter, F.; Voit, B. I.; Mourey, T. H. *Macromolecules* **1994**, *27*, 1611-1616.

⁴ Wooley, K. L.; Hawker, C. J.; Lee, R.; Fréchet, J. M. J. *Polym. J.* **1994**, *26*, 187-197.

⁵ Turner, S. R.; Voit, B. I.; Mourey, T. H. *Macromolecules* **1993**, *26*, 4617-4623.

⁶ Ralph, P.; Hawker, C. J.; Fréchet, J. M. J. *Macromolecules* **1993**, *26*, 4809-4813.

⁷ Miller, T. M.; Neenan, T. X.; Kwock, E. W.; Stein, S. M. *J. Am. Chem. Soc.* **1993**, *115*, 356.

⁸ Uhrich, K. E.; Hawker, C. J.; Fréchet, J. M. J.; Turner, S. R. *Macromolecules* **1992**, *25*, 4583-4587.

⁹ Kim, Y. H. *J. Am. Chem. Soc.* **1992**, *114*, 4947.

¹⁰ Kim, Y. H.; Webster, O. W. *Macromolecules* **1992**, *25*, 5561-5572.

¹¹ Hawker, C. J.; Lee, R.; Fréchet, J. M. J. *J. Am. Chem. Soc.* **1991**, *113*, 4583-4595.

¹² Mathias, L. J.; Carothers, T. W. *J. Am. Chem. Soc.* **1991**, *113*, 4043.

¹³ (a) Gibson, H. W.; Bheda, M. C.; Engen, P. T. *Prog. Polym. Sci.* **1994**, *19*, 843-945. (b) Amabilino, D. B.; Stoddart, J. F. *Chem. Rev.*, **1995**, *95*, 2725-2828. (c) Philp, D.; Stoddart, J. F. *Angew. Chem. Int. Engl.* **1996**, *35*, 1154-1196. (d) Gibson, H. W. in *Large Ring Molecules*, (ED: J. A. Semlyen) J. Wiley and Sons, New York, **1996**, pp. 191-262.

polyrotaxanes, in which the rotaxane unit is a pendant group or side chain moiety. Two different types of main chain polyrotaxanes (Scheme 10.1, Types **10.2** & **10.2'** and Types **10.3** & **10.3'**) were conceived.^{13a,13d} To our knowledge, however, only main chain polyrotaxanes of Types **10.2** & **10.2'** have been constructed¹³⁻²⁰ until recently when we applied the rotaxane concept in the field of branched polymers, i.e., preparation of mechanically-linked branched and/or crosslinked polymers **10.4**, a main chain polyrotaxane, and **10.5**, a side chain polyrotaxane, by *in situ* threading during the reaction (either polymerization or pendant group modification) with hydrogen bonding as the driving force.¹⁹ While the branching or crosslinking points are non-covalent, similar to conventional branched polymers, they are also thermally stable because in-chain macrocycles in **10.4** or pendent macrocycles in **10.5** play the role of blocking groups.¹⁹

¹⁴ (a) Wenz, G. *Macromol. Symp.* **1994**, *87*, 11-16. (b) Weickenmeier, M.; Wenz, G. *Macromol. Rapid. Commun.* **1996**, *17*, 731-736. (c) Steinbrunn, M. B.; Wenz, G. *Angew. Chem. Int. Ed. Engl.* **1996**, *35*, 2139-2142. (d) Heermann, W.; Keller, B.; Enz, G. *Macromolecules* **1997**, *30*, 4966.

¹⁵ (a) Born, M.; Ritter, H. *Acta Polym.* **1994**, *45*, 68-72. (b) Born, M.; Ritter, H. *Angew. Chem. Int. Ed. Engl.* **1995**, *34*, 309-311. (c) Born, M.; Ritter, H. *Adv. Mater.* **1996**, *8*, 149-151. (d) Born, M.; Ritter, H. *Macromol. Rapid Commun.* **1996**, *17*, 197-202.

¹⁶ (a) Harada, A.; Li, J.; Kamachi, M. *Macromolecules* **1994**, *27*, 4538-4543. (b) Harada, A.; Okada, M.; Li, J.; Kamachi, M. *Macromolecules* **1995**, *28*, 8406-8411. (c) Harada, A.; Li, J.; Kamachi, M. *J. Chem. Soc., Chem. Commun.* **1997**, 1413-1415.

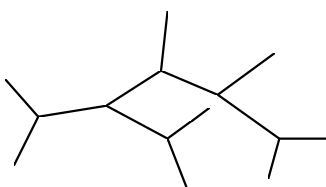
¹⁷ (a) Shen, Y. X.; Xie, D.; Gibson, H. W. *J. Am. Chem. Soc.* **1994**, *116*, 537-548. (b) Gibson, H. W.; Liu, S.; Lecavalier, P.; Wu, C.; Shen, Y. X. *J. Am. Chem. Soc.* **1995**, *117*, 852-874. (c) Gibson, H. W.; Liu, S.; Gong, C.; Ji, Q.; Joseph, E. *Macromolecules* **1997**, *30*, 3711-3727.

¹⁸ (a) Gong, C.; Gibson, H. W. *Macromolecules* **1996**, *29*, 7029-7033. (b) Gong, C.; Gibson, H. W. *Macromol. Chem. Phys.* **1997**, *198*, 2321-2332. (c) Gong, C.; Ji, Q.; Glass, T. E.; Gibson, H. W. *Macromolecules*, **1997**, *30*, 4087-4813. (d) Gong, C.; Gibson, H. W. *Angew. Chem. Int. Ed. Engl.* **1997**, in press. (e) Gong, C.; Gibson, H. W. *Macromolecules* **1997**, in press.

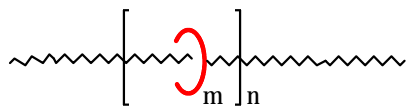
¹⁹ (a) Gong, C.; Gibson, H. W. *J. Am. Chem. Soc.* **1997**, *119*, 5862-5866. (b) Gong, C.; Gibson, H. W. *J. Am. Chem. Soc.* **1997**, *119*, 8585-8561.

²⁰ (a) Owen, J.; Hodge, P. *J. Chem. Soc., Chem. Commun.* **1997**, 11-12. (b) Mason, P. E.; Parsons, I. W.; Tolley, M. S. *Angew. Chem. Int. Ed. Engl.* **1996**, *35*, 2238. (c) Gibson, H. W.; Liu, S.; Shen, Y. X.; Bheda, M. C.; Lee, S.-H.; Wang, F. *NATO ASI Series*, Kluwer Acad. Pub., Dordrecht, the Netherlands, Series C, Vol. 456 **1995**, pp. 41-58. (d) Loveday, D.; Wilkes, G. L.; Bheda, M. C.; She, Y. X.; Gibson, H. W. *J. Macromol. Sci.-Pure Appl. Chem.* **1995**, *A32(1)*, 1-27.

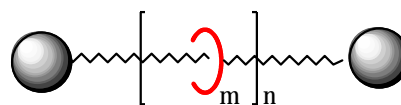
Scheme 10.1



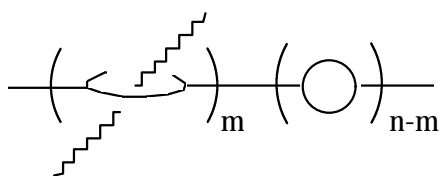
10.1. conventional branched polymer



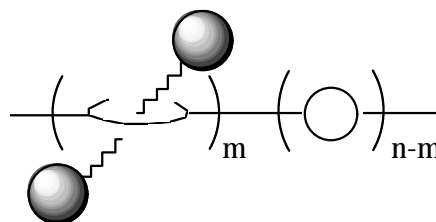
10.2. linear main chain polypseudorotaxane



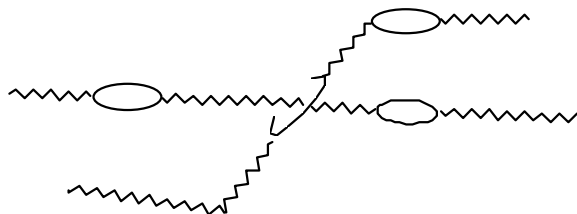
10.2'. linear main chain polyrotaxane



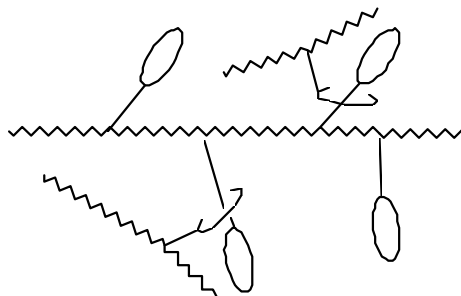
10.3. linear main chain polypseudorotaxane



10.3'. linear main chain polyrotaxane



10.4. branched main chain polyrotaxane



10.5. branched side chain polyrotaxane

In addition to the chemical compositions of the backbone and the cyclic, the properties of polyrotaxanes mainly depend on the extent of threading (m/n, average number of cyclics per repeat unit).¹³ To achieve significant threading efficiency, a strong attractive force between the cyclic and linear species, a driving force for threading, is indeed necessary.¹³ Two types of driving forces have often been used: inclusion complexation for cyclodextrin-based polyrotaxanes¹⁴⁻¹⁶ and hydrogen bonding for crown ether-based polyrotaxanes.¹⁷⁻¹⁹ While it was well demonstrated in Stoddart's group that self-assembly accomplished by π -stacking, hydrogen bonding and dipolar-dipolar interactions between electron rich phenylene-based crown ethers and electron poor 4,4'-bipyridinium salts, played a very powerful and important role in the field of supramolecular chemistry,²¹ only a few polyrotaxanes of Type **10.2** were prepared based on such driving forces. Polypseudorotaxanes were prepared by threading a bisparaquat cyclophane onto a linear polymer bearing hydroquinone moieties in solutions without physical properties reported.^{20a,20b} Polypseudorotaxanes of Type **10.2** with polyurethane backbones containing paraquat moieties were also prepared by threading bisphenylene-based crown ethers.^{20c,20d}

Here, we report an approach to prepare new classes of both linear and branched polyrotaxanes of Type **10.3** by self assembly of a preformed poly(ester crown ether) with 1) a low molar mass 4,4'-bipyridium derivative (paraquat) and 2) a preformed polymer containing paraquat moieties, respectively. Some properties of the polyrotaxanes both in solution and solid states were studied.

10.2 Results and Discussion

10.2.1 Synthesis of precursors

In order to prepare the desired polyrotaxanes of Type **10.3** (Scheme 10.1) by self assembly, both 4,4'-bipyridinium salts and polymeric crown ethers are necessary. Bis(5-hydroxymethyl-m-phenylene)-32-crown-10 (**10.6**) is a perfect macrocycle for this purpose

because its ring size and chemical composition ensure its ability to complex with paraquat²¹ and the reactive hydroxyl groups are feasible for polymerization with other monomers.¹⁹

Macrocyclic **10.6** (Scheme 10.2) was synthesized by a reported procedure.²² It was then quantitatively converted into bis(5-acetoxymethyl-*m*-phenylene)-32-crown-10 (**10.7**) by reaction with acetyl chloride in THF.²² The solution polycondensation of **10.6** with sebacoyl chloride afforded poly[bis(5-methylene-1,3-phenylene)-32-crown-10 sebacate] (**10.8**) (Scheme 10.2). Because -OH groups can H-bond with crown ether macrocycles^{18,19} to induce threaded structures **10.4**, in order to obtain linear polymer DMSO was used as a cosolvent to depress such threading during polymerization.¹⁹ **10.7** was used for the model complexation study since it has very similar structure to the cyclic units in polyester **10.8**. N,N'-Bis(β -hydroxyethyl)-4,4'-bipyridinium 2PF₆⁻ (**10.9**) was prepared from 4,4'-bipyridine and β -hydroxyethyl iodide, followed by counterion exchange.²³ The purpose of the ion exchange is to increase the solubility of the paraquat salt in organic solvents.²¹

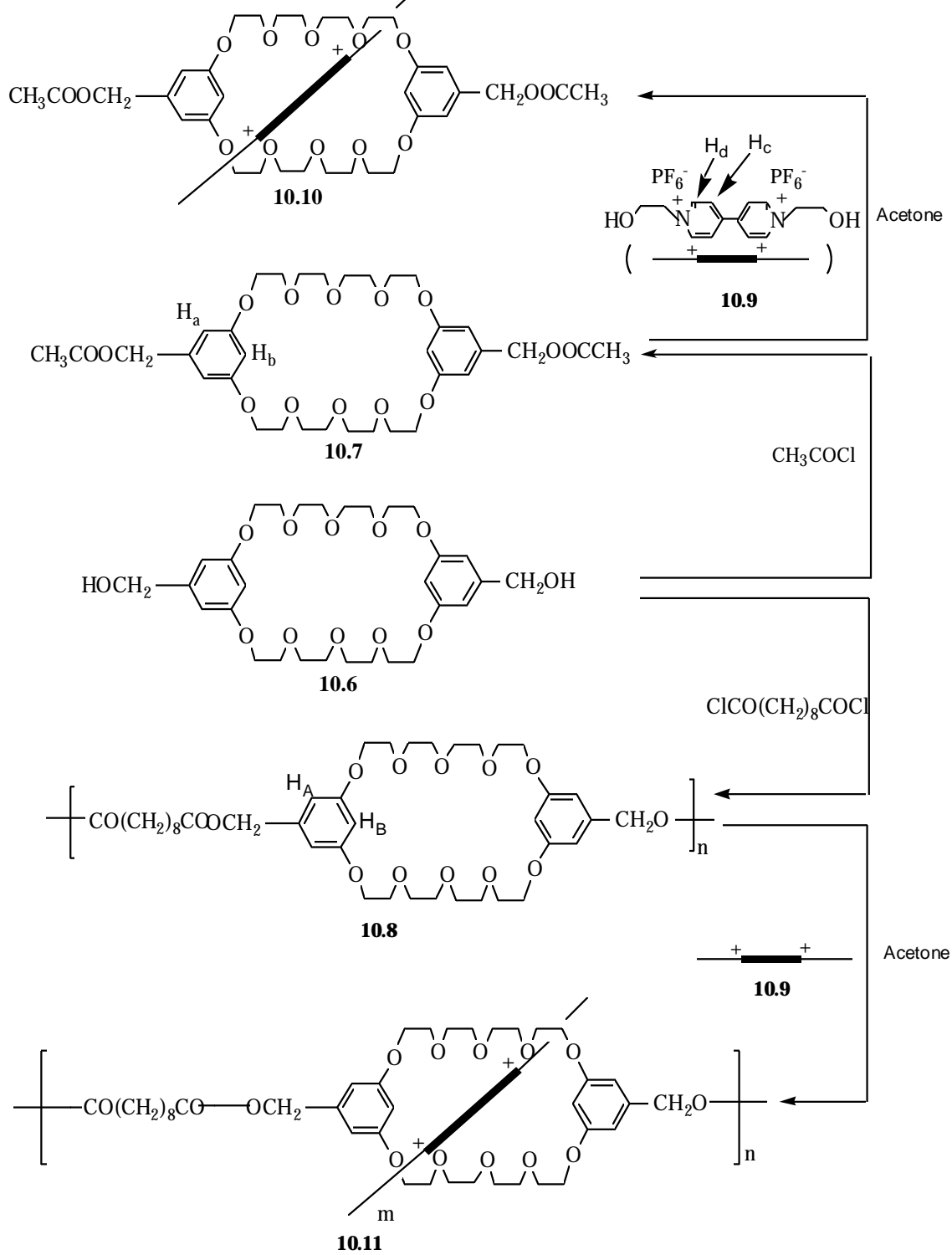
To study interpenetration of preformed polymers, copolyurethane **10.14** (Scheme 10.3) was prepared by refluxing a solution of N,N'-bis(β -hydroxyethyl)-4,4'-bipyridinium 2PF₆⁻ (**10.9**), poly(tetramethyleneoxide) (**10.12**, PTMO, dihydroxy terminated, M_n=1 kg/mol, a = 19) and 4,4'-methylenebis(*p*-phenyl isocyanate) (MDI, **10.13**) in a mixture of diglyme and CH₃CN.

²¹ (a) Allwood, B. L.; Spencer, N.; Shahriari-Zavareh, H.; Stoddart, J. F.; Williams, D. J. *J. Chem. Soc., Chem. Commun.* **1987**, 106-109. (b) Asakawa, M.; Ashton, P. R.; Ballardini, R.; Balzani, V.; Belohradsky, M.; Gandolfi, M. T.; Kocian, O.; Prodi, L.; Raymo, F. M.; Stoddart, J. F.; Venturi, M. *J. Am. Chem. Soc.* **1997**, *119*, 302-310.

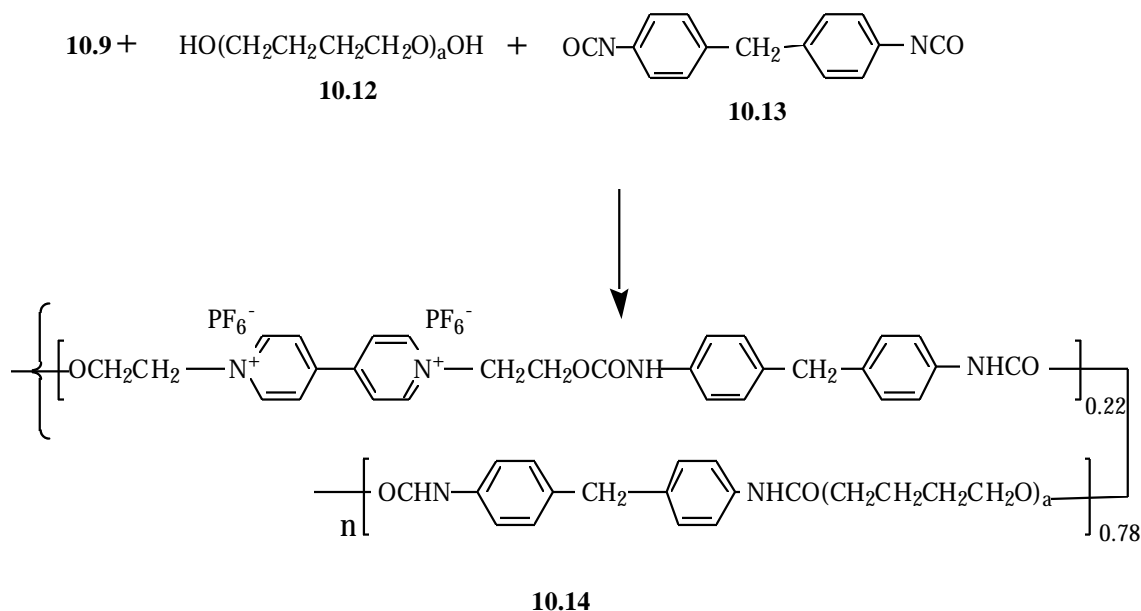
²² Gibson, H. W.; Nagvekar, D. S. *Can. J. Chem.*, **1997**, *75*, xxx.

²³ Shen, Y. X.; Engen, P. T.; Berg, M. A. G.; Merola, J. S.; Gibson, H. W. *Macromolecules* **1992**, *25*, 2786-2788.

Scheme 10.2



Scheme 10.3



10.2.2 Complexation

i. Model study: monorotaxane 10.10

Stoddart's group extensively studied the complexation of bisphenylene-based crown ethers with paraquats.^{13,21} More specifically, they found that bis(m-phenylene)-32-crown-10 can complex with N,N'-bis(β -hydroxyethyl)-4,4'-bipyridinium 2PF₆⁻. While the equilibrium constant (K) was measured by UV spectroscopy at ambient temperature, no enthalpy change (ΔH) and entropy change (ΔS) were reported so far. These data are very important in terms of quantitatively understanding the complexation process. To compare with the polymeric system **10.11** more accurately, paraquat **10.9** and diester cyclic **10.7** were used for the model complexation in the present study. Here, we demonstrated the successful utilization of proton NMR spectroscopy to meet this purpose.

As soon as **10.7** and **10.9** were mixed, the solution turned yellow, indicating the rapid formation of [2]rotaxane **10.10**. Relative to those of pure **10.7** (Figure 10.1a at 21.8 °C and Figure 10.1d at 38 °C, respectively), the time averaged signals of the protons H_a and H_b of the cyclic were shifted upfield after complexation (Figure 10.1b and Figure 10.1c, respectively),

proving the formation of rotaxane **10.10**.^{13,21,23} Increasing temperature depressed the formation of rotaxane **10.10** because the complexation is exothermic, indicated by the fact that the protons H_a and H_b were shifted downfield towards the uncomplexed species at higher temperature while the compositions of the solution remained unchanged (Figure 10.1b and Figure 10.1c).

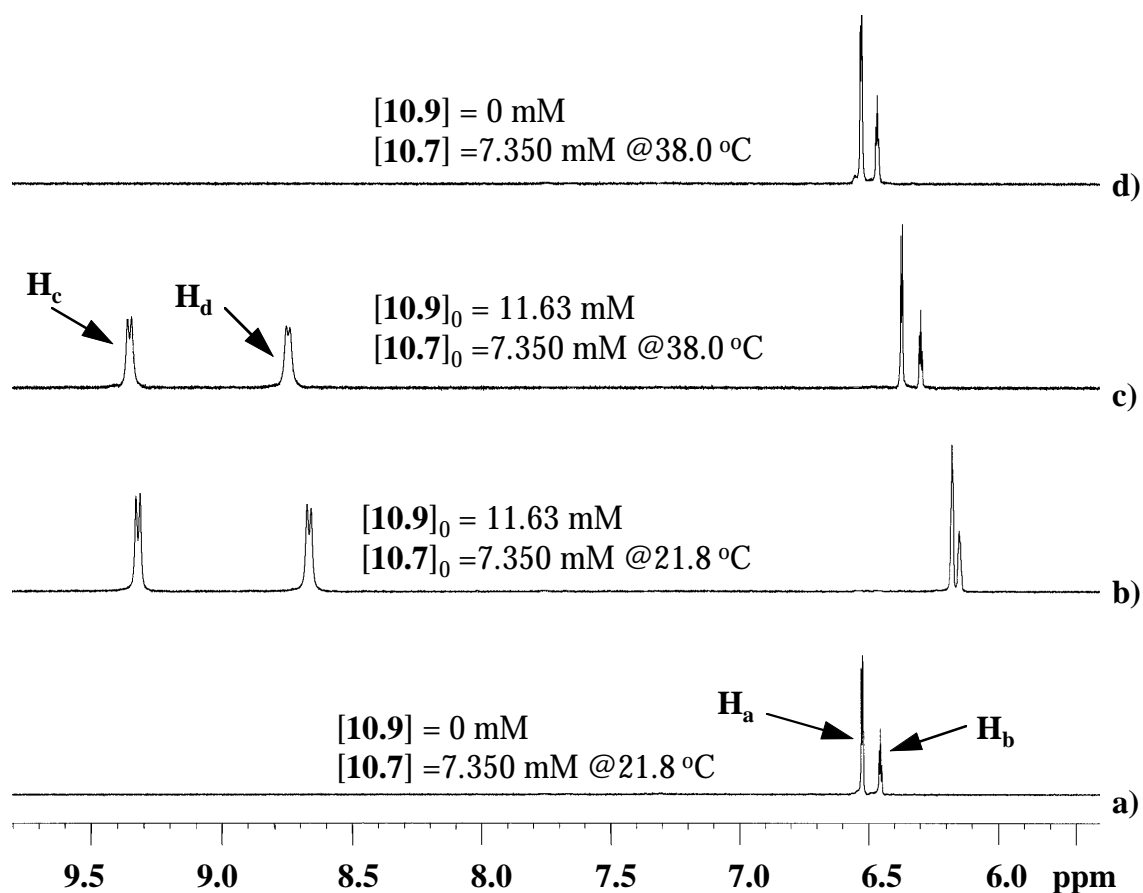


Figure 10.1. The expanded aromatic regions of the 400 MHz proton NMR spectra for a) and d) **10.7**, and b) and c) solutions of **10.7** and **10.9** in acetone-*d*₆.

Only time averaged signals were observed because the complexation was a rapid exchange process relative to the NMR time scale.^{13,20,21} To calculate the equilibrium

constant K , the Benesi-Hildebrand method, continuous titration, was employed.²⁴ According to this method, the continuous addition of **10.9** into a solution of **10.7** gives the corresponding time averaged signals, e.g., for proton H_a , and the Δ values ($\Delta = \delta_f - \delta$ where δ and δ_f are the time averaged chemical shifts of the partially complexed and the free or uncomplexed forms, e.g., pure **10.7**, respectively), whose inverse values are plotted vs. $1/[\mathbf{10.9}]_0$ in the form $1/\Delta = 1/(\Delta_0 K[\mathbf{10.9}]_0) + 1/\Delta_0$, where $\Delta_0 = \delta_f - \delta_c$ (δ_c is the chemical shift of the totally complexed form, e.g., protons H_a and H_b of **10.10**).

Table 10.1. The chemical shifts of protons H_a and H_b of **10.7** upon complexation with different amounts of **10.9** in acetone at different temperatures^a

$[\mathbf{10.9}]_0$ (mM)	21.8 °C δ_a/δ_b^b (ppm)	30.0 °C δ_a/δ_b (ppm)	38.0 °C δ_a/δ_b (ppm)	46.0 °C δ_a/δ_b (ppm)	54.0 °C δ_a/δ_b (ppm)
0	6.523/6.452	6.525/6.458	6.527/6.464	6.529/6.469	6.531/6.475
11.63	6.177/6.149	6.239/6.191	6.312/6.246	6.370/6.296	6.417/6.340
23.25	6.084/6.069	6.154/6.106	6.230/6.162	6.292/6.214	6.353/6.269
27.44	6.073/6.059	6.144/6.097	6.219/6.150	6.283/6.200	6.343/6.253
39.23	6.040/6.031	6.095/6.056	6.162/6.096	6.232/6.148	6.302/6.209
44.18	6.034/6.025	6.092/6.049	6.156/6.087	6.221/6.134	6.286/6.189
65.16	6.018/6.011	6.073/6.030	6.133/6.063	6.191/6.104	6.261/6.159
122.4	5.990/5.990	6.033/5.993	6.082/6.013	6.136/6.042	6.194/6.081

^a $[\mathbf{10.7}]_0$ constant at 7.350 mM; temp: ± 0.1 °C.

^b δ_a/δ_b : the chemical shifts of the protons H_a and H_b , respectively; ± 0.001 ppm.

To determine K , ΔH and ΔS , the chemical shifts of protons H_a and H_b were measured by both varying $[\mathbf{10.9}]_0$ and temperature with $[\mathbf{10.7}]_0$ at 7.350 mM in acetone (Table 10.1) and the corresponding Δ values were calculated (Table 10.2). The $1/\Delta$ values were plotted against $1/[\mathbf{10.9}]_0$ (Figure 10.2a-e based on proton H_a and Figure 10.3a-e based on proton H_b).

²⁴ H. A. Benesi, J. H. Hildebrand, *J. Am. Chem. Soc.*, **1949**, *71*, 2703-2710; H. Tsukube, H. Furuta, A. Odani, Y., Takeda, Y. Kudo, Y. Inone, Y. Liu, H. Sakamoto, K. Kimura, *Comprehensive Supramolecular Chemistry*, Vol. 6 (EDS: J. L. Atwood, J. E. D. Davies, D. D. MacNicol, F. Vögtle), Pergamon, Oxford, UK, **1996**, pp 425-482.

The slope and intercept of these Benesi-Hildebrand plots afforded Δ_0 and K as intercept = $1/\Delta_0$ and slope = $1/(K\Delta_0)$ (Table 10.3). Protons H_a and H_b gave essentially the same K values and free energy changes (ΔG) at a given temperature (Table 10.3), confirming the accuracy and reproducibility of the employed method.

Table 10.2. The chemical shift changes of protons H_a and H_b of **10.7** (7.350 mM initially) upon complexation with different amounts of **10.9** in acetone at different temperatures

[10.9] ₀ (mM)	21.8 °C Δ_a/Δ_b^a (ppm)	30.0 °C Δ_a/Δ_b (ppm)	38.0 °C Δ_a/Δ_b (ppm)	46.0 °C Δ_a/Δ_b (ppm)	54.0 °C Δ_a/Δ_b (ppm)
0	0.000/0.000	0.000/0.000	0.000/0.000	0.000/0.000	0.000/0.000
11.63	0.346/0.303	0.286/0.267	0.215/0.218	0.159/0.173	0.114/0.135
23.25	0.439/0.383	0.371/0.352	0.297/0.302	0.237/0.255	0.178/0.206
27.44	0.450/0.393	0.381/0.361	0.308/0.314	0.246/0.269	0.188/0.222
39.23	0.483/0.421	0.430/0.402	0.365/0.368	0.297/0.321	0.229/0.266
44.18	0.489/0.427	0.433/0.409	0.371/0.377	0.308/0.335	0.245/0.286
65.16	0.505/0.441	0.452/0.428	0.394/0.401	0.338/0.365	0.270/0.316
122.4	0.533/0.462	0.492/0.465	0.445/0.451	0.393/0.427	0.337/0.394

^a Δ_a/Δ_b : the chemical shifts changes of the protons H_a and H_b compared to those of pure **10.7** at the same temperature, respectively; ± 0.002 ppm.

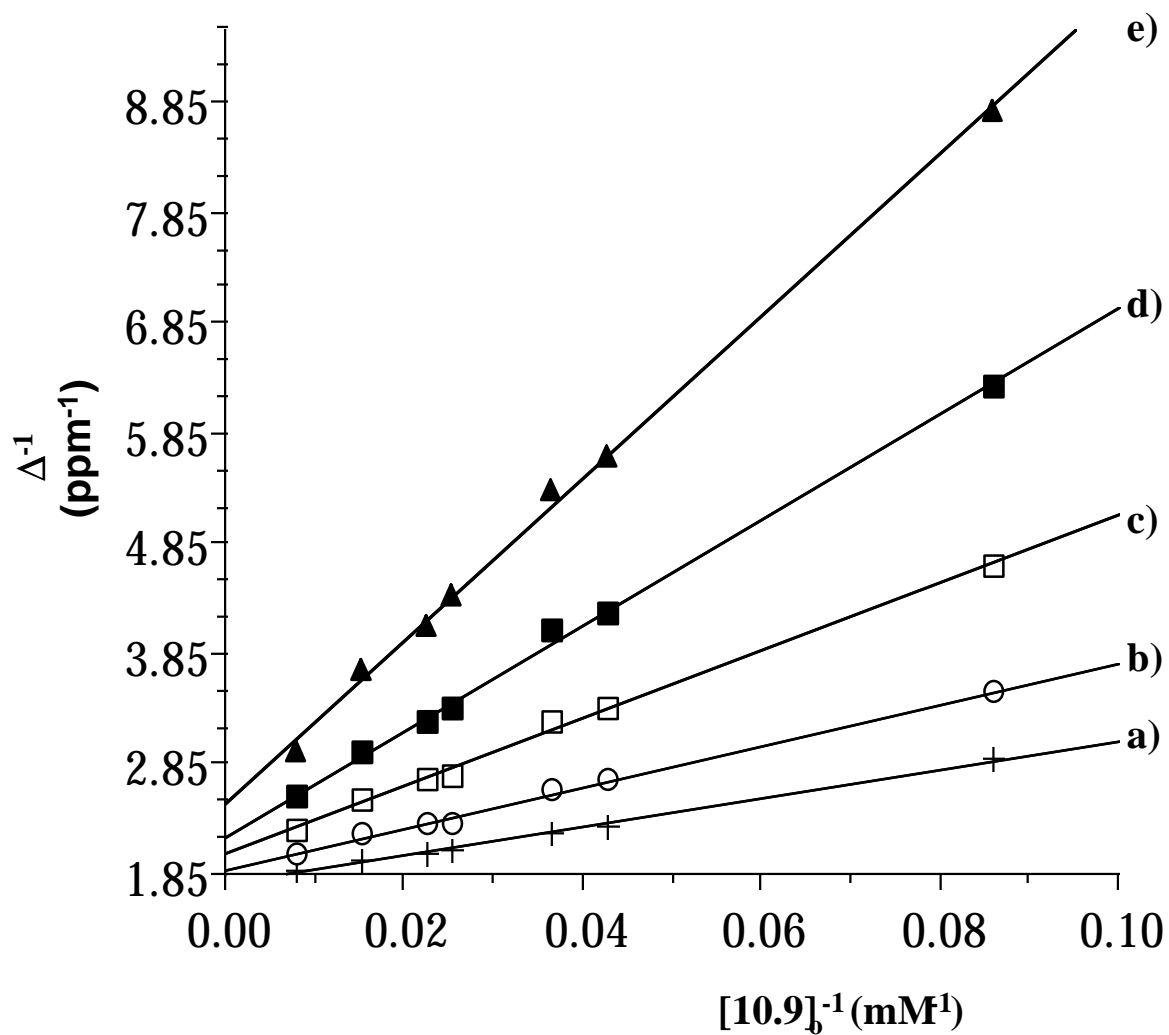


Figure 10.2. The Benesi-Hildebrand plots based on proton H_a for the formation of [2]rotaxane 10.10 with [10.7]₀ = 7.350 mM at a) 21.8 °C, b) 30.0 °C, c) 38.0 °C, d) 46.0 °C and e) 54.0 °C in acetone.

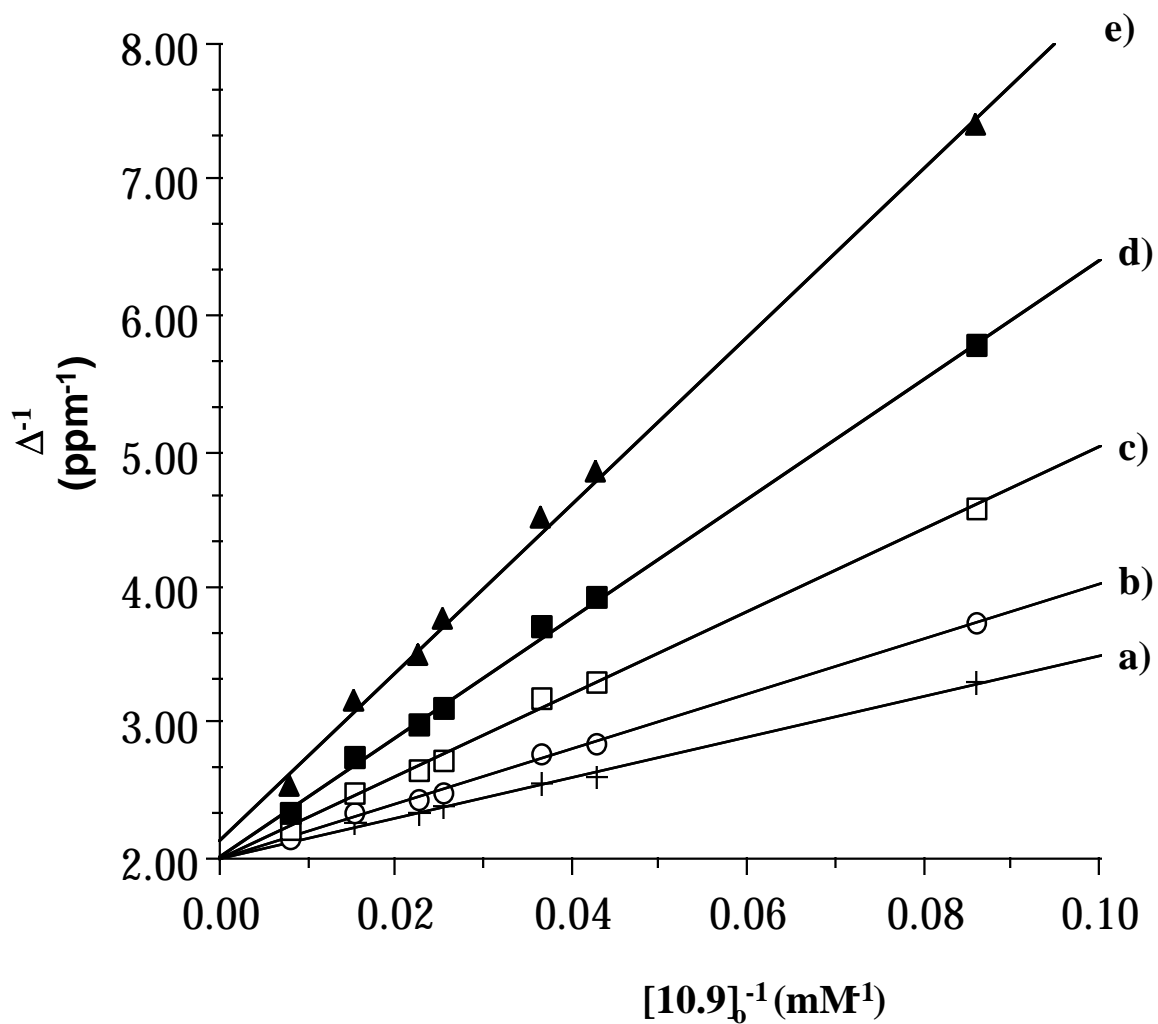


Figure 10.3. The Benesi-Hildebrand plots based on proton H_b for the formation of [2]rotaxane 10.10 with [10.7]_o = 7.350 mM at a) 21.8 °C, b) 30.0 °C, c) 38.0 °C, d) 46.0 °C and e) 54.0 °C in acetone.

Table 10.3. The results from Benesi-Hildebrand plots for complexation of **10.7** and **10.9**^a

Figure	Temp. (°C)	Slope (mM.ppm ⁻¹)	Intercept (ppm ⁻¹)	R ²	K ^b (M ⁻¹)	ΔG ^b (kJ.mol ⁻¹)	Δ _o (ppm)
10.2a	21.8	12.97	1.755	0.996	135.3	-12.03	0.570
10.3a	21.8	14.86	2.007	0.996	135.1	-12.03	0.498
10.2b	30.0	18.72	1.894	0.996	101.2	-11.64	0.528
10.3b	30.0	20.33	1.994	0.998	98.1	-11.56	0.502
10.2c	38.0	30.84	2.025	0.995	65.7	-10.83	0.494
10.3c	38.0	30.40	1.994	0.997	65.6	-10.83	0.502
10.2d	46.0	47.91	2.190	0.997	45.7	-10.14	0.457
10.3d	46.0	43.96	2.026	0.998	46.1	-10.16	0.494
10.2e	54.0	73.62	2.482	0.998	33.7	-9.626	0.403
10.3e	54.0	61.76	2.155	0.998	34.9	-9.722	0.464

^a based on proton H_a for Figure 10.2 and proton H_b for Figure 10.3.

^b estimated relative error: 5 %.

With Δ and Δ_o values at hand, the fraction of **10.7** existing as rotaxane **10.10** was calculated as Δ/Δ_o (Table 10.4 and Figure 10.4 based on the proton H_b). While as Table 10.3 shows, proton H_a and H_b gave similar results, proton H_b, we believe, produces somewhat more accurate data because it has more constant Δ_o over the studied temperature range. Since ΔG is more negative and K is higher at lower temperature (Table 10.3), the fraction of rotaxane **10.10** increased with lower temperature at a given concentration. On the other hand, at a given temperature, the conversion increased with more paraquat **10.9**, agreeing with the equilibrium process.

Table 10.4. The fraction of **10.7** (7.350 mM initially) complexed with **10.9**^a

[10.9] _o (mM)	21.8 °C	30.0 °C	38.0 °C	46.0 °C	54.0 °C
0	0.000/0.000	0.000/0.000	0.000/0.000	0.000/0.000	0.000/0.000
11.63	0.610/0.608	0.542/0.532	0.435/0.434	0.348/0.350	0.283/0.291
23.25	0.770/0.769	0.703/0.701	0.601/0.602	0.512/0.516	0.442/0.444
27.44	0.789/0.789	0.722/0.719	0.623/0.625	0.538/0.545	0.467/0.478
39.23	0.847/0.845	0.814/0.801	0.739/0.733	0.650/0.650	0.568/0.573
44.18	0.858/0.857	0.820/0.815	0.751/0.751	0.674/0.678	0.608/0.616
65.16	0.886/0.886	0.856/0.853	0.798/0.799	0.740/0.739	0.670/0.681
122.4	0.935/0.928	0.932/0.926	0.901/0.898	0.860/0.864	0.836/0.849

^a x_a/x_b : based Δ_a and Δ_b , respectively; estimated relative error: 5 %.

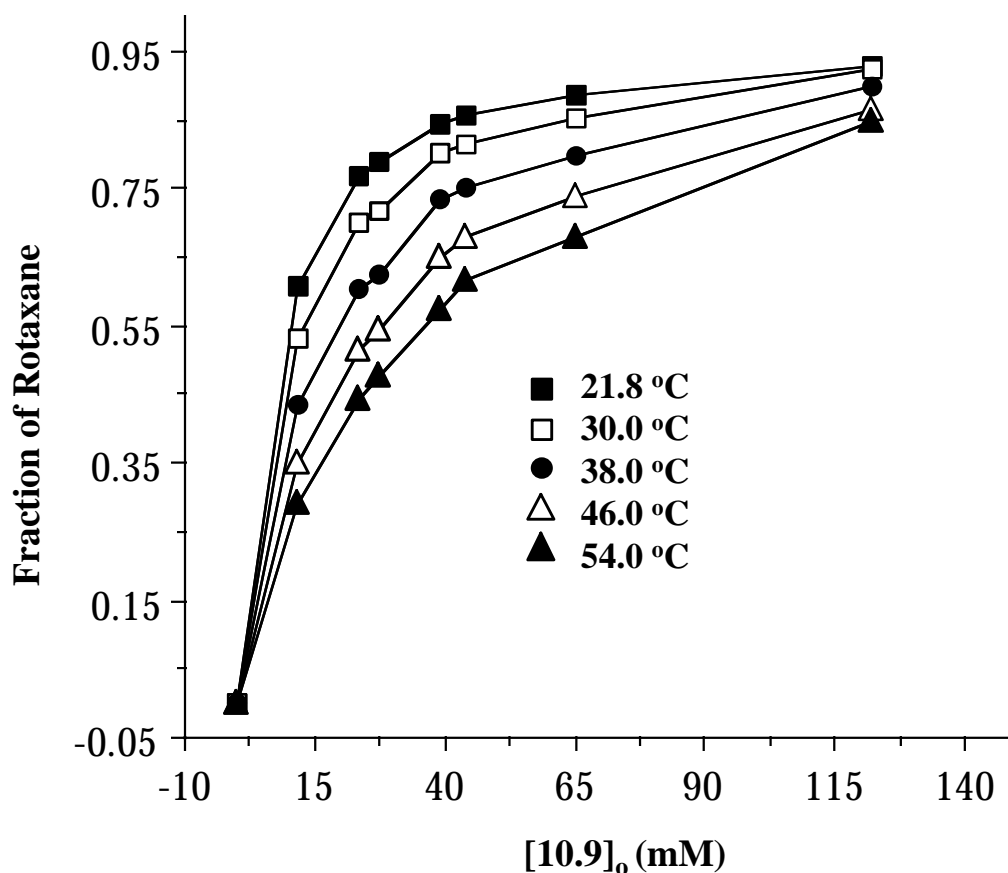


Figure 10.4. The relationship of the fraction of rotaxane **10.10** vs. the feed concentration of **10.9** with $[10.7]_o = 7.350$ mM in acetone at different temperatures.

The van't Hoff plots (Figure 10.5a and 10.5b, and Table 5.5) afforded more valuable information, ΔH and ΔS (-34.6 kJmol^{-1} and $-76.2 \text{ JK}^{-1}\text{mol}^{-1}$ based on proton H_b and -35.7 kJmol^{-1} and $-79.7 \text{ JK}^{-1}\text{mol}^{-1}$ based on proton H_a , respectively). The negative enthalpy agrees with strong interactions, π -stacking accompanied by H-bond and dipole-dipole interactions, between the crown ether and the paraquat. The negative entropy is obvious because rotaxane **10.10** is more organized and rigid than the individual starting materials **10.7** and **10.9**.

Thus proton NMR spectroscopy can be effectively used for quantitative characterization of these supramolecular systems. Considering that no ΔH and ΔS values have been reported for the complexation between the crown ethers and paraquat derivatives, despite the fact that the complexation has widely been used to construct supramolecules,^{13,20-23} the present result is important in terms of fundamental understanding of these systems.

Table 10.5. The enthalpy and entropy changes from van't Hoff plots for the complexation of **10.7** with **10.9**, and **10.8** with **10.9** at different temperatures in acetone^a

Figures	System	Slope (K)	Intercept	R ²	ΔH^b (kJ.mol ⁻¹)	ΔS^b (J.mol ⁻¹ K ⁻¹)
10.5a	7+9	4160	-9.17	0.997	-34.6	-76.2
10.5b	7+9	4290	-9.59	0.995	-35.7	-79.7
10.5c	8+9	2360	-4.25	0.953	-19.6	-35.3
10.5d	8+9	2320	-4.21	0.985	-19.3	-35.0

^a based on proton H_a for Figure 10.5a, proton H_b for Figure 10.5b, proton H_A for Figure 10.5c and proton H_B for Figure 10.5d.

^b estimated relative error: 5 %.

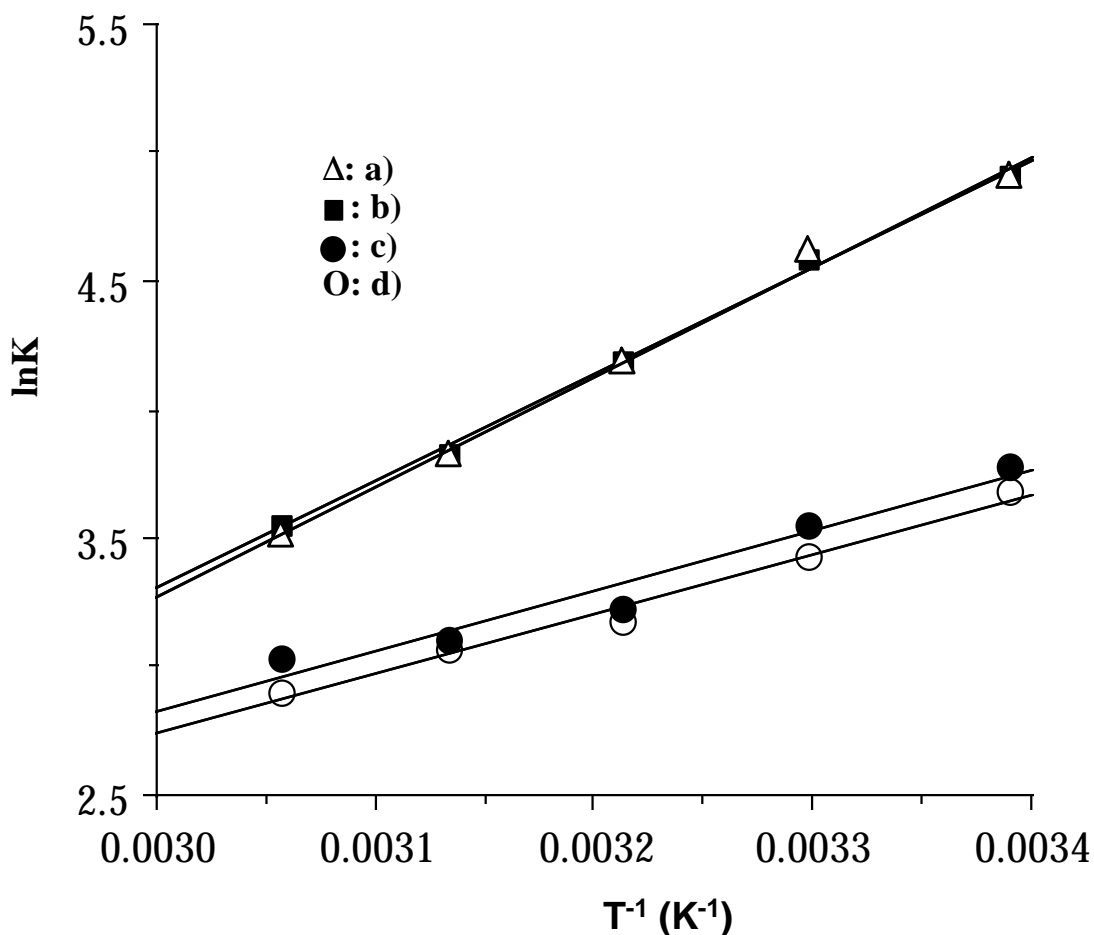


Figure 10.5. The van't Hoff plots: a) for the model system (10.7 + 10.9) based on proton H_a, b) for the model system (10.7 + 10.9) based on proton H_b, c) for the polymeric system (10.8 + 10.9) based on proton H_A, and d) for the polymeric system (10.8 + 10.9) based on proton H_B.

ii. Polyrotaxane 10.11

The model complexation study proved that the diester functional cyclic **10.7** can effectively complex with paraquat **10.9**. Therefore, poly(ester crown ether) **10.8** is expected to complex with paraquat **10.9** to afford desired polyrotaxane **10.11** (Scheme 10.2).

Not surprisingly, as soon as **10.9** was added to a solution of **10.8** in acetone, an orange color immediately appeared, indicating the rapid formation of polyrotaxane **10.11**. Again, direct evidences were obtained from proton NMR studies. Compared to those of pure **10.8** (Figure 10.6a), the signals of the aromatic protons H_A and H_B of the macrocyclic moiety in polyrotaxane **10.11** (Figure 10.6b-c) shifted upfield; this is consistent with the expected complexation process, polypseudorotaxane formation, i.e., the existence of through space interactions because of π stacking between these two components.^{13,21,23} Increasing temperature disfavors the formation of **10.11** as manifested by the fact that the signals of protons H_A and H_B shifted downfield (Figure 10.6c-e) at higher temperature. It is worth noting that all these signals are time averaged since no separate peaks corresponding to threaded and unthreaded structures exist in the spectra. Therefore, although the cyclic component was incorporated into the backbone, the complexation between poly(crown ether) **10.8** and **10.9** is still rapid relative to the proton NMR time scale.

As demonstrated for the model system, to quantitatively understand the formation of polyrotaxane **10.11**, the chemical shifts of protons H_A and H_B at different solution compositions and temperatures are necessary. Therefore, a solution of **10.8** in acetone was continuously titrated with **10.9** at different temperatures. The measured chemical shifts of protons H_A and H_B are summarized in Table 10.6 and the corresponding Δ values were calculated relative to those of pure **8** (Table 10.7). According to the slopes and intercepts of Benesi-Hildebrand plots (Figure 10.7 based on proton H_A and Figure 10.8 based on proton H_B), Δ_0 and the equilibrium constants (K values) as well as the free energy changes for the formation of polyrotaxane **10.11** at different temperatures were calculated as the intercept = $1/\Delta_0$ and the slope = $1/(K \cdot \Delta_0)$ (Table 10.8). From the van't Hoff plots based on these K values (Figure 10.5c for proton H_A and Figure 10.5d for proton H_B), ΔH and ΔS were derived to be -19.3 kJmol^{-1} and $-35.0 \text{ Jmol}^{-1}\text{K}^{-1}$ based on proton H_B and -19.6 kJmol^{-1} and $-35.4 \text{ Jmol}^{-1}\text{K}^{-1}$ based on proton H_A, respectively (Table 10.5). Therefore, the formation of polyrotaxane **11** is favored by the enthalpy term but disfavored by the entropy term.

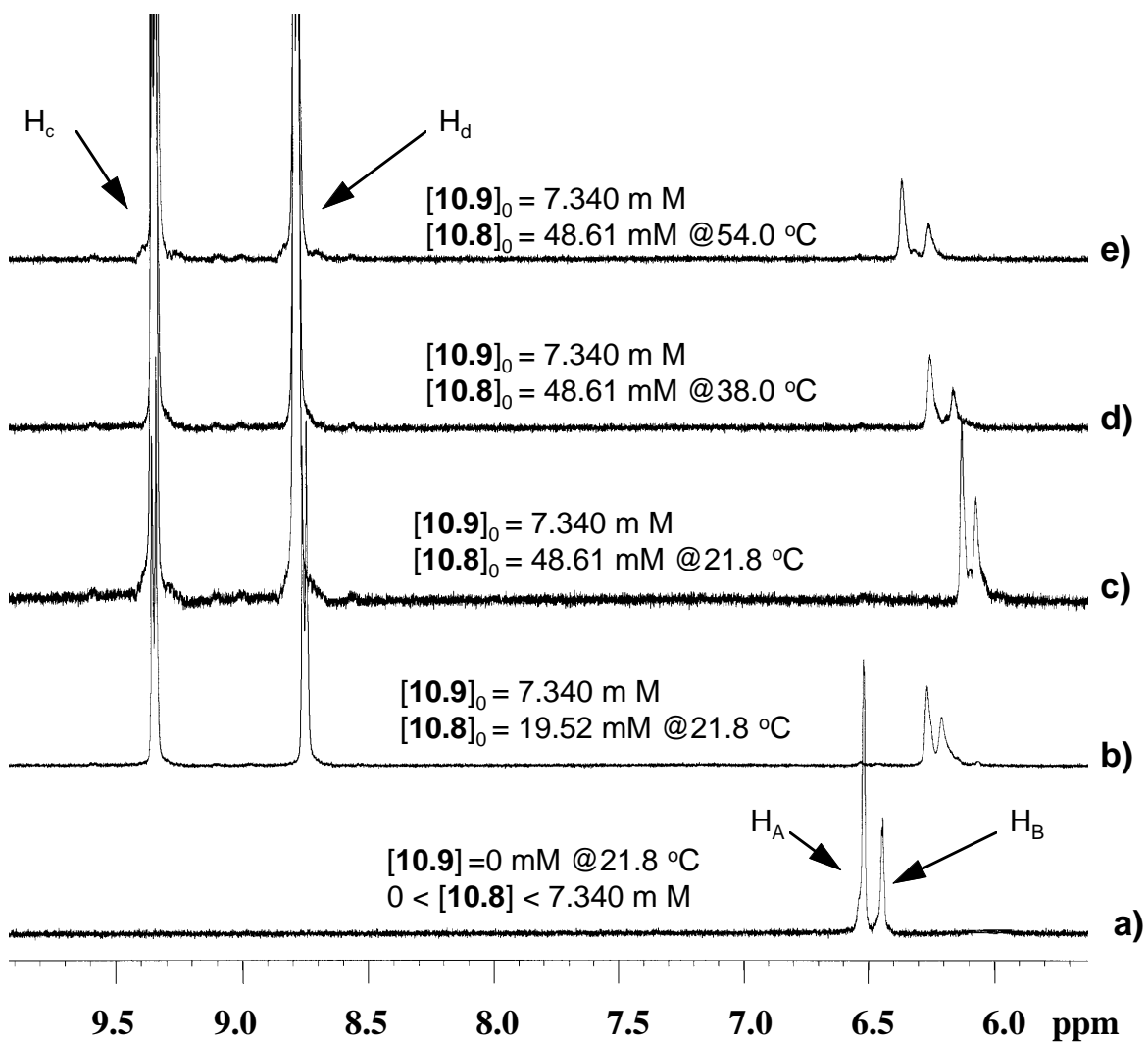


Figure 10.6. The expanded aromatic regions of the 400 MHz proton NMR spectra for a) 10.8 and b-e) solutions of 10.8 and 10.9 in acetone- d_6 .

Table 10.6. The chemical shifts of protons H_A and H_B of **10.8** upon complexation with different amounts of **10.9** in acetone at different temperatures^a

[10.9] _o (mM)	21.8 °C δ _A /δ _B ^b (ppm)	30.0 °C δ _A /δ _B (ppm)	38.0 °C δ _A /δ _B (ppm)	46.0 °C δ _A /δ _B (ppm)	54.0 °C δ _A /δ _B (ppm)
0	6.517/6.441	6.521/6.447	6.520/6.453	6.521/6.459	6.527/6.466
11.16	6.330/6.271	6.375/6.307	6.413/6.339	6.441/6.364	6.465/6.391
19.52	6.265/6.206	6.316/6.242	6.366/6.287	6.404/6.320	6.439/6.356
32.54	6.179/6.119	6.248/6.172	6.304/6.215	6.355/6.260	6.398/6.306
37.43	6.167/6.111	6.224/6.150	6.289/6.136	6.343/6.245	6.390/6.291
42.55	6.149/6.094	6.213/6.137	6.272/6.183	6.329/6.229	6.377/6.278
48.61	6.126/6.070	6.194/6.117	6.250/6.160	6.315/6.211	6.364/6.255
67.00	6.095/6.042	6.156/6.079	6.218/6.121	6.275/6.166	6.330/6.217
100.8	6.062/6.010	6.118/6.040	6.179/6.078	6.237/6.117	6.294/6.167

^a [**10.8**]_o constant at 7.340 mM; temp: ± 0.1 °C.

^b δ_A/δ_B: the chemical shifts of the protons H_A and H_B, respectively (± 0.001 ppm).

Table 10.7. The chemical shift changes of protons H_A and H_B of **10.8** (7.340 mM initially) upon complexation with different amounts of **10.9** in acetone at different temperatures

[10.9] _o (mM)	21.8 °C Δ _A /Δ _B ^a (ppm) ^a	30.0 °C Δ _A /Δ _B (ppm)	38.0 °C Δ _A /Δ _B (ppm)	46.0 °C Δ _A /Δ _B (ppm)	54.0 °C Δ _A /Δ _B (ppm)
0	0/0	0/0	0/0	0/0	0/0
11.16	0.187/0.170	0.146/0.140	0.107/0.114	0.080/0.095	0.062/0.075
19.52	0.252/0.235	0.205/0.205	0.154/0.166	0.117/0.139	0.088/0.110
32.54	0.338/0.322	0.273/0.275	0.216/0.238	0.166/0.199	0.129/0.165
37.43	0.350/0.330	0.297/0.297	0.231/0.257	0.178/0.214	0.137/0.175
42.55	0.368/0.347	0.308/0.310	0.248/0.270	0.192/0.230	0.150/0.188
48.61	0.391/0.371	0.327/0.330	0.270/0.293	0.206/0.248	0.163/0.211
67.00	0.422/0.399	0.365/0.368	0.302/0.332	0.246/0.293	0.197/0.249
100.8	0.455/0.431	0.403/0.407	0.341/0.375	0.284/0.342	0.233/0.299

^a Δ_A/Δ_B: the chemical shifts changes of protons H_A and H_B compared to those of pure **10.8** at the corresponding temperatures, respectively (± 0.002 ppm).

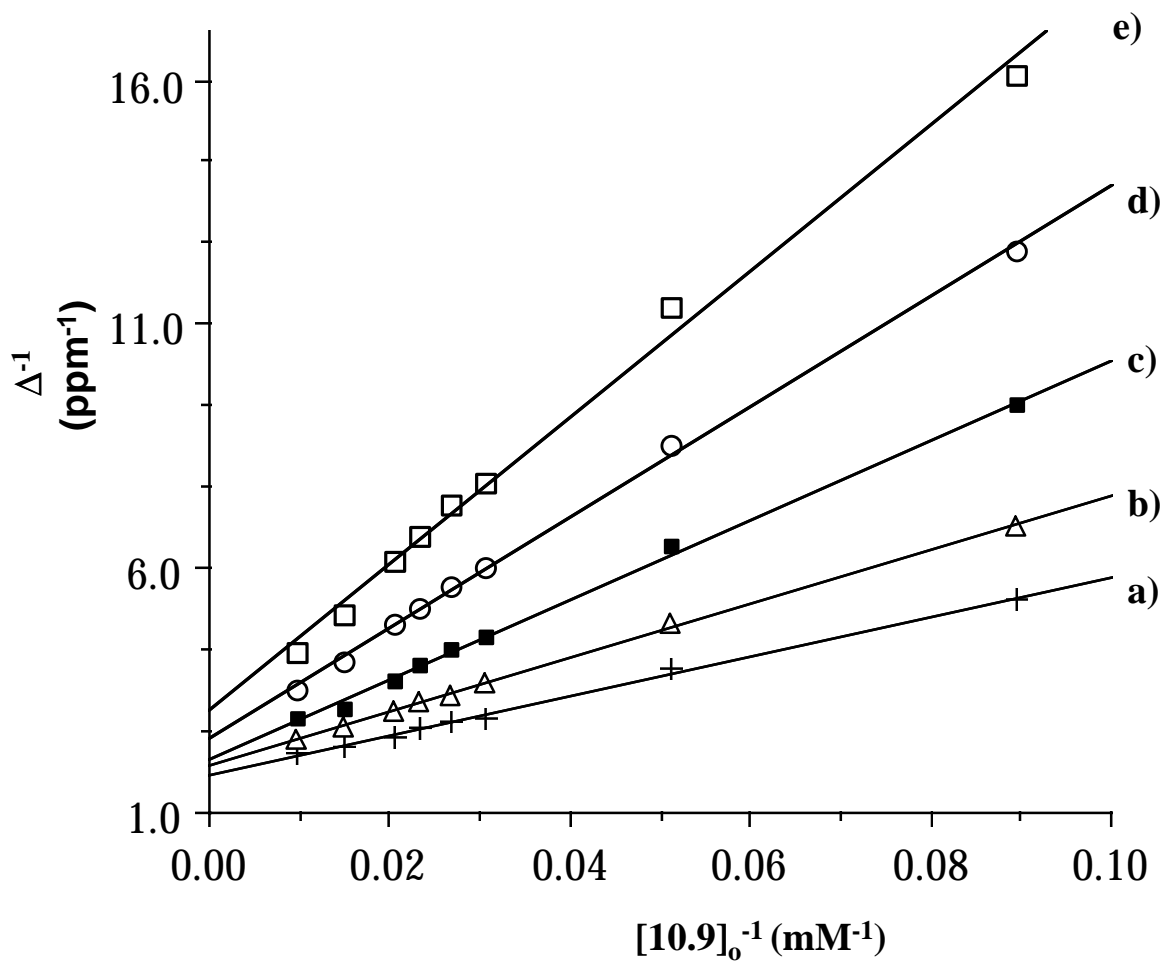


Figure 10.7. The Benesi-Hildebrand plots based on proton H_A for the formation of polyrotaxane 10.11 with $[10.8]_0 = 7.340 \text{ mM}$ at a) $21.8 \text{ }^\circ\text{C}$, b) $30.0 \text{ }^\circ\text{C}$, c) $38.0 \text{ }^\circ\text{C}$, d) $46.0 \text{ }^\circ\text{C}$ and e) $54.0 \text{ }^\circ\text{C}$ in acetone.

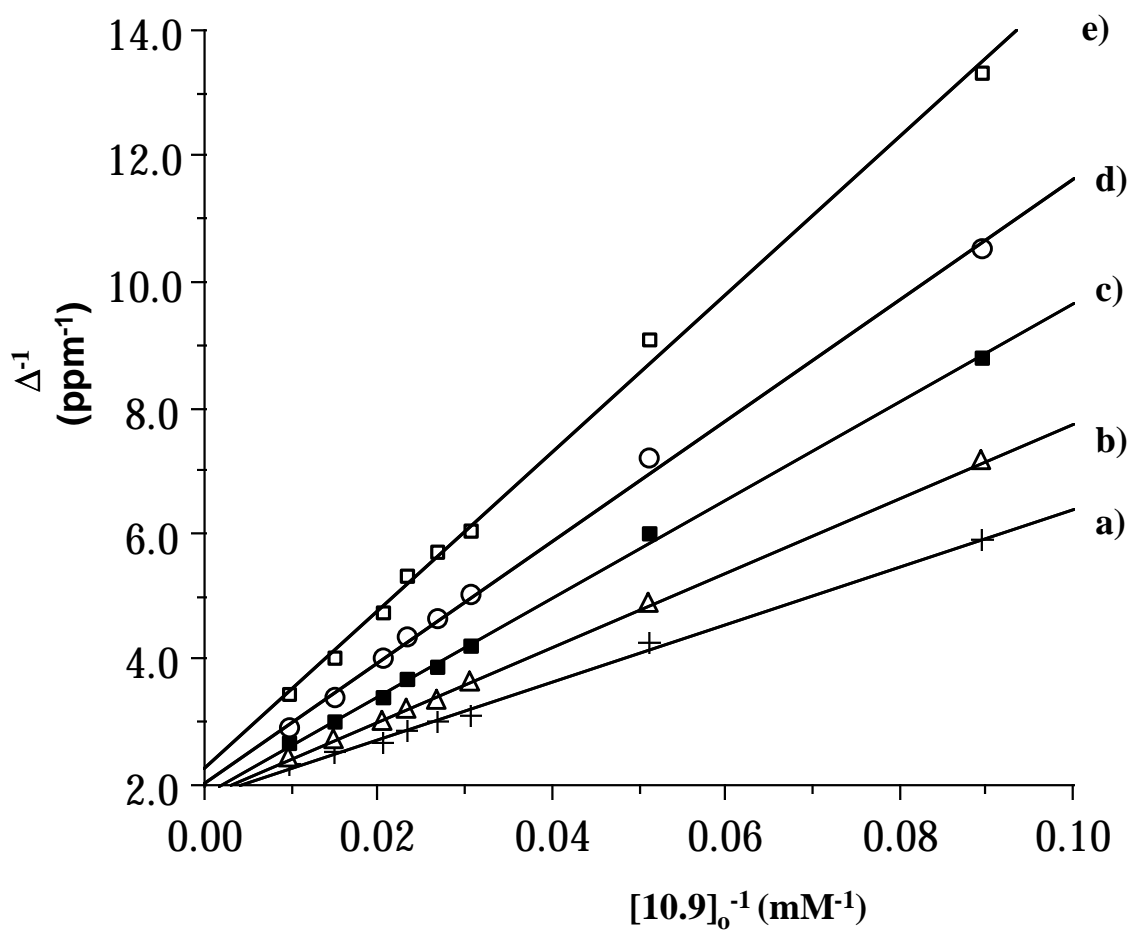


Figure 10.8. The Benesi-Hildebrand plots based on proton H_B for the formation of polyrotaxane 10.11 with [10.8]₀ = 7.340 mM at a) 21.8 °C, b) 30.0 °C, c) 38.0 °C, d) 46.0 °C and e) 54.0 °C in acetone.

Table 10.8 The results of the complexation of **10.8** and **10.9** based on Benesi-Hildebrand plots^a

Figure	Temp. (°C)	Slope (mM.ppm ⁻¹)	Intercept (ppm ⁻¹)	R ²	K ^b (M ⁻¹)	ΔG ^b (kJ.mol ⁻¹)	Δ _o (ppm)
10.7a	21.8	40.40	1.772	0.997	43.9	-9.274	0.564
10.8a	21.8	45.70	1.808	0.997	39.6	-9.021	0.553
10.7b	30.0	55.38	1.936	0.999	35.0	-8.961	0.517
10.8b	30.0	59.25	1.828	1.000	32.4	-8.766	0.547
10.7c	38.0	82.25	2.070	0.997	25.2	-8.348	0.483
10.8c	38.0	77.82	1.861	0.998	23.9	-8.211	0.537
10.7d	46.0	113.1	2.515	0.998	22.2	-8.226	0.398
10.8d	46.0	95.81	2.067	0.998	21.6	-8.153	0.484
10.7e	54.0	149.5	3.095	0.993	20.7	-8.242	0.323
10.8e	54.0	125.7	2.268	0.997	18.0	-7.862	0.441

^a based on proton H_A for Figure 10.7 and proton H_B for Figure 10.8.

^b estimated relative error: 5%.

Compared to the model system of **10.7** and **10.9**, K (Table 10.5) for the polymeric system is much lower at a given temperature. The difference, we believe, is because the cyclic units of polymer **10.8** are less flexible than those of monomeric **10.7**. For π -stacking to occur, the phenyl rings of the cyclic have to rotate toward each other relative to their parallel but non-overlapped conformation in the uncomplexed state.^{21a,25} As soon as they are incorporated into the polymer backbone, the rotation of these phenyl rings becomes much more difficult because it involves local or probably more extensive chain movement; this

²⁵ The crystal structure of bis(m-phenylene)-32-crown-10 indicates an open cavity (4.9 x 7.8 Å), which undergoes a small conformational change when it complexes with paraquat.^{21a} However, bis(5-carbomethoxy-1,3-phenylene)-32-crown-10 in the solid state has a collapsed cavity (0.75 x 7.8 Å), perhaps due to crystal packing forces and not intrinsic conformational preferences: Y. Delaviz, J. S. Merola, M. A. G. Berg and H. W. Gibson, *J. Org. Chem.* **1995**, *60*, 516-522.

leads to enthalpic penalties and consequently a lower K value. Thus ΔH is more negative for the model system. On the other hand, the ethyleneoxy units of the cyclic moiety in polymer **10.8** are restricted and expected to be less flexible relative to free macrocycle **10.7**, while both of them will be rigidified upon complexation with **10.9**; this results in a more negative ΔS for the model system than for the polymeric system. Thus while the enthalpic term favors monorotaxane **10.10**, the entropic term favors polyrotaxane **10.11**.

Therefore the threading efficiency (m/n) of polyrotaxane **10.11** can be simply controlled by varying temperature and concentration; that is the m/n values (Δ/Δ_0) of polypseudorotaxanes **10.11** increased with higher ratio of **10.9** vs. poly(crown ether) **10.8** at a given temperature as well as lower temperature at given concentrations (Table 10.9 and Figure 10.9).

Table 10.9. Threading efficiencies of **10.11** formed under different conditions
with $[\mathbf{10.8}]_0 = 7.340$ mM

$[\mathbf{10.9}]_0$ (mM)	21.8 °C m/n ^a	30.0 °C m/n ^a	38.0 °C m/n ^a	46.0 °C m/n ^a	54.0 °C m/n ^a
0	0/0	0/0	0/0	0/0	0/0
11.16	0.331/0.307	0.282/0.256	0.221/0.212	0.201/0.196	0.192/0.170
19.52	0.447/0.425	0.397/0.375	0.319/0.309	0.294/0.287	0.272/0.249
32.54	0.599/0.582	0.528/0.503	0.447/0.443	0.417/0.411	0.399/0.374
37.43	0.620/0.597	0.574/0.543	0.478/0.479	0.447/0.442	0.424/0.397
42.55	0.652/0.628	0.596/0.567	0.513/0.503	0.482/0.475	0.464/0.426
48.61	0.693/0.671	0.632/0.603	0.559/0.546	0.518/0.512	0.505/0.478
67.00	0.748/0.722	0.706/0.673	0.625/0.618	0.618/0.605	0.610/0.565
100.8	0.807/0.779	0.779/0.744	0.706/0.698	0.714/0.707	0.721/0.678

^a x_A/x_B : based on Δ_A and Δ_B , respectively; estimated relative error: $\pm 5\%$.

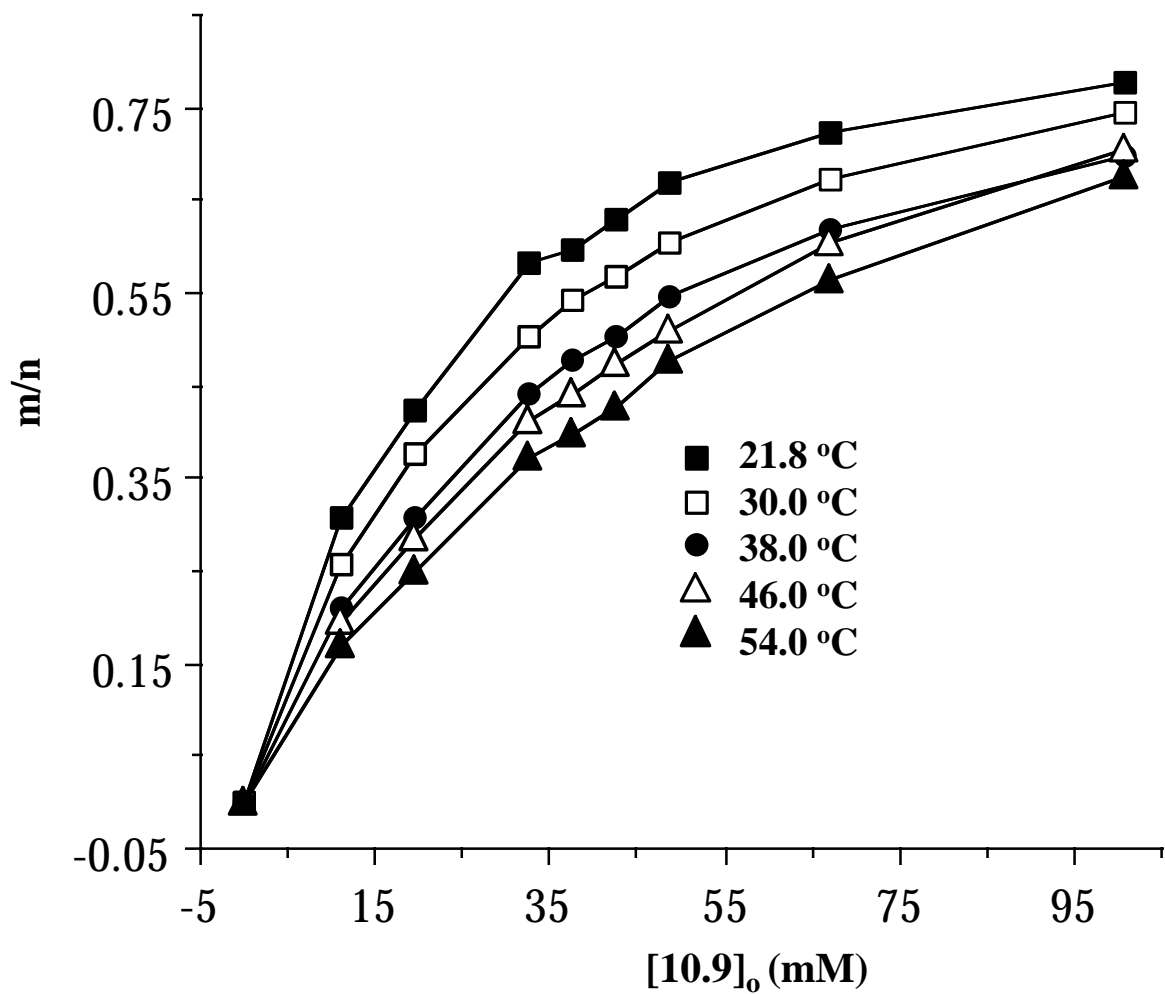


Figure 10.9 The relationship of threading efficiency (m/n) of 10.11 vs. the feed concentration of 10.9 with $[10.8]_0 = 7.340$ mM in acetone at different temperatures.

10.2.3. Physical Properties of Polyrotaxanes 10.11.

i Solubility.

In order to understand the effect of m/n on the solubility of polyrotaxane **10.11**, samples were prepared by slowly cooling acetone solutions of **10.8** and **10.9** to -78 °C followed by freeze-drying. Since $\Delta H = -19.3 \text{ kJ}\cdot\text{mol}^{-1}$ and $\Delta S = -35.0 \text{ J}\cdot\text{K}^{-1}\cdot\text{mol}^{-1}$, K is $2.18 \times 10^3 \text{ M}^{-1}$ under such conditions and the obtained solid had m/n values closely related to the feed composition (Table 10.10). As expected, these materials were orange, indicating that the polyrotaxane structure **10.11** remained in the solid state.

Table 10.10. The solubilities of **10.8**, **10.9** and **10.11**^a

	[10.8] ₀ ^b (mM)	[10.9] ₀ ^b (mM)	m/n ^c	Acetone	THF	CH ₃ CN	DM F
10.9	0	7.60	--	Y	N	Y	Y
10.8	<7.60 ^d	0	0	P	Y	N	Y
10.11	7.60	1.90	0.232	Y ^{9,8}	Y ⁸ ,P ⁹	N	Y ^{9,8}
10.11	7.60	3.80	0.428	Y ^{9,8}	Y ⁸ ,P ⁹	[Y ^{9,8} /N ⁸ ,Y ⁹] ^e	Y ^{9,8}
10.11	7.60	5.70	0.642	Y ^{9,8}	Y ⁸ ,P ⁹	[Y ^{9,8} /N ⁸ ,Y ⁹] ^e	Y ^{9,8}
10.11	7.60	7.60	0.783	Y ^{9,8}	Y ⁸ ,P ⁹	Y ^{9,8}	Y ^{9,8}
10.11	7.60	15.2	0.946	Y ^{9,8}	Y ⁸ ,P ⁹	Y ^{9,8}	Y ^{9,8}
10.11	7.60	22.8	0.971	Y ^{9,8}	Y ⁸ ,P ⁹	Y ^{9,8}	Y ^{9,8}

^a Y^x: component x totally soluble; P^x: x component partially soluble; insoluble part and precipitate were identified by solubility in CH₃CN and THF and confirmed by ¹H NMR.

^b The initial concentrations of **10.8** and **10.9**.

^c The threading efficiencies of solid **10.11** from freeze-drying calculated based on $K = 2.18 \times 10^3 \text{ M}^{-1}$ at -78 °C.

^d polymer **10.8** by itself only partially soluble in acetone.

^e Initially both components were soluble but polymer **10.8** precipitated in less than 10 seconds.

Since paraquat **10.9** and starting polymer **10.8** had different solubilities, the solubility of polyrotaxane **10.11** is expected to be dependent on the threading efficiency (Table 10.10). Not surprisingly, all the polyrotaxanes were soluble in DMF since it is a good solvent for both components. While polymer **10.8** is only partially soluble in acetone, a good solvent for paraquat **10.9**, all polyrotaxanes were soluble in acetone with an orange color and no precipitation was observed over days. The absence of a precipitate over days at room temperature indicated that only a small amount of threading (m/n much lower than that specified in Table 10.10) is necessary to retain polymer **10.8** in acetone.

While polymer **10.8** is totally soluble in THF and paraquat **10.9** is not soluble at all, the polyrotaxanes **10.11** even up to $m/n=0.971$ were initially soluble except for a small amount of uncomplexed paraquat (the difference between m/n and the feed ratio). However, a few seconds later, more paraquat **10.9** from disassociation of **10.11** precipitated as a white solid. Since all solutions were orange and the precipitation stopped shortly after dissolution, the solubility of paraquat **10.9** was indeed enhanced by the complexation with polymer **10.8**.

CH_3CN is a good solvent for paraquat **10.9** but poor for polymer **10.8**. However, all polyrotaxanes **10.11** with $m/n \geq 0.428$ were soluble while **10.11** ($m/n=0.232$) was not; this means that a certain amount of paraquat is necessary for polyrotaxane **10.11** to be soluble. Interestingly, while no insoluble materials were observed over weeks for **10.11** with a feed ratio of **10.9** vs. **10.8** at one or greater, for **10.11** with the ratio lower than 0.75, **10.8** precipitated over a couple minutes, indicating the occurrence of dethreading upon dissolution.

ii. Viscosity.

To study the effect of the formation of the polyrotaxane structure on chain conformation, the specific viscosity and reduced viscosity were measured at different feed ratios of **10.9** vs. **10.8** at constant concentration of **10.8** (Table 10.11). To eliminate the possible interference of the excess paraquat **10.9**, the viscosities were also calculated by subtracting the flow time contributed by **10.9**.

As the results show, the incremental viscosity caused by **10.9** is negligible over the measured concentration range, i.e., η'_{sp}/C and η'_{sp} are very close to η_{sp}/C and η_{sp} (Table

10.11). Since K is 39.6 M^{-1} (Table 10.8), the corresponding m/n values were calculated. The results in Table 10.11 afford information in terms of understanding the polyrotaxane conformation. Polyrotaxane **10.11** with $m/n=0.430$ had a reduced viscosity (0.215) and specific viscosity (0.122 dL/g) twice as high as those (0.122 and 0.0689 dL/g, respectively) of **10.11** with $m/n=0.054$. Overall, the higher m/n , the higher the viscosities polyrotaxane **10.11** had (Figure 10.10); this clearly indicates that **10.11** with higher m/n had larger hydrodynamic volume, i.e., **10.11** became more and more rigid and adopted a more extended chain conformation.

Table 10.11. The viscosities and glass transition temperatures of **10.11** with different threading efficiencies^a

	[10.8] ₀ ^b (mM)	[10.9] ₀ ^b (mM)	m/n ^c	$\dot{\eta}_{sp}$ ^d $\times 10^2$	$\dot{\eta}_{sp}/C$ ^d $\times 10^2$ (dL/g)	η_{sp} ^d $\times 10^2$	η_{sp}/C ^d $\times 10^2$ (dL/g)	m/n ^e	T_g ^f (°C)
10.8	--	--	0	--	--	--	--	0	-6.3
10.11	7.427	1.857	0.054	6.82	12.0	6.89	12.2	--	--
10.11	7.427	3.714	0.104	7.61	13.4	7.70	13.6	0.45	45
10.11	7.427	5.570	0.150	8.30	14.7	8.41	14.8	0.64	86
10.11	7.427	7.427	0.192	9.28	16.4	9.42	16.6	0.78	116
10.11	7.427	14.85	0.329	10.7	18.9	11.0	19.4	--	--
10.11	7.427	22.28	0.430	11.8	20.8	12.2	21.5	--	--

^a Measured with Cannon L12 viscometer in acetone at 21.8 °C at the concentrations specified.

^b The feed concentration of polymer **10.8** (repeat unit basis) and **10.9**, respectively; 7.427 mM of **10.8** equals 0.5667 g/dL.

^c Calculated based on $K = 39.6 \text{ M}^{-1}$ in acetone at 21.8 °C.

^d $\dot{\eta}_{sp} = (t-t_0')/t_0'$ and $\dot{\eta}_{sp}/C = (t-t_0')/t_0'C$ where t and t_0' are the flow times of the solution of **10.8** and **10.9** and solution of pure **10.9** (the concentrations of **10.9** were same for both solutions) in acetone at 21.8 °C, respectively, and C is concentration of **10.8**. $\eta_{sp} = (t-t_0'')/t_0''$ and $\eta_{sp}/C = (t-t_0'')/t_0''C$ ($t_0'' =$ flow time of acetone).

^e Calculated based on $K=2.18 \times 10^3 \text{ M}^{-1}$ because the samples for T_g were obtained by freeze-drying at -78 °C.

^f Measured by DSC at scan rate of 10 °C/min.

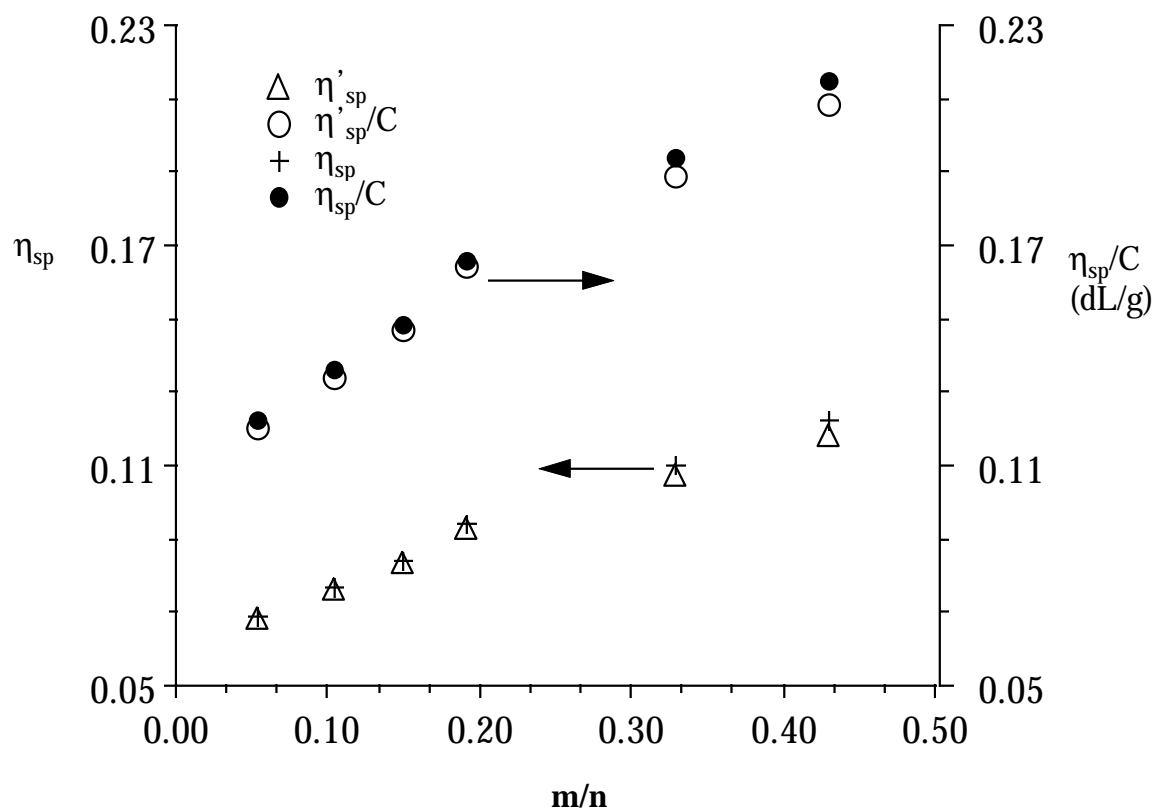


Figure 10.10. The relationship of viscosities of **10.11** vs. the threading efficiency in acetone at 21.8 °C.

iii. Glass Transition Temperatures, Melt Threading and Dethreading.

The samples from the viscosity measurements were freeze-dried in an acetone/dry-ice bath under high vacuum for the thermal analysis. According to K ($2.18 \times 10^3 \text{ M}^{-1}$) calculated from ΔH and ΔS at this temperature, m/n values of the resulting **10.11** were close to the feed ratio of **10.9** vs. **10.8** (Table 10.11). Their deep orange color indicated the rotaxane structures. This is very important because it means that polypseudorotaxanes in the solid state can simply be prepared and thus physical properties and applications in the solid state can be explored.

While uncomplexed polymer **10.8** was a colorless viscous material with glass transition temperature, $T_g = -6.3 \text{ }^\circ\text{C}$, **10.11** (m/n = 0.640) was a glassy orange material with

$T_g = 86\text{ }^\circ\text{C}$, indicating that **10.11** is more rigid than **10.8**. Overall, the higher m/n is, the higher the T_g is (Table 10.11). All these results agree with expectations. The cyclic moiety contains very flexible ethyleneoxy units which explains the low T_g of polymer **10.8**. Upon complexation with paraquat, the flexibility (the mobility of cyclic) is restricted and thus the higher m/n is, the more rigid the polyrotaxane **10.11** is.

The polyrotaxanes upon heating above the glass transition temperatures lost their color, indicating that dethreading occurs. Slow cooling and reheating did not bring the color back; instead a glass transition temperature corresponding to uncomplexed polymer **10.8** was observed. Therefore, the dethreading is not reversible under these conditions, probably because paraquat has a melting point well beyond the observed temperature range and quickly phase separates once dethreading takes place.

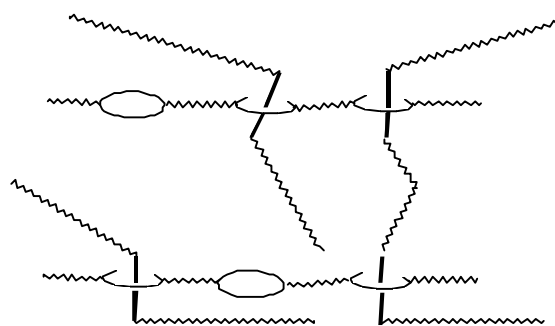
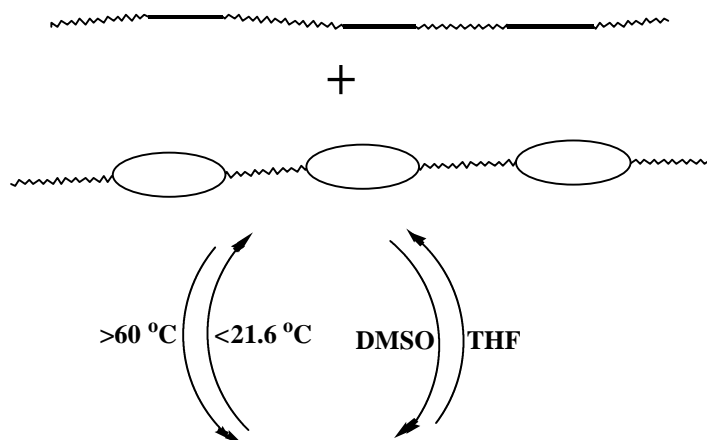
Thus these materials could be used as ceiling temperature indicators, e.g., for storage and shipping of perishables. The change in color from orange to nearly colorless takes place if T_g is exceeded. Since T_g can be controlled by m/n, a useful range of temperature sensors can be “dialed-in”.

10.2.4 Reversible mechanically-linked branched polymers: interpenetration of preformed polymers

According to the above study, it is expected that poly(sebacate crown ether) **10.8** will knit with polyurethane **10.14** containing paraquat moieties to form interpenetrated branched polymers **10.15** with rotaxane units as linkages (Scheme 10.4). If enough threading is achieved, crosslinked **10.16** will form as a precipitate. However, to characterize the interpenetrated rotaxane structure, a soluble polymer is necessary. Thus only a small amount of paraquat, an average two paraquat moieties per polymer chain, was incorporated into **10.14** for the present study.

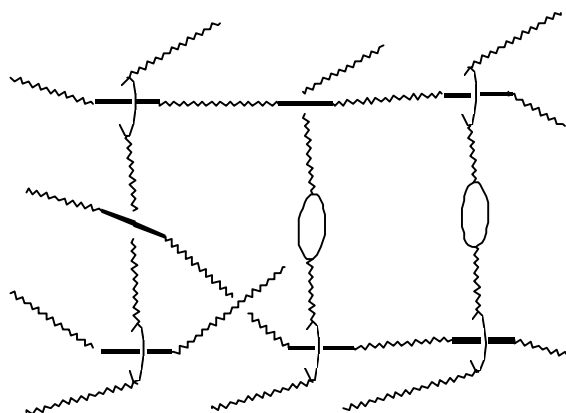
Not surprisingly, as soon as polyester **10.8** (colorless) and polyurethane **10.14** (light yellow) were mixed in THF at room temperature, a deep orange color appeared. This indicates that self assembly occurs rapidly. More directly, compared to the spectrum of pure **10.8** (Figure 10.11a), the signals of protons H_A and H_B of the macrocyclic units of **10.8** in its

Scheme 10.4



Branched 10.15

or



Crosslinked 10.16

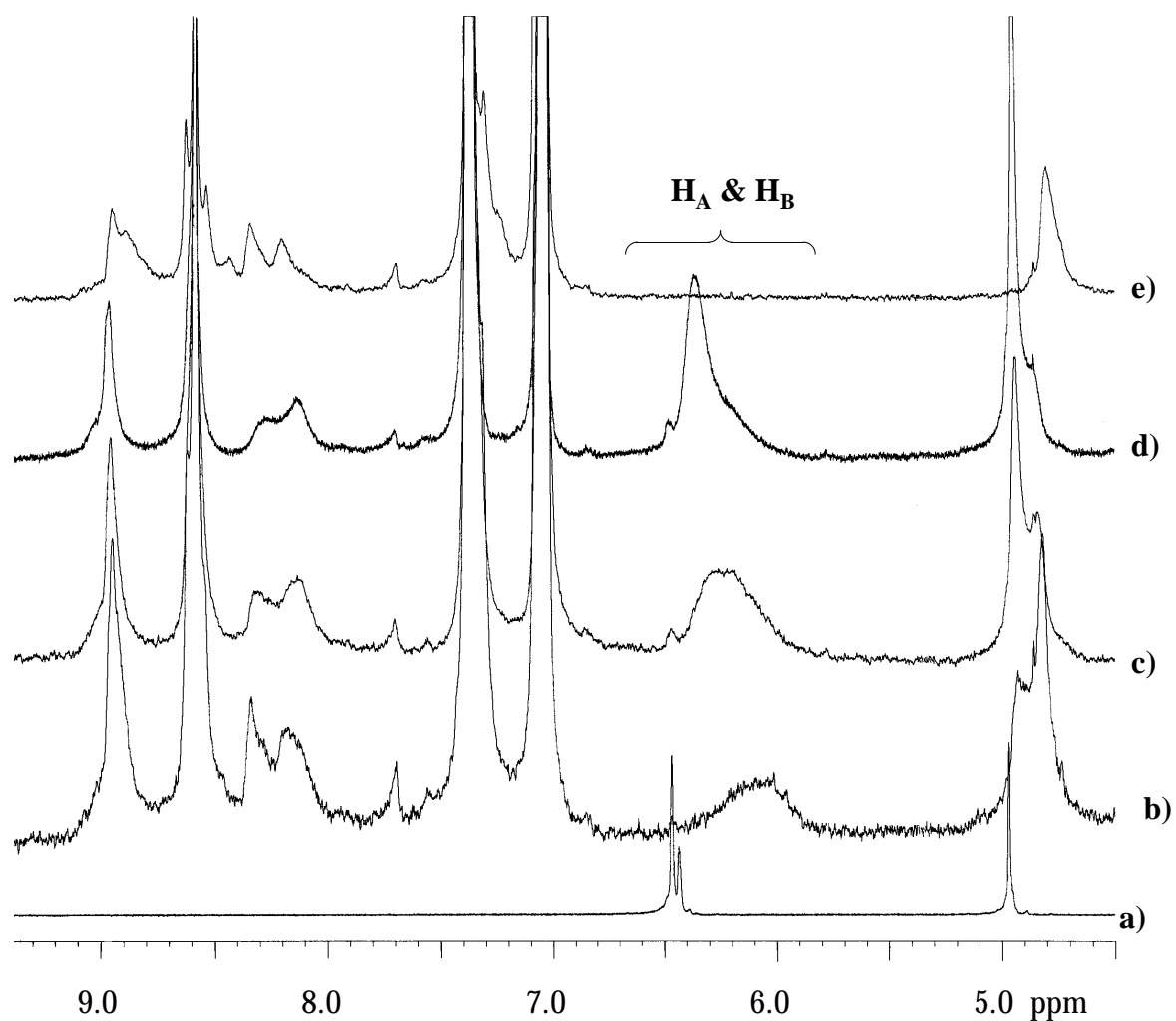


Figure 10.11. The expanded 400 MHz proton NMR spectra of solutions of 10.8 and 10.14: (a) $[10.14]_0 = 0$ mM and $[10.8]_0 = 1.43$ mM; (b) $[10.14]_0 = 3.82$ mM and $[10.8]_0 = 1.43$ mM; (c) $[10.14]_0 = 3.82$ mM and $[10.8]_0 = 4.00$ mM; (d) $[10.14]_0 = 3.82$ mM and $[10.8]_0 = 12.58$ mM and (e) $[10.14]_0 = 3.82$ mM and $[10.8]_0 = 0$ mM in THF- d_8 at 21.6 °C (all concentrations are based on cyclic units for 10.8 and bipyridinium moieties for 10.14).

mixtures with **10.14** (Figure 10.11b-d) were shifted upfield.²⁶ Therefore, proton NMR directly proved the formation of interpenetrating structures. The extreme breadth of these signals also agrees with the proposed branched structure **10.15** which causes slower relaxation. As shown in Figure 10.11, the chemical shifts of protons A and B increase with more polyester **10.8** because a lower fraction of cyclic units is occupied by the bipyridinium moieties. It was also found that the shapes and chemical shifts of the signals for protons A and B did not change with mixing time up to 24 hrs; this indicates that the self assembly occurs within 30 seconds, the shortest time for a spectrum to be acquired.

If the interpenetration indeed occurs, both a higher molecular weight and polydispersity (PDI) are expected for **10.15** compared to its precursors polyester **10.8** and polyurethane **10.14**. Therefore, molecular weights of different solutions of **10.8** and **10.14** were measured by GPC with polystyrene standards at room temperature (Table 10.12). Compared to those ($M_n = 11.9$ kg/mol and PDI = 3.78) from GPC measurements in salt solution with universal calibration, molecular weights of polyurethane **10.14** were totally different in THF with polystyrene standards ($M_n = 1.46$ kg/mol and PDI = 6.43) (Table 10.1); this is attributed to the polyelectrolyte effect. Thus the values in Table 10.12 do not reflect true molecular weights of **10.15**. However, they do reflect changes of molecular weight and PDI since they were measured under identical conditions at the same overall concentration of polyurethane **10.14**. Indeed, upon the addition of 1 g of poly(ester crown ether) **10.8** into a solution of 20 g of polyurethane **10.14** in 1 L of THF, both the molecular weight and PDI increased (Table 10.12 and Figure 10.12); this directly proved that larger supramolecules **10.15** were indeed formed by self assembly. PDI as high as 46.5 and M_w as high as 164

²⁶ DMSO as cosolvent prevented H-bonding between **6** and its hydroxy groups and no rotaxane structure (branching point) was formed.¹⁹ Therefore the obtained polymer **8** was linear with PDI = 1.97. It was used for the preparation of main chain polypseudorotaxanes **11**. This explains the fact no uncomplexed signals exist in **11** (Figure 6). **8** was also prepared by the same procedure but using only diglyme as solvent and thus the obtained **8** with PDI = 4.60 (used for preparation of branched polyrotaxane **15**, Table 12) was branched because of the rotaxane formation.¹⁹ The crown ether moieties threaded by linear species do not have enough room to accommodate another linear component and the corresponding protons H_A and H_B remained at the original position (the minor peaks at 6.4-6.5 ppm in Figure 10.11b, c, d) while the major peaks shifted upfield upon complexation with **14**.

kg/mol were reached despite the fact that the individual polymers **10.8** and **10.14** have M_w of 36.9 kg/mol and 9.41 kg/mol, respectively (Table 10.12 and Figure 10.12). These results are also consistent with the proposed interpenetrating structure **10.15** (Scheme 10.4).

Table 10.12. The GPC results for **10.8**, **10.14** and **10.15**

products	[10.8] ₀ (g/L ^a ; mM ^b)	[10.14] ₀ (g/L ^a / mM ^c)	M_n^d (kg/mol)	M_w^d (kg/mol)	PDI ^d
10.8	3.00; 3.93	0	8.01	36.9	4.60
10.15	1.00; 1.31	20.0; 3.82	2.66	26.1	9.80
10.15	2.00; 2.62	20.0; 3.82	3.25	37.3	11.5
10.15	4.00; 5.24	20.0; 3.82	3.17	53.7	16.9
10.15	6.00; 7.86	20.0; 3.82	3.37	70.2	20.8
10.15	8.00; 10.48	20.0; 3.82	3.53	164.0	46.5
10.14	0	20.0; 3.82	1.46	9.41	6.43

a) based on polymer.

b) based on cyclic repeat unit.

c) based on bipyridinium salt moiety.

d) measured by GPC with polystyrene standards in THF at 22.0 °C.

Since the complexation of the crown ether and bipyridinium units is an equilibrium, its extent can be controlled by temperature and solvent; the higher the temperature is, the lower the association constant is. Thus it occurred to us that **10.15** can dissociate into the starting polymers **10.8** and **10.14** under the influence of external forces. Indeed, in DMSO, the chemical shifts of protons H_A and H_B of the cyclic moiety in polyester **10.8** did not change upon mixing (Figure 10.13); this indicates that no complexation occurred. Therefore, **10.15** formed in THF can simply be dissociated by addition of DMSO. In addition, the signals were as sharp as those of pure **10.8**, indicating that the signal broadening in THF was indeed because of the branched structure of **10.15** but not due to the simple addition of **10.14**. Moreover, it was found that the signals for protons H_A and H_B in a solution of **10.8** and **10.14**

in THF (21.6 °C, Figure 10.11c) shifted downfield and became less broad when the temperature was increased to 31.7 °C and back to that of uncomplexed **10.8** at 60 °C (Figure 10.13d); the branching structure **10.14** also depends on temperature; lower temperatures favor its formation.

Use of higher paraquat loadings should enable self assembly of networks that behave like thermosets, but which can be easily processed and reprocessed.

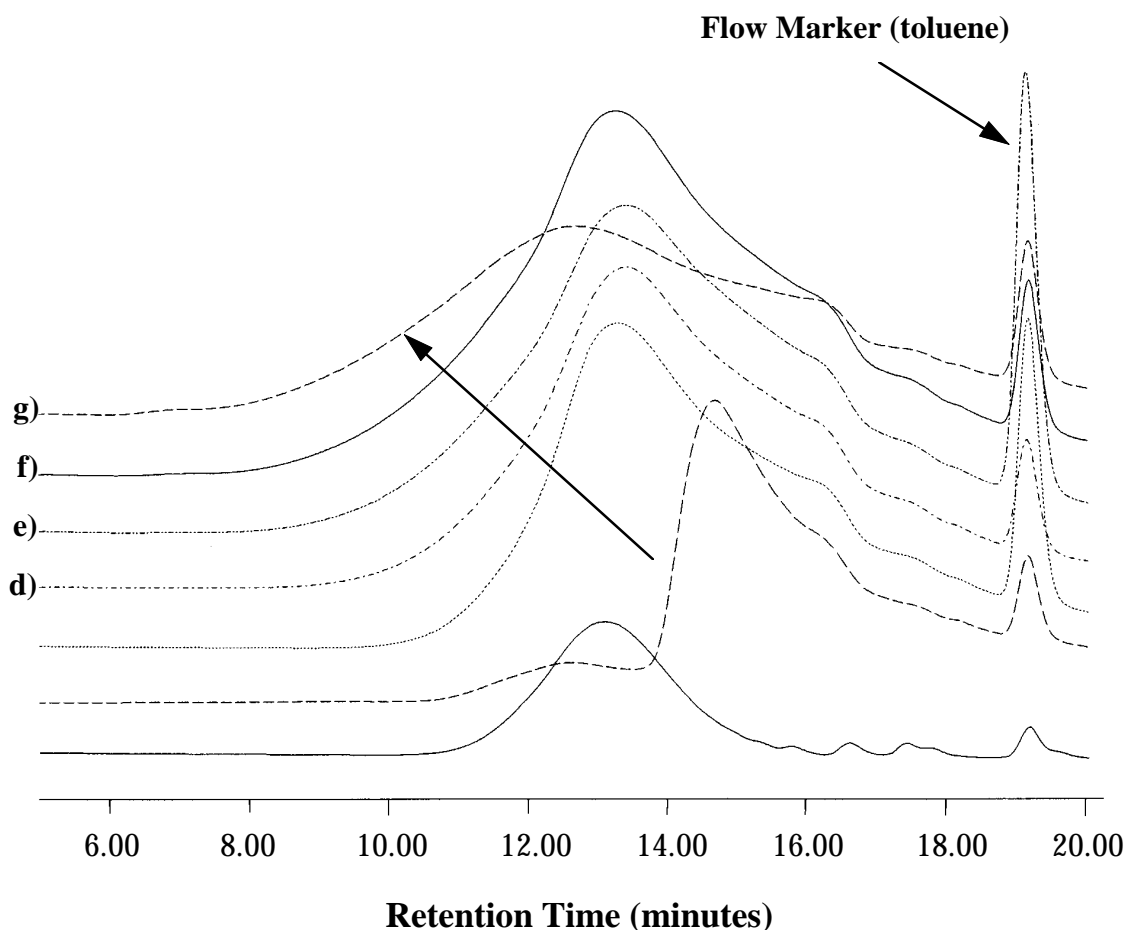


Figure 10.12. The GPC traces of solutions of (a) $[10.8]_0 = 3.93$ mM and $[10.14]_0 = 0$ mM; (b) $[10.8]_0 = 0$ mM and $[10.14]_0 = 3.83$ mM; (c) $[10.8]_0 = 1.31$ mM and $[10.14]_0 = 3.82$ mM; (d) $[10.8]_0 = 2.62$ mM and $[10.14]_0 = 3.82$ mM; (e) $[10.8]_0 = 5.24$ mM and $[10.14]_0 = 3.82$ mM; (f) $[10.8]_0 = 7.86$ mM and $[10.14]_0 = 3.82$ mM; (g) $[10.8]_0 = 10.48$ mM and $[10.14]_0 = 3.82$ mM in THF at 21.6 °C (UV detector).

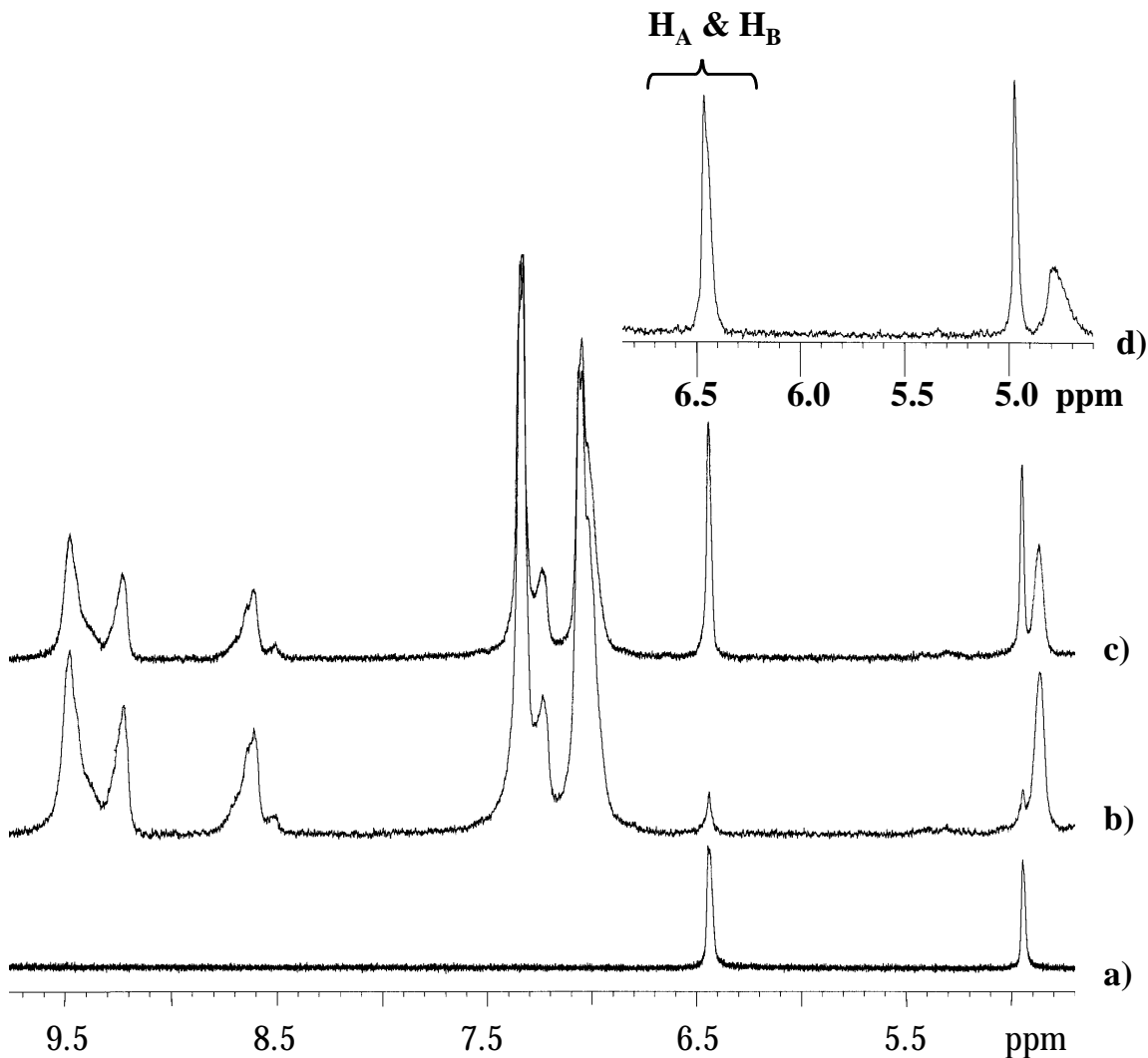


Figure 10.13. Expanded 400 MHz proton NMR spectra of solutions of **10.8** and **10.14**: (a) $[10.14]_0 = 0$ mM and $[10.8]_0 = 1.43$ mM; (b) $[10.14]_0 = 3.82$ mM and $[10.8]_0 = 1.43$ mM; (c) $[10.14]_0 = 3.82$ mM and $[10.8]_0 = 4.00$ mM in $\text{DMSO-}d_6$ at 21.6 °C and (d) $[10.14]_0 = 3.82$ mM and $[10.8]_0 = 1.43$ mM in $\text{THF-}d_8$ at 60.0 °C.

10.3 Conclusions

An approach for new main chain polyrotaxanes of Type **10.2** (Scheme 10.1) was described. Polypseudorotaxane **10.11** was effectively formed by threading linear paraquat **10.9** through the cavities of the cyclic repeat units of polymacrocyclic **10.8**. The formation of the polyrotaxane structure in solution was proved by both the color change and proton NMR

spectroscopy. Importantly, the corresponding solid state polyrotaxane was simply prepared by a freeze-drying procedure without use of blocking groups. Polyrotaxane **10.11** with higher m/n had higher viscosity because of chain conformational changes. Because of its higher rigidity, **10.11** also had higher T_g than starting backbone **10.8**, depending on the loading. The solubility of **10.8** was also altered by the formation of polyrotaxane **10.11**.

The m/n value of polyrotaxane **10.11** increased with increasing amounts of paraquat salt **10.9** as well as decreasing temperature. The values of K, ΔH and ΔS provide the basis for predicting the threading efficiency for the preparation of analogous polyrotaxanes. Compared to the model system of **10.9** with simple **10.7**, both ΔH and ΔS for the polyrotaxane system are less negative, indicating that the enthalpy term favors the formation of [2]rotaxane **10.10** while the entropy terms do so for the formation of polyrotaxane **10.11**. Since paraquat **10.9** bears two terminal -OH groups, **10.11** can further react, e.g., with diisocyanates, to form very interesting networks.

In addition, a novel method for the construction of interpenetrating branched polymers was demonstrated for the first time by self assembly of bipyridinium salt units of a preformed polyurethane and crown ether moieties of a polymeric crown ether. The physically linked structure is reversible, depending on environmental conditions, e.g., solvent and temperature. This concept is suitable for lots of other polymer systems incorporating crown ether and bipyridinium moieties and suggests several potential applications.

10.4 Experimental Section.

Chemical Reagents and Measurements

All chemicals were reagent grade and used directly as received from Aldrich unless otherwise specified. All solvents were HPLC or GC grade. Bis(5-hydroxymethyl-m-phenylene)-32-crown-10 (**10.6**)²², bis(5-acetoxymethyl-m-phenylene)-32-crown-10 (**10.7**)²² and paraquat diol **10.9**²³ were prepared by well-established procedures. Proton NMR spectra, reported in ppm, were obtained on a 400 MHz Varian spectrometer using acetone- d_6 or DMSO- d_6 . The absolute molecular weights of the polymers were measured by GPC with a Waters 150C ALC/GPC chromatograph equipped with a differential refractometer detector or

an on-line differential viscometric detector (Viscotek 150R) coupled in parallel using the universal calibration. The relative molecular weights of polymers were measured by GPC equipped with a UV detector using PS standards. T_g 's were measured with a Perkin-Elmer thermal analysis system at a rate of 10 °C/minute; all reported values were the centers of transitions from first heating.

Poly(ester crown ether) 10.8.

Sebacoyl chloride (**10.7**) (150.0 mg, 0.6272 mmol) and bis(5-hydroxymethyl-m-phenylene)-32-crown-10 (**10.3**) (374.3 mg, 0.6272 mmol) were dissolved in a mixture of anhydrous diglyme and DMSO (4 mL, 1:1 by volume). Polymerization proceeded at 60 °C for 2 days under the protection of N₂. The product was purified by precipitation into MeOH (100 mL) to afford **10.8** (421.1 mg, 88 %). ¹H NMR (DMSO-*d*₆ ppm) δ 6.52 (br s, ArH, 4H), 6.44 (br s, ArH, 2H), 5.01 (br s, ArCH₂O, 4H), 4.06 (br s, ArCH₂CH₂O, 8H), 3.78 (br s, ArCH₂CH₂O, 8H), 3.61 (br s, ArCH₂CH₂OCH₂, 16H), 2.34 (br s, OOCH₂, 4H), 1.62 (br s, OOCH₂CH₂, 4H), 1.32 (br s, OOCH₂CH₂CH₂CH₂, 8H). $M_n = 14.9$ kg/mol and PDI = 1.97 by GPC with polystyrene standards.²⁶

Polyurethane 10.14.

To a 15 mL flask containing a mixture of anhydrous diglyme and CH₃CN (3 mL, 1:1) were added N,N'-bis(β-hydroxyethyl)-4,4'-bipyridinium 2PF₆ (**10.9**) (151.6 mg, 0.2828 mmol), poly(tetramethyleneoxide) diol (**10.12**) ($M_n = 1000$, dihydroxy-terminated) (660.0 mg, 0.6660 mmol) and 4,4'-methylenebis(*p*-phenyl isocyanate) (**10.13**) (235.9 mg, 0.9426 mmol). The solution was refluxed for 12 h. The product was purified by precipitation into water to afford polyurethane **10.14** (712 mg, 68 %). Based on proton NMR, the paraquat units represent 0.22 mole fraction of repeat units. Molecular weight: $M_n = 11.9$ kg/mol and PDI = 3.78 by GPC with universal calibration in NMP (10⁻³ M LiBr).

VITA

Mr. Caiguo Gong was born on January 9, 1965 in Jianyin, an east coast city of Jiangsu province, P. R. China. After he graduated from Changzhou Light Industry Institute in 1984, he was employed by YiXing First Plastics Factory as a plastics processing engineer until 1988 when he started his graduate study in Department of Polymer Materials at East China University of Chemical Technology. After he received his Master degree in Engineering in 1991, he had worked on processing polymer fibers in Jiangsu Textile Research Institute as a research engineer for three years. He started his Ph.D. study in the Department of Chemistry at Virginia Polytechnic Institute and State University in August 1994 and joined Dr. Gibson's group shortly after.